Dynamics Controlling the Seasonal Cycle of Congo Basin Evaporation



David Crowhurst

Keble College

University of Oxford

A thesis submitted for the degree of

Doctor of Philosophy

Trinity Term 2021

Abstract

Evaporation is an integral component of Congo Basin climate and a crucial moisture source for basin rainfall. However, the dynamics controlling the climatological seasonal cycle of basin evaporation are unclear. Therefore, this thesis aims to make progress towards a complete understanding of the dynamics controlling the seasonal cycle of Congo Basin evaporation. Knowledge of these dynamics will provide a theoretical framework useful for advancing basin hydrological science, and a baseline against which global climate models can be evaluated.

The LandFlux-EVAL evaporation benchmark product is used in this thesis as a point of reference for Congo Basin evaporation. On the basin-wide average, LandFlux-EVAL evaporation increases from January to its one peak in March, is stable between March and April, decreases from April to a trough in July, and recovers between July and January. Evaporation is also lower at the November rainfall peak than the March rainfall peak, despite similar rainfall in the CHIRPS2 rainfall product. Using the ERA5-Land reanalysis, which effectively reproduces the pattern of lower evaporation in November than March in LandFlux-EVAL, this thesis derives plausible dynamics responsible for this feature of the seasonal cycle. Lower surface downward shortwave radiation (DSR) is a plausible driver of lower leaf area index (LAI) in the rainforest and north-eastern savannah, which is the main reason for lower transpiration, and therefore lower evaporation, in November.

As evaporation differs substantially between the basin's evergreen rainforest and deciduous savannah, to expand beyond the difference between the peaks a regional approach is used based on land cover type. Collectively, the dynamics that explain why evaporation is suppressed at the November rainfall peak relative to the March rainfall peak, and the dynamics controlling the seasonal cycles of evaporation in the rainforest and savannah, will explain what controls the seasonal cycle of evaporation on the basin-wide average. Therefore, this thesis seeks to derive plausible dynamics controlling the seasonal cycle of evaporation in these two ecoregions.

However, the thesis finds that ERA5-Land effectively reproduces the seasonal cycle of evaporation from LandFlux-EVAL in the savannah only. Therefore, the following plausible dynamics are derived from ERA5-Land controlling the savannah's seasonal cycle of evaporation. These are considered from November to November to account for evaporation in one wet and one dry season. Between November and March, an increase in surface DSR explains an increase in LAI, transpiration and evaporation. Between March and April, the effects of a decrease in rainfall and increase in surface DSR offset one another, leading to stable evaporation. Between April and July, a decrease in rainfall explains why evaporation falls. Between July and November, early green-up and an increase in rainfall explain why evaporation recovers.

The lack of agreement between ERA5-Land and LandFlux-EVAL in the basin's rainforest precludes the use of ERA5-Land to derive the dynamics controlling the seasonal cycle of evaporation here. However, this thesis suggests that using a sub-grid rainfall scheme in the land surface model of the next version of ERA5-Land could bring the seasonal cycle of evaporation from ERA5-Land into good agreement with LandFlux-EVAL in the rainforest and allow the next version of this reanalysis to be used to derive the dynamics controlling the seasonal cycle of evaporation here. This could then achieve a complete understanding on the basin-wide average of why the seasonal cycle of Congo Basin evaporation behaves as it does.

Table of contents

Abstract i
Acknowledgements vi
List of tables viii
List of figures x
List of acronyms xviii
1 Introduction 1
1.1 Background and rationale 2
1.2 Aim and research questions 7
1.3 Congo Basin rainfall regime 8
1.3.1 Tropical rain belt 10
1.3.2 Jet streams and mesoscale convective systems 13
1.3.3 Congo Basin cell 15
1.3.4 Sources of moisture for Congo Basin rainfall 16
1.4 Congo Basin evaporation regime 19
1.4.1 Thesis definition of evaporation 19
1.4.2 Review of previous research 19
1.4.3 Relevance of the seasonal cycle of evaporation 24
1.4.4 Revealing basin evaporation dynamics 27
1.5 Congo Basin evaporation in land surface models 31
1.5.1 Errors in the partitioning of evaporation into its components 32
1.5.2 Identifying how to improve reanalysis evaporation 37
1.6 Thesis format 39
2 Data and methods 40
2.1 Introduction 41
2.2 Data 41
2.2.1 Reference data sets 41
2.2.2 CMIP5 models 43
2.2.3 Reanalysis data sets 45
2.3 Methods 46
2.3.1 Seasonal cycles 46
2.3.2 GCM and reanalysis evaluation 46

3 Evaluation of evaporation climatology for the Congo Basin wet seasons in 11 global climate models 49
Authorship declaration 49
Abstract 50
3.1 Introduction 51
3.1.1 Process-based evaluation of Congo Basin evaporation 53
3.1.2 Aims 54
3.2 Data and methods 55
3.2.1 Domain 55
3.2.2 AGCMs 56
3.2.3 Reference data sets 58
3.2.4 Methods 60
3.2.4.1 Root mean square error analysis 60
3.2.4.2 Process-based evaluation 62
3.3 Annual cycles of rainfall and evaporation in the Congo Basin 62
3.4 Evaporation partitioning in the Congo Basin wet seasons 69
3.4.1 Canopy evaporation 69
3.4.2 Transpiration 70
3.4.3 Soil evaporation 72
3.5 Discussion 73
3.6 Conclusions 76
Acknowledgements 78
Appendix A 79
A.1 Canopy evaporation 79
A.2 Transpiration 80
A.3 Soil evaporation 80
4 Contrasting controls on Congo Basin evaporation at the two rainfall peaks 82
Authorship declaration 82
Abstract 83
4.1 Introduction 84
4.1.1 Lower evaporation in November than March in the Congo Basin 85
4.1.2 Aims 89
4.2 Data and methods 90
4.2.1 Domain and evaporation reference data 90
4.2.2 Reanalysis data 91

4.2.3 Methods ... 93
4.3 Lower evaporation in November than March ... 94
4.3.1 Regions ... 94
4.3.2 ERA5-Land v MERRA-2 ... 95
4.3.3 Rainforest ... 96
4.3.4 Eastern savannah ... 98
4.4 Contrasting controls on transpiration at the two rainfall peaks ... 99
4.4.1 Leaf area index (LAI) and vapour pressure deficit (VPD) ... 100
4.4.2 Lower LAI in November than March ... 102
4.4.2.1 Northern rainforest ... 104
4.4.2.2 Southern rainforest ... 107
4.4.2.3 North-eastern savannah ... 107
4.4.2.4 South-eastern savannah ... 108
4.4.3 Lower VPD in November than March in the northern rainforest ... 108
4.5 Summary and discussion ... 110
4.5.1 Contrasting controls on Congo Basin evaporation at the two rainfall peaks 111
4.5.2 Consistency with the Budyko framework ... 114
4.6 Conclusions ... 115
Acknowledgements ... 117
Appendix B ... 118
B.1 LAI ... 118
B.2 VPD ... 118
B.3 VWC ... 119
B.4 Surface DSR ... 119
5 Understanding the dynamics controlling the seasonal cycle of Congo Basin evaporation using a regional approach ... 120
Authorship declaration ... 120
Abstract ... 121
5.1 Introduction ... 122
5.1.1 Background ... 123
5.1.2 Aims ... 126
5.2 Data and methods ... 127
5.2.1 Ecoregions ... 127
5.2.2 Evaporation reference data ... 127
5.2.3 Reanalysis data ... 129

5.2.4 Methods 129
5.3 Seasonal cycles of evaporation for the rainforest and savannah 131
5.4 Seasonal cycles of the evaporation components for the savannah 133
5.5 Controls on the seasonal cycle of transpiration in the savannah 136
5.5.1 Variables for analysis 136
5.5.2 Leaf area index and vapour pressure deficit 137
5.5.3 Controls on the seasonal cycle of LAI 139
5.5.3.1 November to April 140
5.5.3.2 April to November 141
5.5.4 Controls on the seasonal cycle of VPD 142
5.6 Controls on canopy and soil evaporation in the savannah's dry season 145
5.7 Overestimation in evaporation in the rainforest in ERA5-Land and MERRA-2 149
5.8 Discussion 153
5.8.1 Controls on the seasonal cycle of evaporation in the savannah 154
5.8.2 Consistency with the Budyko framework 158
5.8.3 Improving rainforest evaporation in ERA5-Land and MERRA-2 160
5.9 Conclusions 163
Acknowledgements 164
6 Conclusions 165
6.1 Introduction 166
6.2 Research question 1 167
6.2.1 Findings 167
6.2.2 Limitations of the research approach 170
6.2.3 Implications of the findings for the field 171
6.3 Research question 2 172
6.3.1 Findings 172
6.3.2 Limitations of the research approach 174
6.3.3 Implications of the findings for the field 175
6.4 Fulfilment of thesis aim and thesis contribution to knowledge 177
6.5 Suggestions for future work 178
6.5.1 Congo Basin climate dynamics 178
6.5.2 Use of sub-grid rainfall in GCMs and reanalyses to improve evaporation .. 181
6.6 Concluding comments 185
7 References 186

Acknowledgements

There are many people I would like to thank for helping me to carry out my DPhil. I am incredibly grateful to my supervisors, Professor Richard Washington and Professor Simon Dadson, for their invaluable support throughout my research. Richard – thank you for providing such clarity of thought and never missing the big picture. Simon – thank you for excellent advice along the journey and for being such a positive mentor.

Thanks are also due to the members of the Oxford African Climate Research Group for insightful discussions over the past four and a half years. I am particularly grateful to Dr. Ellen Dyer, Dr. Neil Hart and Dr. Rachel James for providing excellent feedback at the Transfer and Confirmation steps and to Dr. Sebastian Engelstaedter for his computational support. I would also like to extend thanks to the members of the Oxford Hydrology Group for their constructive input. In particular, I am grateful to Professor Jian Peng for his scientific direction, which improved Chapter 4. I am also thankful to the reviewers and editors of Journal of Geophysical Research: Atmospheres and Climate Dynamics for their reviews on my results chapters, which helped me improve them.

I am grateful for the opportunity to have carried out internships at the Centre for Ecology and Hydrology (CEH) and the Met Office during my DPhil. Many thanks to Dr. Jon Evans and Dr. Ross Morrison at CEH, who oversaw my work on the evaporation data system for COSMOS-UK, and Dr. Emma Fiedler at the Met Office, who helped me to improve my data analysis skills. I am also grateful to Richard for the opportunity to be an observer at the Radcliffe Meteorological Station. I enjoyed being interviewed for an article on the BBC News website when I observed the wettest day in Oxford for 50 years.

I would like to formally thank the Natural Environment Research Council for funding my doctoral studentship. This funding allowed me to present my research at several national and international conferences. I am also grateful to the American Geophysical Union for providing me with a travel grant to attend the Congo Basin Chapman Conference in Washington DC in 2018. This conference was a unique opportunity to meet other scientists working on the climate and hydrology of the Congo Basin and helped to shape my research.

Many thanks are also due to my examiners, Dr. Wilfried Pokam and Dr. Neil Hart, for reviewing this thesis and conducting my viva.

Finally, I would like to give heartfelt thanks to my family and friends who have kept me going all the way through. Without you, this thesis would not have been possible.

List of tables

Table 2.1 Reference data sets 41

Table 2.2 Reanalysis data sets 45

Table 3.1 AGCMs used and details about their evaporation components..... 57

Table 3.2 Reference data sets used in this chapter..... 59

Table 3.3 AGCM rankings for 30-year mean (1979-2008) annual cycles of rainfall and evaporation in the Congo Basin (14°S to 4°N, 18°E to 29°E). CHIRPS2 rainfall (1981-2008) and LandFlux-EVAL evaporation (1989-2005) are used as reference datasets... 61

Table 3.4 Models selected for the composites analysed within this chapter 61

Table 3.5 30-year mean (1979-2008) difference in total evaporation and its components in the Congo Basin (14°S to 4°N, 18°E to 29°E) between March and November, from model composites with unrealistic and realistic evaporation. Units are mm day^{-1} 74

Table 4.1 November minus March rainfall (mm day^{-1}) and evaporation (mm day^{-1}), averaged over the Congo Basin (14°S to 4°N, 18°E to 30°E) from four reanalysis data sets and two reference data sets..... 88

Table 4.2 Further details on LandFlux-EVAL and the reanalyses evaluated in this chapter. Monthly climatologies are produced by averaging over 1989-2005 92

Table 4.3 Sixteen-year mean (1989-2005) November minus March surface energy budget averaged over the northern rainforest (2°S to 1°N, 18°E to 30°E) from ERA5-Land . 109

List of figures

Figure 1.1 a Domain used in this thesis and **b** domain used in Creese and Washington (2016). Dots on **b** indicate gauges contributing to Climate Research Unit rainfall data.. 8

Figure 1.2 Land cover map of Africa. Data are sourced from the European Space Agency Climate Change Initiative Land Cover map (2017). Domain used in this thesis is shown with a red box. Sub-domains in blue indicate the rainforest and the savannah..... 9

Figure 1.3 Long-term mean (1989-2005) seasonal cycle of rainfall (mm day^{-1}) from 5 rainfall data sets. Averaged over the basin domain (14°S to 4°N, 18°E to 30°E)..... 10

Figure 1.4 Long-term mean (1989-2005) rainfall over Africa (mm day^{-1}) from CHIRPS2 in **a** January, **b** March, **c** July, **d** November, and **e** January 11

Figure 1.5 Key features of the Tropical African rainfall regime. Source: Creese (2018). Used with permission 13

Figure 1.6 Schematic showing the features of the Congo Basin Cell. Source: Longandjo and Rouault (2020). © American Meteorological Society. Used with permission..... 16

Figure 1.7 Seasonal cycle of evaporation (mm mon^{-1}) from several evaporation products, averaged over the period 2000-2010. R15 refers to the basin's northern rainforest. R19 refers to the basin's southern savannah. Source: Trambauer et al. (2014)..... 21

Figure 1.8 Mean seasonal cycles of EVI (dimensionless), rainfall (mm mon^{-1}) and solar irradiation (kWh m^{-2}) from 2003-2013 averaged over the 0° to 5°N, 12°E to 19°E domain. Source: Philippon et al. (2016). Reprinted with permission from Elsevier..... 23

Figure 1.9 Conceptual Budyko framework defining different evaporation regimes. EF denotes the evaporative fraction, or the ratio of latent heat flux to total net radiation. Source: Seneviratne et al. (2010). Reprinted with permission from Elsevier 25

Figure 1.10 Maps of flux tower sites contributing to the FLUXNET network. **a** shows global distribution and **b** shows African distribution alone. Source: Weerasinghe et al. (2020). Map data © Google (2020) 28

Figure 1.11 Ensemble mean of the global ratio of transpiration to evaporation (dimensionless) from 108 different data sets. Source: Wei et al. (2017) 32

Figure 1.12 Global canopy interception loss derived from an analytical model. Units of mm $year^{-1}$. Source: Miralles et al. (2010) 33

Figure 3.1 Thirty-year mean (1979–2008) evaporation across the African continent (mm day^{-1}), from a composite mean of the 11 AMIP models used in this chapter. Congo Basin domain used in this chapter (14°S to 4°N, 18°E to 29°E) is shown by a red box 55

Figure 3.2 Thirty-year mean (1979–2008) annual cycles of **a** rainfall (mm day^{-1}) and **b** evaporation (mm day^{-1}) in the Congo Basin (14°S to 4°N, 18°E to 29°E), from 11 AMIP

models, and their ensemble mean. CHIRPS2 rainfall (1981–2008) and LandFlux-EVAL evaporation (1989–2005) are used as reference data sets..... 64

Figure 3.3 Thirty-year mean (1979–2008) evaporation (mm day^{-1}) for March, July, and November, from the AGCM ensemble mean, models with unrealistic evaporation, models with realistic evaporation, and LandFlux-EVAL. AGCM standard deviations are also included. Domain analysed in this chapter (14°S to 4°N, 18°E to 29°E) is shown by a red box in the first panel 65

Figure 3.4 Thirty-year mean (1979–2008) annual cycles of **a** rainfall (mm day^{-1}) and **b** evaporation (mm day^{-1}) in the Congo Basin (14°S to 4°N, 18°E to 29°E). Rainfall annual cycles are from models with unrealistic rainfall, the AGCM ensemble mean, and models with realistic rainfall. Evaporation annual cycles are from models with unrealistic evaporation, the AGCM ensemble mean, and models with realistic evaporation. CHIRPS2 rainfall and LandFlux-EVAL evaporation are used as reference data sets ... 67

Figure 3.5 Thirty-year mean (1979–2008) annual cycle of canopy evaporation (mm day^{-1}) in the Congo Basin (14°S to 4°N, 18°E to 29°E) from models with unrealistic total evaporation, the AGCM ensemble mean, and models with realistic total evaporation.. 70

Figure 3.6 Thirty-year mean (1979–2008) annual cycle of transpiration (mm day^{-1}) in the Congo Basin (14°S to 4°N, 18°E to 29°E) from models with realistic total evaporation, the AGCM ensemble mean, and models with unrealistic total evaporation 71

Figure 3.7 Thirty-year mean (1979–2008) annual cycle of soil evaporation (mm day^{-1}) in the Congo Basin (14°S to 4°N, 18°E to 29°E) from models with unrealistic total evaporation, the AGCM ensemble mean, models with realistic total evaporation, and models which contain a credible scheme for soil evaporation (refer to section 3.4.3) .. 73

Figure 4.1 Sixteen-year mean (1989-2005) seasonal cycles of **a** rainfall (mm day^{-1}) and **b** evaporation (mm day^{-1}) averaged over the Congo Basin (14°S to 4°N, 18°E to 30°E), from four reanalyses, CFSR (Saha et al. 2010), ERA5-Land (Hersbach et al. 2020), MERRA-2 (Gelaro et al. 2017) and NCEP-2 (Kanamitsu et al. 2002), and two reference data sets, CHIRPS2 rainfall (Funk et al. 2015) and LandFlux-EVAL evaporation (Mueller et al. 2013) 87

Figure 4.2 Sixteen-year mean (1989-2005) evaporation across Africa (mm day^{-1}) from the LandFlux-EVAL synthesis data set. Congo Basin domain used in this chapter (14°S to 4°N, 18°E to 30°E) is shown with a red box 90

Figure 4.3 16-year mean (1989-2005) November minus March evaporation (mm day^{-1}) difference maps from **a** LandFlux-EVAL, **b** ERA5-Land, and **c** MERRA-2. The domain used in this chapter (14°S to 4°N, 18°E to 30°E) is shown with a red box. Sub-domains are shown with blue boxes and indicate the two regions in LandFlux-EVAL where evaporation is lower in November than March: (1) the rainforest, and (2) the eastern savannah. Dots are grid points where the difference between March and November is statistically significant ($p<0.05$) 94

Figure 4.4 Sixteen-year mean (1989-2005) **a** November minus March canopy evaporation (mm day^{-1}), **b** November minus March soil evaporation (mm day^{-1}), and **c** November minus March transpiration (mm day^{-1}), difference maps from ERA5-Land. Domains are as for Figure 4.3. Dots are grid points where the difference between March and November is statistically significant ($p<0.05$) 97

Figure 4.5 Sixteen-year mean (1989-2005) **a** November minus March LAI (m^2 m^{-2}), and **b** November minus March VPD (kPa), difference maps from ERA5-Land. Domains are as for Figure 4.3, with additional sub-division into the northern rainforest, southern rainforest, north-eastern savannah and south-eastern savannah. Dots are grid points where the difference between March and November is statistically significant ($p<0.05$) 101

Figure 4.6 a Sixteen-year mean (1989-2005) November minus March VWC (%) difference map from ERA5-Land, where domains are as for Figure 4.5, and dots are grid points where the difference between March and November is statistically significant ($p<0.05$). **b-e** Sixteen-year mean (1989-2005) water budget diagrams from ERA5-Land for **b** the northern rainforest, **c** the southern rainforest, **d** the north-eastern savannah, and **e** the south-eastern savannah 105

Figure 4.7 16-year mean (1989-2005) **a** November minus March surface DSR (W m^{-2}), **b** November minus March top-of-atmosphere DSR (W m^{-2}), **c** November minus March cloud forcing (W m^{-2}), and **d** November minus March atmospheric forcing (W m^{-2}), difference maps from ERA5-Land. Domains are as for Figure 4.5. Dots are grid points where the difference between March and November is statistically significant ($p<0.05$). Figure 4.7a is equal to Figure 4.7b + Figure 4.7c + Figure 4.7d 106

Figure 4.8 Flow chart showing contrasting controls on evaporation at the two rainfall peaks in the four sub-domains around the basin. The results in each sub-domain are consistent with the Budyko framework for evaporation. The collective of these contrasting controls provides a plausible explanation for why there is lower evaporation in November than March on the basin-wide average 113

Figure 5.1 Land cover map for Africa. Data are sourced from the European Space Agency Climate Change Initiative Land Cover map (2017). The Congo Basin domain used in this chapter (14°S to 4°N, 18°E to 30°E) is shown with a red box. Sub-domains in blue indicate the two ecoregions analysed: the rainforest to the north (5°S to 4°N, 18°E to 30°E), and the savannah to the south (14°S to 5°S, 18°E to 30°E) 128

Figure 5.2 Sixteen-year mean (1989-2005) seasonal cycles of evaporation (mm day^{-1}) for **a** the basin-wide average, **b** rainforest, and **c** savannah. Data from ERA5-Land, MERRA-2 and LandFlux-EVAL 133

Figure 5.3 Sixteen-year mean (1989-2005) seasonal cycles of rainfall (mm day^{-1}) and evaporation (mm day^{-1}) for the savannah. **a** Seasonal cycles begin in January and end in January. **b** Seasonal cycles begin in November and end in November. All data from ERA5-Land..... 134

Figure 5.4 Sixteen-year mean (1989-2005) seasonal cycles of evaporation and its three components (mm day^{-1}) for the savannah. All data from ERA5-Land 135

Figure 5.5 Sixteen-year mean (1989-2005) seasonal cycles of **a** LAI (m^2 m^{-2}) and transpiration (mm day^{-1}), and **b** VPD (kPa) and transpiration (mm day^{-1}), for the savannah. All data from ERA5-Land 138

Figure 5.6 Sixteen-year mean (1989-2005) seasonal cycles of **a** soil VWC (%) and LAI (m^2 m^{-2}), **b** rainfall and (evaporation plus runoff) (mm day^{-1}), **c** surface DSR (W m^{-2}) and LAI (m^2 m^{-2}), and **d** TOA DSR, cloud forcing and atmospheric forcing (W m^{-2}), for the savannah. Shadings in panel **b** refer to soil moisture accumulation or soil moisture depletion (mm). All data from ERA5-Land 140

Figure 5.7 Sixteen-year mean (1989-2005) seasonal cycles of **a** soil VWC (%), **b** net radiation, latent heat flux and sensible heat flux (W m^{-2}), **c** near-surface air temperature (°C) and SVP (kPa), **d** specific humidity (g kg^{-1}) and AVP (kPa) and **e** SVP, AVP and VPD (kPa), for the savannah. All data from ERA5-Land 144

Figure 5.8 Sixteen-year mean (1989-2005) seasonal cycles of **a** rainfall (mm day^{-1}), and canopy evaporation (mm day^{-1}), **b** LAI (m^2 m^{-2}) and canopy evaporation (mm day^{-1}), **c** VPD (kPa) and canopy evaporation (mm day^{-1}), and **d** wind speed (m s^{-1}), and canopy evaporation (mm day^{-1}), for the savannah's dry season. All data from ERA5-Land ... 146

Figure 5.9 Sixteen-year mean (1989-2005) seasonal cycles of **a** soil VWC (%) and soil evaporation (mm day^{-1}), **b** net radiation (W m^{-2}) and soil evaporation (mm day^{-1}), and **c** LAI (m^2 m^{-2}) and soil evaporation (mm day^{-1}), for the savannah's dry season. All data from ERA5-Land 148

Figure 5.10 Sixteen-year mean (1989-2005) seasonal cycles of evaporation and its three components (mm day^{-1}) for the rainforest. **a** Data are from the ERA5-Land reanalysis. **b** Data are from the MERRA-2 reanalysis..... 150

Figure 5.11 Flow chart showing plausible dynamics controlling the seasonal cycle of evaporation between November and March during the savannah's wet season 154

Figure 5.12 Flow chart showing plausible dynamics controlling the seasonal cycle of evaporation between March and April during the savannah's dry season 155

Figure 5.13 Flow chart showing plausible dynamics controlling the seasonal cycle of evaporation between April and July during the savannah's dry season..... 156

Figure 5.14 Flow chart showing plausible dynamics controlling the seasonal cycle of evaporation between July and November during the savannah's dry season..... 157

Figure 6.1 Sixteen-year mean (1989-2005) November minus March rainfall (mm day^{-1}) difference map from CHIRPS2. The domain used in this thesis is shown with a red box (14°S to 4°N, 18°E to 30°E). Dots are grid points where the difference between March and November is statistically significant ($p<0.05$)..... 179

List of acronyms

AEJ-N	African Easterly Jet - North
AEJ-S	African Easterly Jet - South
AGCM	Atmosphere-only Global Climate Model
AMIP	Atmospheric Model Intercomparison Project
AVP	Actual Vapour Pressure
CFSR	Climate Forecast System Reanalysis
CHIRPS2	Climate Hazards Group Infrared Precipitation with Station data version 2
CH-TESSEL	Carbon-Hydrology Tiled ECMWF Scheme for Surface Exchanges Over Land (the land surface model of the ECMWF reanalysis)
CMIP3	Coupled Model Intercomparison Project Phase 3
CMIP5	Coupled Model Intercomparison Project Phase 5
CMIP6	Coupled Model Intercomparison Project Phase 6
COSMOS-UK	Cosmic-ray Soil Moisture Observing System in the UK
DfID	Department for International Development
DRC	Democratic Republic of the Congo
DSR	Downward Shortwave Radiation
ECMWF	European Centre for Medium-Range Weather Forecasts
EF	Evaporative Fraction
ERA5	Fifth generation of the ECMWF reanalysis
ERA5-Land	High-resolution version of ERA5 for land surface variables
ERA-Interim	Fourth generation of the ECMWF reanalysis
ESGF	Earth System Grid Federation

EVI	Enhanced Vegetation Index
FCFA	Future Climate for Africa
GCM	Global Climate Model
GEWEX	Global Energy and Water Exchanges
GLEAM	Global Land Evaporation Amsterdam Model
ICOS	Integrated Carbon Observing System
ILEAPS	Integrated Land Ecosystem-Atmosphere Process Study
IMPALA	Improving Model Processes for African Climate (DfID project)
LAI	Leaf Area Index
LLW	Low-Level Westerlies
LSM	Land Surface Model
MAM	March-April-May
MCS	Mesoscale Convective System
MEJ	Mid-level Easterly Jet
MERRA-2	Second generation of the Modern-Era Retrospective analysis for Research and Applications (NASA reanalysis)
MODIS	Moderate Resolution Imaging Spectroradiometer
NCEP-2	Second generation of the National Centers for Environmental Prediction reanalysis
NERC	Natural Environment Research Council
RCM	Regional Climate Model
RMSE	Root Mean Square Error
SON	September-October-November
SST	Sea Surface Temperature
SVP	Saturated Vapour Pressure

TEJ	Tropical Easterly Jet
TOA	Top-Of-Atmosphere
UK	United Kingdom
UMFULA	Uncertainty reduction in Models For Understanding deveLopment Applications (DfID project)
VPD	Vapour Pressure Deficit
VWC	Volumetric Water Content (a measure of soil moisture)

1 Introduction

1.1 Background and rationale

The climate of the Congo Basin is complex and not well understood. In particular, there is no satisfactory explanation for what shapes the seasonal cycle of basin rainfall. Nicholson (2018a) challenged the assumption that the inter-tropical convergence zone controls the seasonal cycle of rainfall and called for additional research on this cycle. Factors that could interact to shape the seasonal cycle of rainfall include the north-south migration of the rain belt (Nikulin and Hewitson 2019), teleconnections to modes of variability such as the El-Niño Southern Oscillation and the Madden-Julian Oscillation (Hart et al. 2019; Raghavendra et al. 2020), regional atmospheric circulations (Cook and Vizy 2016; Longandjo and Rouault 2020), atmospheric jets (Kuete et al. 2020; Munday et al. 2021), mesoscale convective systems (MCSs) (Taylor et al. 2018; Alber et al. 2021; Hartman 2021), and land-atmosphere coupling (Dyer et al. 2017; Sori et al. 2017).

Knowledge of the dynamics controlling the seasonal cycle of basin rainfall is required as a point of reference against which climate models can be compared. Climate models are the only tools available to understand how the future climate might evolve, but many models have problems representing rainfall in the Congo Basin. Washington et al. (2013) identified a wide spread in rainfall magnitudes across global climate models (GCMs) from the fifth phase of the Coupled Model Intercomparison Project (CMIP5) in the Congo Basin in all seasons. Given that there is such a wide spread in rainfall historically, and GCMs have not been evaluated to assess their realism, it is unclear which climate models are producing the most realistic simulation of rainfall in the basin. Models must effectively reproduce historical climate for their future projections to be trusted, but the lack of knowledge on which GCMs adequately represent basin rainfall means that it is

unclear which GCMs produce the most reliable rainfall projections (Haensler et al. 2013; Aloysius et al. 2016). The consequence of this is that climate change adaptation planners have insufficient evidence necessary to inform their decisions. This lack of evidence is problematic as the Democratic Republic of the Congo (DRC) has a low adaptive capacity (Washington et al. 2006) and changing rainfall patterns could impact subsistence agriculture, energy and water supply (Bele et al. 2015; Sonwa et al. 2017). By developing an understanding of the various factors controlling the seasonal cycle of basin rainfall, it may be possible to provide a set of dynamics controlling this cycle against which GCMs can be evaluated to ensure that they reproduce this cycle effectively.

Additionally, developing knowledge of the dynamics controlling the seasonal cycle of basin rainfall is needed before future changes in basin rainfall can be fully characterised (Howard and Washington 2019). To obtain the most comprehensive understanding of the future climate system, it is necessary to reveal how the present-day climate system operates first, and then to evaluate how the climate system in the present day will adjust through time as the planet warms (Dunning 2018).

Land-atmosphere coupling is partially responsible for the seasonal cycle of rainfall in the basin (Hohenegger 2020). This coupling is divided into two ‘legs’: the terrestrial leg that defines how land surface biophysical characteristics affect the rate of evaporation itself (Dirmeyer 2011), and the atmospheric leg that governs the flow of evaporated moisture from the surface, through the atmosphere and back to the surface as rainfall (Dirmeyer et al. 2014). A few studies have examined the atmospheric leg of the Congo Basin by researching moisture recycling, which is defined as the process by which a portion of

evaporated water from the land surface contributes to rainfall over the same region (Pokam et al. 2012; Dyer et al. 2017; Sori et al. 2017). These studies agree that evaporation from the land surface is an integral component of Congo Basin climate and a crucial moisture source for basin rainfall in all seasons. However, there are discrepancies between studies on the amount of water recycled. Dyer et al. (2017) found that approximately 25% of the rainfall in the basin is sourced from land surface evaporation, while Sori et al. (2017) found this ratio to be 50%.

Although the atmospheric leg has received some research attention, the terrestrial leg of the Congo Basin has received less, and the dynamics controlling the climatological seasonal cycle of Congo Basin evaporation are unclear. Ndehedehe et al. (2018) argued that research on the dynamics controlling the seasonal cycle of basin evaporation would provide a theoretical framework useful for advancing hydrological science in this region. Fisher et al. (2017) also argued that knowledge of evaporation and the dynamics that control the evaporation seasonal cycle would be helpful for scientific applications such as biodiversity assessment, climate and cloud formation, agricultural management, and water resource management.

Knowledge of these evaporation dynamics would also provide a baseline for evaporation against which GCMs can be evaluated. Berg and Sheffield (2019) argued that adequately representing evaporation in GCMs is crucial for generating a realistic representation of the climate. This is because evaporation is part of the water balance and is an essential component of the hydrological cycle. Errors in evaporation could lead to an inaccurate biosphere-atmosphere equilibrium, with implications for rainfall. As basin evaporation

contributes substantially to basin rainfall (Dyer et al. 2017; Sori et al. 2017), evaluating model evaporation against known evaporation dynamics could increase confidence in GCM simulations and projections of basin rainfall and allow adaptation planning to be based upon credible information.

For the above reasons, there is a strong rationale to make progress towards understanding the dynamics controlling the climatological seasonal cycle of Congo Basin evaporation, and research to do this will be carried out in this thesis. The thesis research will begin the development of the theoretical framework suggested by Ndehedehe et al. (2018) and contribute helpful knowledge for scientific applications both within basin climate research and further afield (Fisher et al. 2017).

However, there are challenges in researching these evaporation dynamics, as long-term in situ records of evaporation and its controls are currently unavailable for the basin (Alsdorf et al. 2016). Without these records, this thesis will need to undertake research using alternative contemporary data sources. As both GCMs and reanalyses produce an extensive range of variables for climate research on global scales, data from these products will be used to understand evaporation dynamics in the Congo Basin on the basin-wide average. For initial exploratory research on evaporation and its components, GCMs will be the data source of choice. However, when researching what drives these components, reanalyses will be the data source of choice as they are constrained by observations and potentially provide a more realistic representation of key drivers such as radiation and soil moisture.

As there is little agreement between contemporary reanalyses on their simulation of the hydrological cycle in the Congo Basin (Maidment et al. 2015; Hua et al. 2019), it is necessary to confirm that reanalyses effectively reproduce evaporation from reliable reference data before they can be used. In this thesis, the LandFlux-EVAL evaporation benchmark product (Mueller et al. 2013) will be used as a reliable reference point for basin evaporation. If a reanalysis product effectively reproduces evaporation from LandFlux-EVAL for credible reasons in a specific part of the basin, it will then be possible to use data from the reanalysis to understand the dynamics which control the seasonal cycle of evaporation there.

However, as the basin has a diversity of land cover types with differing densities of vegetation, it is unlikely that good agreement between a contemporary reanalysis product and LandFlux-EVAL will be achieved for the whole Congo Basin. This is because land surface models (LSMs) included in reanalyses have been shown to overestimate evaporation in areas of high leaf area index (LAI) in the past (Wang and Eltahir 2000; Wang et al. 2006), and contemporary reanalyses appear to suffer from similar problems (Martens et al. 2020). Where no agreement can be found between reanalyses and LandFlux-EVAL, then evaporation dynamics cannot be understood using them.

Therefore, as it is unlikely that there will be good agreement between reanalyses and LandFlux-EVAL in all parts of the basin, this thesis also seeks to identify possible ways to improve reanalyses to bring them into good agreement with LandFlux-EVAL for the part(s) of the basin where this is needed. Achieving this agreement could then allow data from reanalyses to be used in future work to advance understanding of the dynamics controlling the seasonal cycle of evaporation in the Congo Basin.

1.2 Aim and research questions

This thesis aims to make progress towards an understanding of the dynamics controlling the climatological seasonal cycle of Congo Basin evaporation. This will be achieved by addressing two research questions:

1. What do GCM and reanalysis data reveal about the dynamics controlling the climatological seasonal cycle of Congo Basin evaporation?

2. Where no agreement is found between reanalyses and LandFlux-EVAL evaporation, how could the reanalyses be improved to bring them into good agreement, thereby allowing evaporation dynamics to be derived from the reanalyses in future work?

The present chapter will continue by making a case for the analysis to follow. Firstly, the chapter will describe the domain studied in this thesis and provide a brief overview of the Congo Basin rainfall regime to provide the necessary background. Secondly, the chapter will review previous research on the Congo Basin evaporation regime, justify in more detail why researching the dynamics controlling the seasonal cycle of evaporation is essential, and explain in more depth the approach that will be taken to move towards an understanding of these dynamics. Thirdly, the chapter will outline current knowledge on the problems that LSMs have in simulating Congo Basin evaporation, and explain in more depth the approach that will be taken to identify how basin evaporation could be improved in contemporary reanalysis products.

1.3 Congo Basin rainfall regime

In this thesis, the domain chosen covers 14°S to 4°N, 18°E to 30°E (Figure 1.1a). These coordinates differ from those used in previous work by Creese and Washington (2016), which were 10°S to 10°N, 5°E to 35°E (Figure 1.1b).

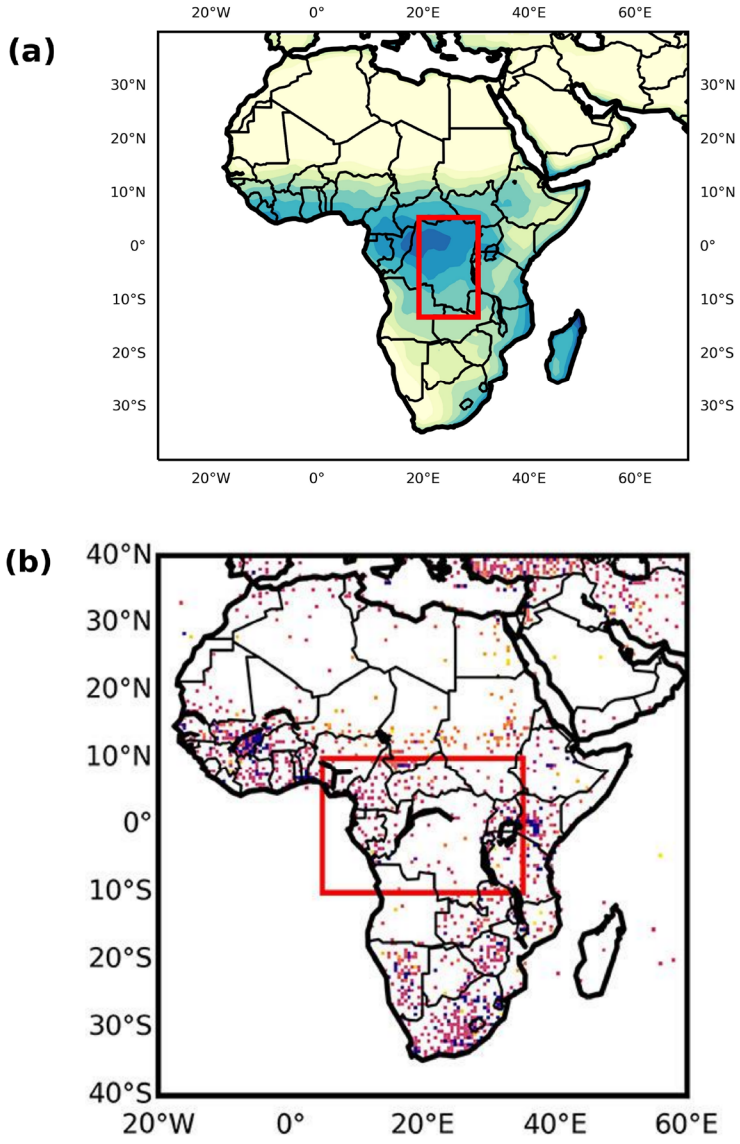


Figure 1.1 a Domain used in this thesis and **b** domain used in Creese and Washington (2016). Dots on **b** indicate gauges contributing to Climate Research Unit rainfall data

It should be noted that variations in domain coordinates will cause seasonal cycles to have different shapes. In contrast to Creese and Washington (2016), this thesis has a narrower basin domain that only covers the land surface, because the thesis focuses on land surface evaporation rather than oceanic evaporation. Additionally, the current domain was selected to cover an area of the DRC containing relatively few in situ rain gauges compared to neighbouring countries (Figure 1.1b). Therefore, the domain chosen covers a region of scientific interest that is under-observed relative to other parts of Central Africa. Finally, as shown in Figure 1.2, the current domain covers two contrasting vegetation types, the densely vegetated rainforest in the north and the less densely vegetated savannah in the south, which could help to clarify basin evaporation from a regional perspective.

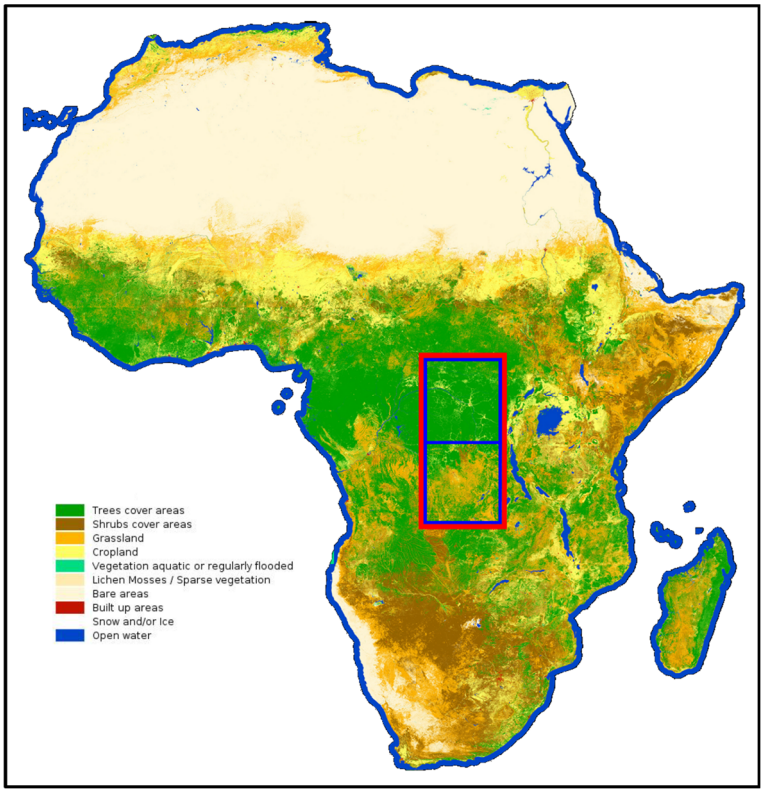


Figure 1.2 Land cover map of Africa. Data are sourced from the European Space Agency Climate Change Initiative Land Cover map (2017). Domain used in this thesis is shown with a red box. Sub-domains in blue indicate the rainforest and the savannah

Alsdorf et al. (2016) found that in December 2013, there were almost ten times more peer-reviewed publications on the climate of the Amazon Basin compared to the Congo Basin. This lack of research was concerning given the crucial role that the Congo Basin plays in regional and global climate systems. However, since this seminal study, several research groups have investigated the dynamics controlling Congo Basin rainfall, and scientific knowledge has improved.

1.3.1 Tropical rain belt

Figure 1.3 shows the long-term mean (1989-2005) seasonal cycle of rainfall averaged over the basin domain used in this thesis from four reanalyses as well as from CHIRPS2 data (Funk et al. 2015). The latter merges satellite rainfall data with station rainfall data to produce a gridded rainfall product at 0.05° x 0.05° resolution.

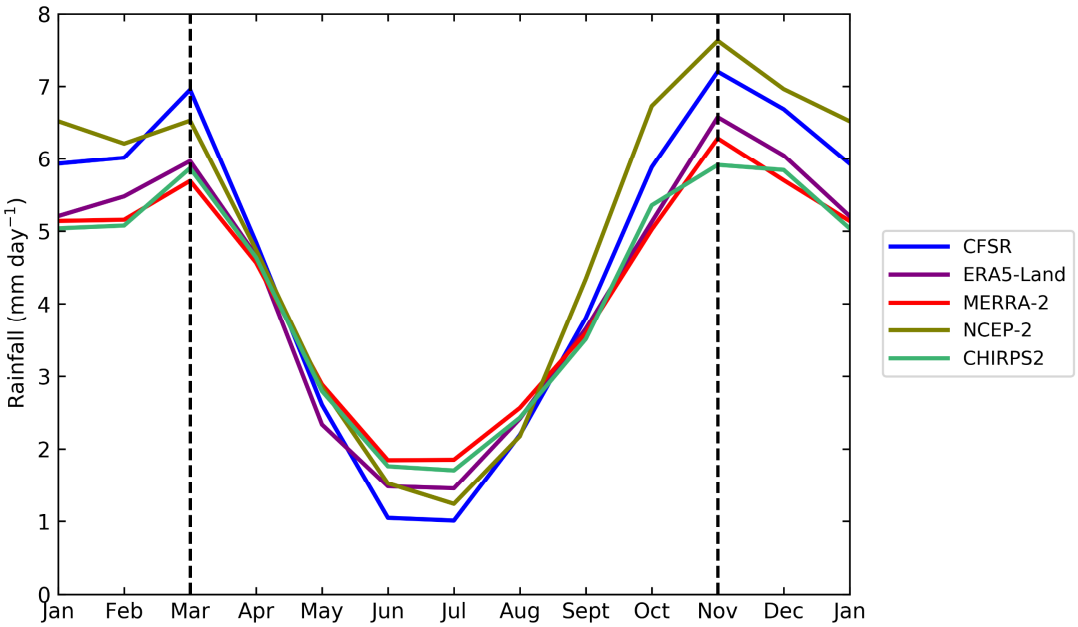


Figure 1.3 Long-term mean (1989-2005) seasonal cycle of rainfall (mm day^{-1}) from 5 rainfall data sets. Averaged over the basin domain (14°S to 4°N, 18°E to 30°E)

In every data set, basin rainfall increases from January to a peak in March, declines to a trough in July, recovers to a peak in November and then decreases slightly between November and January. All reanalyses show that rainfall is slightly higher at the November peak than the March peak, although CHIRPS2 has a similar amount of rainfall at the two peaks.

Figure 1.4 shows the spatial distribution of the seasonal cycle of rainfall from CHIRPS2 at the key turning points of January, March, July, November and January. The seasonal cycle of rainfall is characterised by the north-south migration of the tropical rain belt.

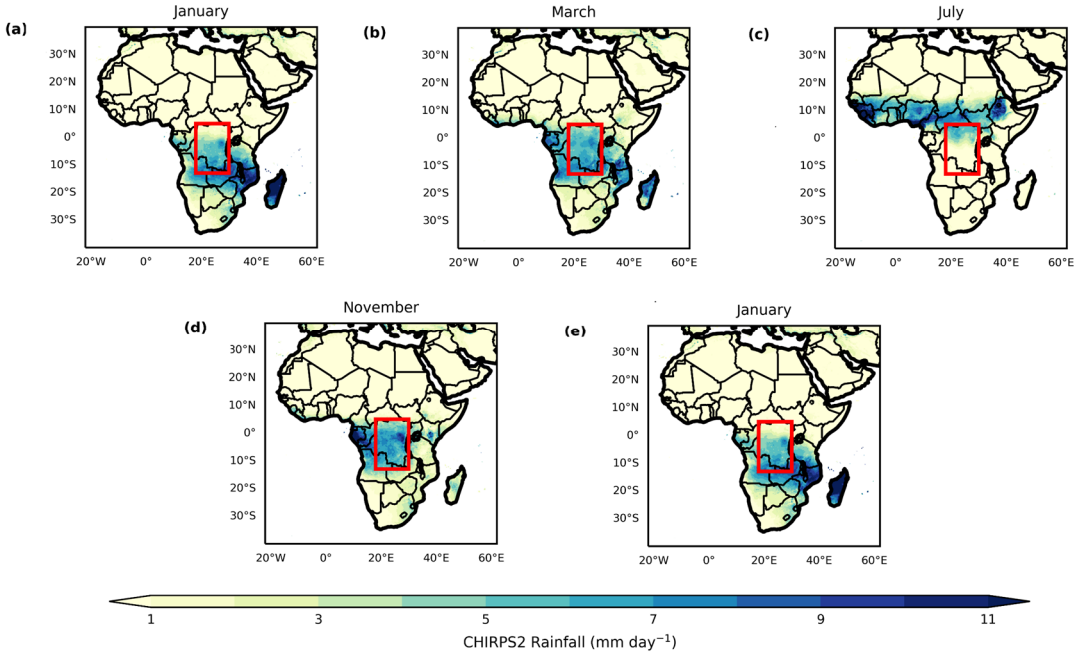


Figure 1.4 Long-term mean (1989-2005) rainfall over Africa (mm day^{-1}) from CHIRPS2 in **a** January, **b** March, **c** July, **d** November, and **e** January

In January, Figure 1.4a shows that the top third of the basin domain is relatively dry, while the middle and bottom thirds are relatively wet. Between January and March, the tropical rain belt migrates northwards. In March, Figure 1.4b shows that the rain belt covers most of the basin domain, explaining why rainfall has increased to a peak during this month. Between March and July, the rain belt continues to migrate northwards, moving mostly out of the basin. In July, Figure 1.4c shows that rainfall has declined to a trough on the domain-wide average but does not fall below 1 mm day^{-1} due to the southern edge of the rain belt still being located within the northern latitudes of the domain. The rain belt then returns southwards between July and November. In November, Figure 1.4d shows that the rain belt again covers most of the domain, explaining why rainfall returns to a peak. Finally, the rain belt moves further south between November and January. Figure 1.4e shows that in January, the top third of the domain is drier, explaining the dip in basin-wide average rainfall between November and January.

Traditionally, researchers have argued that intense solar heating in Tropical Africa causes wind convergence, uplift of moist air, deep convection and heavy rainfall in a rain belt wrapping around the equator at the inter-tropical convergence zone. However, meteorologists have challenged this argument by showing that the surface wind convergence is decoupled from the rain belt at all times of the year (Yang et al. 2015; Dezfuli 2017; Nicholson 2018a). Therefore, solar heating and surface wind convergence cannot explain why the region has high rainfall amounts, and other regional features must explain this. The schematic from Creese (2018) in Figure 1.5 summarises the critical elements of the Tropical African rainfall regime which make the region conducive to high rainfall amounts, and the section that follows describes these features.

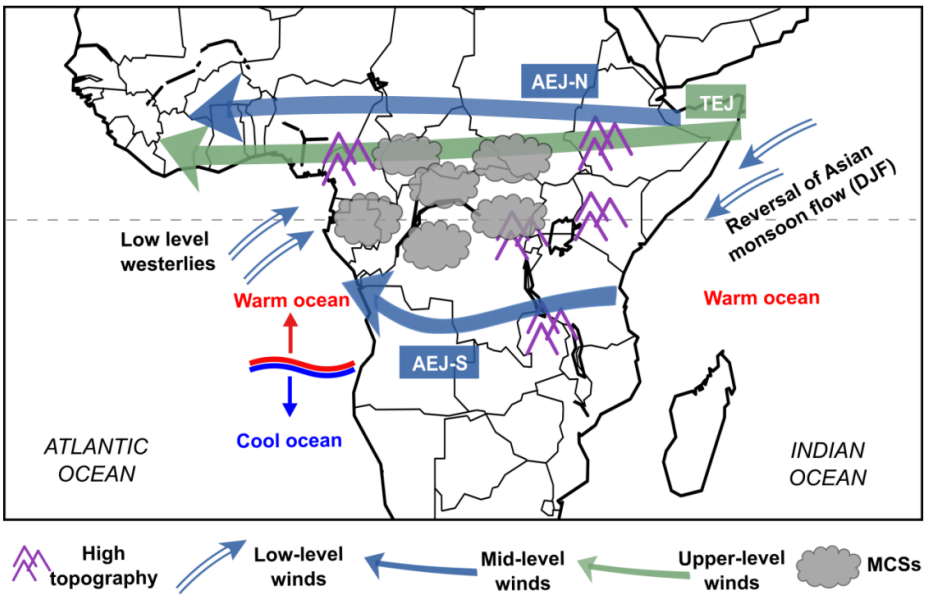


Figure 1.5 Key features of the Tropical African rainfall regime. Source: Creese (2018). Used with permission

1.3.2 Jet streams and mesoscale convective systems

Key features which play a role in the rainfall regime of the Congo Basin are the African Easterly Jet North (AEJ-N), African Easterly Jet South (AEJ-S) and Tropical Easterly Jet (TEJ). The origin of the AEJ-N is the temperature contrast between the warm Sahara and the cool Gulf of Guinea (Nicholson and Grist 2003). The atmosphere responds by generating vertical wind shear to maintain thermal wind balance, producing a strong jet with a core between 750 and 600 hPa. Several factors cause this jet to exist throughout the year, including soil moisture gradients and orography. Kuete et al. (2020) found that the origin of the AEJ-S is the thermal contrast between the hot and dry subtropical Kalahari region and the sub-humid region of the Congo Basin. This jet has a core at 600 hPa, is clearly defined between August and November, and is not present at other times

of the year. The origin of the TEJ is the temperature gradient between the Himalayan Plateau and the Indian Ocean (Dezfuli 2017). This jet is centred at approximately 200 hPa, extends across Africa and reaches maximum wind speeds of 35 ms^{-1}. Nicholson and Klotter (2021) evaluated the TEJ in a range of reanalysis data sets and discussed its driving factors and relationships with Sahelian rainfall.

The AEJ-N is believed to be important for rainfall in the Congo Basin because African easterly waves are known to propagate along it, and these waves can trigger MCS activity through dynamical instability (Wu et al 2009; Farnsworth et al. 2011). MCSs are organised ensembles of clouds that interact to form a contiguous, extensive area of rainfall on the order of 100 km or more on the horizontal scale. MCSs are commonly generated along the western slope of the Rift Valley highlands in the afternoon and propagate south-westward into the basin, producing convective rainfall across the domain (Jackson et al. 2009). MCSs are the major rain-bearing systems across much of Tropical Africa (Taylor et al. 2018). The AEJ-S is not associated with African easterly wave activities (Adebiyi and Zuidema 2016) but is still believed to be important for rainfall in the Congo Basin due to its relationship with mid-level moisture flux convergence. Kuete et al. (2020) found that when the AEJ-S is weak, there is strong zonal mid-level moisture flux convergence between 10°S and the equator, which favours high rainfall over the Congo Basin. These authors also found that when the AEJ-S is strong, there is strong zonal mid-level moisture flux divergence between these latitudes, which favours low rainfall over the Congo Basin. Mechanisms have been proposed linking the TEJ with rainfall over Equatorial Africa, which include upper-level divergence in the jet exit region (Nicholson and Dezfuli 2013; Nicholson and Klotter 2021).

1.3.3 Congo Basin cell

MCSs that develop in the Congo Basin are the primary features responsible for high rainfall in this region. However, if moisture was not supplied to the basin in the mid-levels of the atmosphere, then rainfall could not be delivered by the MCSs. Therefore, to understand the rainfall regime, there is also a need to understand the structure of the atmospheric circulation responsible for delivering moisture to the mid-levels. However, studies differ on the structure of this circulation and its seasonal variation.

Cook and Vizy (2016) argued that between June and October only, low-level westerlies (LLW) form the lower branch of a Walker-type circulation between the Atlantic Ocean and the Congo Basin. The authors suggested that LLW collect evaporated moisture as they travel, firstly from the ocean and secondly from the rainforest inland. Moist air then ascends in the centre of the basin at 20°E resulting in convective activity and intense rainfall. The air returns to the Atlantic Ocean from the Congo Basin at 300 hPa and then descends over the Gulf of Guinea, which completes the circulation.

However, Neupane (2016) provide evidence that suggests that a Walker-type overturning exists during MAM and SON. In contrast, Longandjo and Rouault (2020) argue that a large-scale overturning cell exists all year round. They found a closed, shallow zonal overturning, which they refer to as the ‘Congo Basin Cell’, embedded within a larger-scale Walker-type overturning (Figure 1.6). According to their study, surface wind convergence occurs at 30°E, where surface westerly winds carrying moisture from the Atlantic and the rainforest meet surface easterly winds bringing moisture from the Indian

Ocean. Mass convergence destabilises the atmosphere at low levels, triggering the ascent motion of warm, moist air, which leads to intense convection and rainfall generation. In contrast to previous studies, these authors argued that the Mid-level Easterly Jet (MEJ) forms at 700 hPa due to mechanical work that balances the latent heat release associated with this convection. The schematic in Figure 1.6 suggests that MCSs propagate along this jet and deliver rainfall to the basin. The air then descends over the Gulf of Guinea to complete the local circulation.

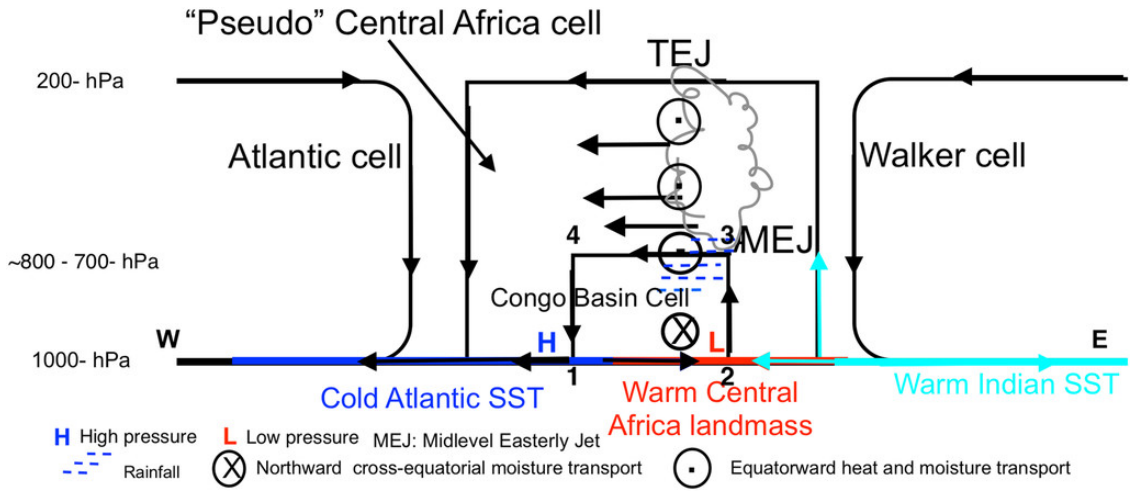


Figure 1.6 Schematic showing the features of the Congo Basin Cell. Source: Longandjo and Rouault (2020). © American Meteorological Society. Used with permission

1.3.4 Sources of moisture for Congo Basin rainfall

In addition to disagreements on the circulation, there is also a lack of agreement between studies on where the moisture for Congo Basin rainfall comes from. Evaporation from the Congo Basin itself, the Indian Ocean and the Atlantic Ocean have each been cited as crucial moisture sources, but there are variations between studies on the relative importance of each.

Estimates of the fraction of Congo Basin rainfall sourced from basin evaporation vary considerably. The percentage of rainfall derived from local evaporation is known as the recycling ratio. Trenberth (1999) found a recycling ratio of less than 20%, Dyer et al. (2017) calculated a ratio of 25% in both wet seasons, Pokam et al. (2012) found ratios of approximately 38% in both wet seasons, while Sori et al. (2017) calculated recycling ratios of over 50% across the entire seasonal cycle. These differences between studies reflect differences in the approaches used to calculate the recycling ratio. Despite the wide spread in recycling ratios, all studies agree that local evaporation does provide a substantial contribution to rainfall in the Congo Basin. Pokam et al. (2012) argued that because the basin has high recycling ratios compared to other world regions, it is essential to study land-atmosphere coupling processes operating here.

Dyer et al. (2017) identified a plausible mechanism by which locally evaporated water could reach the higher levels of the atmosphere before it is returned as rainfall. They showed that in both MAM and SON, evaporated moisture from the rainforest is collected by the LLW, transported to the eastern Congo, uplifted at 30°E, and transported westwards back into the basin in the MEJ at 700 hPa. Therefore, the path of the evaporated moisture is aligned with the low level zonal overturning circulation in Figure 1.6. Moisture arriving in the mid-levels ensures that a high moist static energy is maintained, which is necessary for generating MCSs that produce rainfall (Yang et al. 2015).

Using a water tagging scheme in the Community Earth System Model, Dyer et al. (2017) also found that advection from the Indian Ocean provides a large supply of moisture for Congo Basin rainfall in the wettest months of the year. Figure 11 from their study shows

that moisture inflows from the Indian Ocean peak in the lowest levels of the atmosphere in both MAM and SON. This is consistent with Figure 1.6, where moisture from this ocean is hypothesised to enter the Congo Basin at a near-surface level. This incoming moisture is then supplied to the Congo Basin cell, uplifted to the MEJ and transported into the Congo basin at height. In contrast, using a Lagrangian back tracking algorithm, Sori et al. (2017) found only a limited role for advection from the Indian Ocean, which is consistent with the argument of Van der Ent et al. (2010), who suggested that the high terrain in East Africa acts to block the inflow of moisture.

Other studies have indicated that advection of moisture from the Atlantic Ocean is also an important supply of moisture for Congo Basin rainfall (Balas et al. 2007). For example, Sori et al. (2017) argued that moisture from the Atlantic Ocean makes a large contribution to rainfall at all times of the year. However, Dyer et al. (2017) found that the importance of moisture from the Atlantic varies depending on the season. These authors calculated that the peak contribution from the Atlantic is in SON when LLW are strong and persist through the depth of the lower troposphere. They found that less moisture arrives from the Atlantic in MAM when LLW are weaker and shallower.

To understand the seasonal cycle of basin rainfall, it is essential to understand not just how evaporated moisture is recycled (the atmospheric leg) but also what controls the rate of evaporation to begin with (the terrestrial leg), and the latter will be discussed in the next section.

1.4 Congo Basin evaporation regime

1.4.1 Thesis definition of evaporation

In this thesis, evaporation is defined as the flux of water from the land surface into the atmosphere. Land surface evaporation is usually calculated as the sum of three components: transpiration (stomatal evaporation), canopy evaporation and soil evaporation. The word ‘evaporation’ is used in the present research to refer to this land surface process rather than ‘evapotranspiration’. As discussed by Miralles et al. (2020), there is a scientific rationale to support the use of the former term. Evapotranspiration singles out transpiration and implies that transpiration is the most crucial component. This is problematic in world regions where canopy evaporation and soil evaporation represent a high proportion of the flux. It also lessens research emphasis on canopy evaporation and soil evaporation, which are uniquely important to the evaporation process. Using the word evaporation ensures that no component is implied to be more important than any other. In this thesis, the word evaporation also ensures that the water flux is understood as the collective of its three components.

1.4.2 Review of previous research

Compared to rainfall, there is much less scientific research on Congo Basin evaporation (Alsdorf et al. 2016). Bultot and Griffiths (1972) were amongst the first authors to publish on evaporation in the Congo Basin. These authors published maps of the Congo Basin for potential evaporation, which is the evaporation that would occur if the water supply were

completely sufficient. They argued that potential evaporation does not differ significantly from one season to the next across the basin. The authors found that actual evaporation is equal to potential evaporation in the wet season but less than potential evaporation in the dry season. They also showed that the annual mean actual evaporation is approximately 1200 mm in the central Congo basin but around 800 mm in the southern Congo basin.

Matsuyama et al. (1994) used a global rainfall data set based on station data, alongside runoff data from the Congo River at Kinshasa and vapour flux convergence data from a reanalysis product, to derive estimates of the climatological seasonal cycle of evaporation in the basin as a residual of the water budget. The authors concluded that evaporation is in phase with rainfall in the rainforest to the north, but that the seasonal change in evaporation for the whole basin mainly reflects the character of the savannah to the south. Nicholson et al. (1997) used a climatonomy model to estimate the seasonal cycle of evaporation for a range of locations across Africa, including in the town of Bambesa in the northern Congo Basin. They found that evaporation increases from January to October and then decreases between October and December.

Shem (2006) produced a long-term mean seasonal cycle of evaporation for the whole basin from the Community Climate System Model. Their cycle showed that basin-wide average evaporation peaks in March, falls to a trough in July, recovers to a plateau in November and then returns to its peak in March. More recently, Trambauer et al. (2014) calculated evaporation from a range of climate and hydrological data products for the rainforest and the savannah.

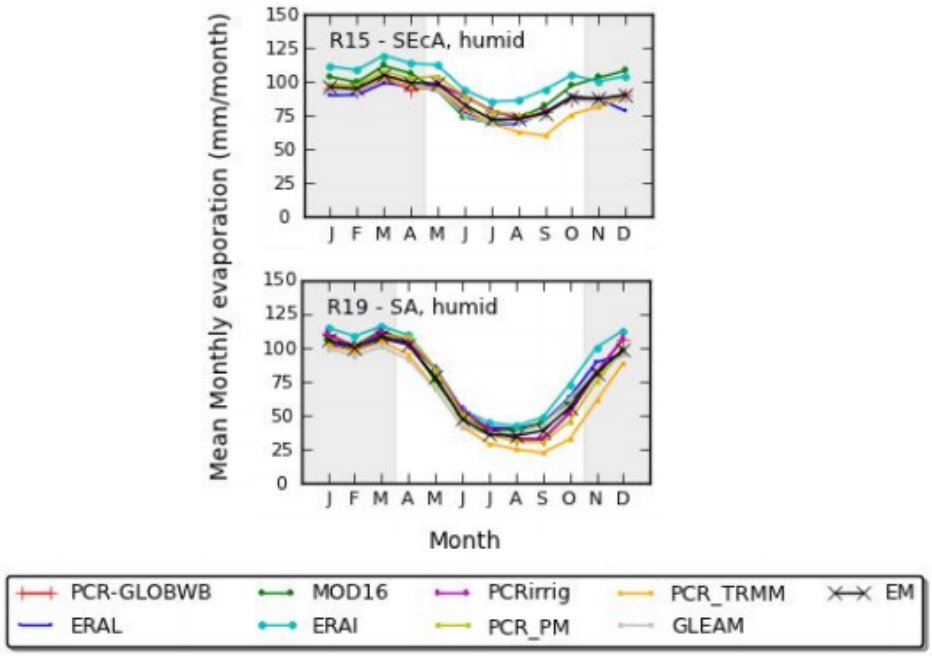


Figure 1.7 Seasonal cycle of evaporation (mm mon^{-1}) from several evaporation products, averaged over the period 2000-2010. R15 refers to the basin's northern rainforest. R19 refers to the basin's southern savannah. Source: Trambauer et al. (2014)

In the rainforest (top panel, Figure 1.7), all products show that evaporation is relatively high from January to April, falls slightly from April to July, and then recovers slowly between July and December. For the savannah (bottom panel, Figure 1.7), all products show that evaporation is relatively high between January and April, decreases between April and August, and then recovers between August and December. Trambauer et al. (2014) noted that their study did not validate the remotely sensed evaporation data against reliable reference products, which implies that their seasonal cycles should be treated with a degree of caution. However, the authors did recommend that the remotely sensed evaporation data should be validated against the LandFlux-EVAL evaporation benchmark product developed by Mueller et al. (2013).

Although climatological seasonal cycles of evaporation within the Congo Basin have been presented in previous studies, the dynamics controlling these proposed shapes are not well understood. However, research has been undertaken to examine the dynamics controlling the seasonal cycle of enhanced vegetation index (EVI) in a small region to the north-west of the basin, outside of the domain studied in this thesis (Gond et al. 2013; Philippon et al. 2016). EVI is a proxy for photosynthetic activity and forest greenness and is therefore closely related to evaporation. This research provides valuable insights on vegetation functioning at a location relatively close to the current thesis domain.

Gond et al. (2013) argued that forest greenness is strongly correlated with rainfall, and to a lesser extent light availability, in this region. The authors suggested that the relative importance of rainfall in shaping forest greenness may be greater in Tropical Africa than in Tropical Amazonia. Philippon et al. (2016) also argued that rainfall in this region shapes the seasonal cycle of forest greenness, but suggested that light availability has an important role as well. These authors analysed seasonal cycles of EVI, rainfall and solar irradiation from remotely sensed data (Figure 1.8) and made hypotheses on what controls the seasonal cycle of EVI.

Their results showed that March-April has the highest EVI level because it has optimal conditions of high rainfall and high solar irradiation. As boreal summer develops, Figure 1.8 shows that EVI decreases. Although rainfall declines, the authors suggested that soil water availability is not a limiting factor, and a pronounced drop in solar irradiation could therefore explain why EVI decreases. Their results also showed that EVI partially recovers by September-October. This recovery could be due to an increase in solar

irradiation at a time of high soil water availability. However, EVI does not fully recover to the level observed in March-April, even though rainfall rises to a peak in September-October which is higher than the rainfall peak in March-April. The authors suggested that lower solar irradiation in September-October could explain why EVI is lower at the second rainfall peak than the first. As boreal winter begins, Figure 1.8 shows that EVI decreases. The authors argued that because solar irradiation is stable, the decrease in EVI is likely to be caused by decreasing rainfall and soil water availability. Finally, at the end of boreal winter, Figure 1.8 shows that EVI increases. As solar irradiation is stable, the authors suggested that the increase in rainfall and soil water availability could explain why EVI recovers.

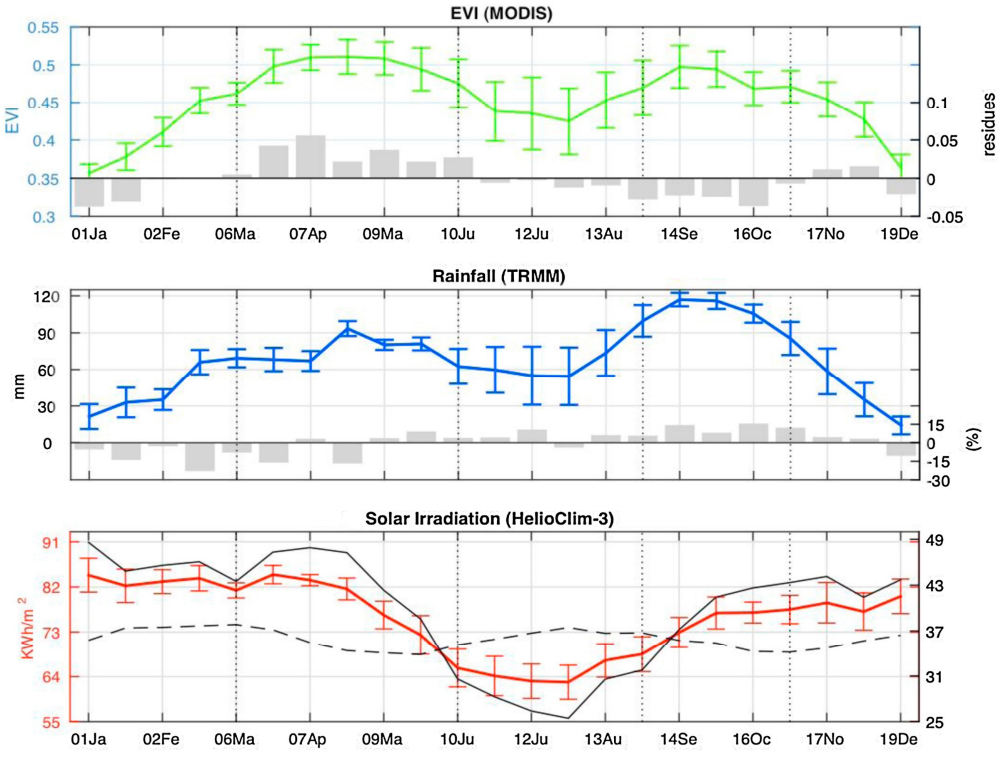


Figure 1.8 Mean seasonal cycles of EVI (dimensionless), rainfall (mm mon^{-1}) and solar irradiation (kWh m^{-2}) from 2003-2013 averaged over the 0° to 5°N, 12°E to 19°E domain. Source: Philippon et al. (2016). Reprinted with permission from Elsevier

Philippon et al. (2016) developed an understanding of the dynamics controlling the seasonal cycle of forest greenness in their region of study. However, for the present thesis domain, the dynamics that control the seasonal cycle of forest greenness and the seasonal cycle of evaporation are poorly understood. Ndehedehe et al. (2018) suggested that in densely vegetated regions of Sub-Saharan Africa with high amplitudes of rainfall and soil moisture, evaporation may be constrained by temperature. In semi-arid areas characterised by grasslands and shrubs, these authors also suggested that evaporation would be a function of soil moisture, which is determined by rainfall. Nevertheless, it remains unclear how the seasonal cycle of evaporation in the thesis domain is partitioned into its three components, and what the dynamics are that control each of the components.

1.4.3 Relevance of the seasonal cycle of evaporation

Ndehedehe et al. (2018) argued that there is a need to study the seasonal distribution of evaporation in Sub-Saharan Africa to provide a theoretical framework that could be used to advance hydrological science. An important challenge in hydrology is understanding the factors that control the surface water and energy budgets, in particular the partitioning of rainfall into evaporation and runoff, and the partitioning of net radiation into latent heat flux and sensible heat flux (Williams et al. 2012). Evaporation is the keystone variable that links the water and energy budgets and plays a central role in the hydrological cycle (Jung et al. 2010; Wang and Dickinson 2012). Without an understanding of the seasonal variation of evaporation (the terrestrial leg), it is impossible to achieve a complete understanding of how the climate system of the Congo Basin works. This is because the biosphere-atmosphere equilibrium and its seasonal variation are critical for driving basin climate patterns.

Hydrologists have derived a conceptual framework, known as the Budyko framework (Budyko 1961; Seneviratne et al. 2010), which defines the terrestrial leg of the land-atmosphere coupling (Figure 1.9). This framework states that in wet evaporation regimes, where soil moisture lies above a critical value, evaporation varies in response to changes in surface solar radiation alone. In dry evaporation regimes, where soil moisture lies below a wilting point, evaporation does not occur as water availability is too low. However, in transition evaporation regimes, where soil moisture lies between the wilting point and the critical value, evaporation varies in response to changes in soil moisture alone. Several other controls may also affect evaporation, but the Budyko framework provides a good representation of the terrestrial leg to first order (Seneviratne et al. 2010).

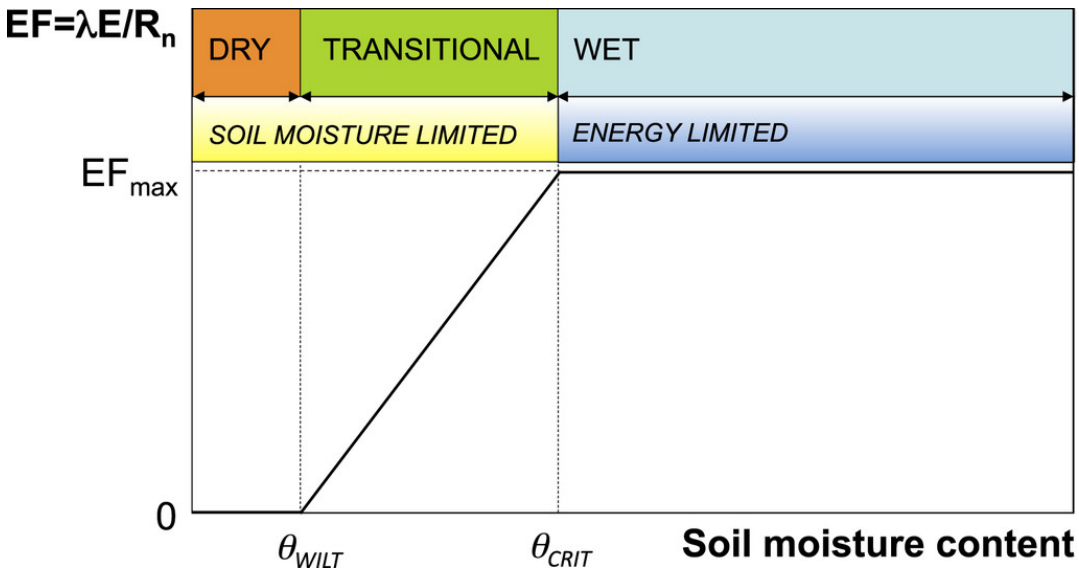


Figure 1.9 Conceptual Budyko framework defining different evaporation regimes. EF denotes the evaporative fraction, or the ratio of latent heat flux to total net radiation. Source: Seneviratne et al. (2010). Reprinted with permission from Elsevier

As knowledge of the terrestrial leg is essential for understanding the climate of the Congo Basin in its entirety, researching the dynamics controlling the seasonal cycle of evaporation in this thesis in the context of the Budyko framework could improve knowledge on how the basin's climate functions. This information could then inform future studies on the climate of the Congo Basin and its links with other regions.

Fisher et al. (2017) argued that developing knowledge on evaporation and its controls is also of importance beyond climate research in sectors including agriculture, water management and ecosystem management. It could be possible to apply information on evaporation and its dynamics to anticipate droughts and minimise water loss through enhanced irrigation scheduling. This could improve agricultural practices in a basin where a large percentage of the population relies on subsistence agriculture (Sonwa et al. 2017).

Knowledge of evaporation and its dynamics is also necessary to evaluate the credibility of GCMs. These models produce projections of changes in many climate variables, including evaporation and its components (Berg and Sheffield 2019). However, GCMs differ in their representation of core hydrological variables in the Congo Basin (Siam et al. 2013; Washington et al. 2013) and have not been evaluated to assess whether they effectively reproduce the dynamics controlling the seasonal cycle of basin evaporation. Therefore, it is unclear which GCMs are producing a realistic simulation of evaporation within the basin, and unclear which models to analyse for projections. Fisher et al. (2017) argued that there is a need to understand how the seasonal cycle of evaporation will change in future because its changes can affect soil water availability for agriculture. These changes can occur both directly, given that evaporation extracts water from the soil, and indirectly, as evaporation affects rainfall, which then feeds back to the soil.

Developing knowledge of the dynamics controlling the seasonal cycle of Congo Basin evaporation will provide a baseline against which GCMs can be evaluated to establish which GCMs effectively reproduce the seasonal cycle of basin evaporation. As basin evaporation contributes to basin rainfall (Dyer et al. 2017; Sori et al. 2017), evaluating GCM evaporation against known evaporation dynamics could allow for confidence to be achieved in GCM simulations and projections of basin rainfall. The main factors contributing to basin rainfall, including evaporation, need to be evaluated for realism in models before confidence in rainfall simulations and projections can be achieved.

1.4.4 Revealing basin evaporation dynamics

The absence of long-term in situ records of evaporation and its controls is one reason why evaporation in the Congo Basin is not well understood compared to other world regions. Figure 1.10a shows the global distribution of eddy covariance flux tower sites contributing to the FLUXNET network in 2015, and Figure 1.10b shows the distribution of these sites for Africa alone. Data from these towers can be used to advance scientific understanding of the evaporation process.

More economically developed countries tend to have a greater number of flux towers, while less economically developed countries tend to have fewer. There are only a small number of flux towers located in Africa, and before October 2020, no flux towers were installed in the Congo Basin (ICOS 2020).

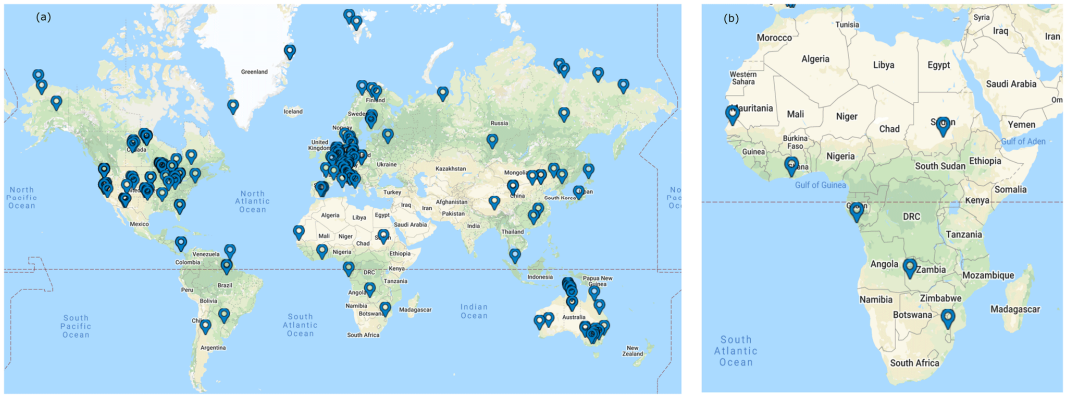


Figure 1.10 Maps of flux tower sites contributing to the FLUXNET network. **a** shows the global distribution and **b** shows the African distribution alone. Source: Weerasinghe et al. (2020). Map data © Google (2020)

An observational network of flux towers was deployed across the Amazon Basin in the 1990s as part of the Large Scale Biosphere-Atmosphere Experiment (Keller et al. 2004). Gas analysers and sonic anemometers installed on each flux tower allow for evaporation fluxes to be computed from the covariance of water vapour content and vertical wind. A wide range of parameters, including net radiation, air temperature and soil water content, are also measured at each tower (Hutyra et al. 2007). These measurements can explain why the seasonal cycle of evaporation in the Amazon Basin has received more research attention than the seasonal cycle of evaporation in the Congo Basin, and have enabled scientific questions on hydrology in the Amazon Basin to be answered (Werth and Avissar 2004; Hasler and Avissar 2007; Maeda et al. 2017; Baker et al. 2021). For example, measurements have been used to determine climatological controls on evaporation in the Amazon Basin's dry season and have shown that evaporation is controlled by net radiation in this season (Restrepo-Coupe et al. 2013). When net radiation increases as the dry season develops, leaf flushing occurs, which increases evaporation even when rainfall decreases (Hasler and Avissar 2007; Myneni et al. 2007).

Another example of a flux tower network providing useful scientific information is the Cosmic-ray Soil Moisture Observing System in the United Kingdom (COSMOS-UK), which was recently installed by the United Kingdom (UK) Centre for Ecology and Hydrology. This network delivers near real-time data on energy and water fluxes, soil volumetric water content (VWC), net radiation, and a wide range of other variables from 50 sites around the UK (Evans et al. 2016; Cooper et al. 2021). The author of this thesis led the development of an evaporation data system for COSMOS-UK that derives evaporation in near-real-time for each station as a residual of the surface energy balance (Crowhurst et al. 2019). This initiative has the potential to transform understanding of evaporation in the UK and enable scientific discoveries through analysis of near real-time in situ observations.

In contrast, in situ observations of the natural environment are scarce in the Congo Basin, and this is possibly due to the high level of political instability, which has hindered the progress of scientific research. The scarcity of in situ hydrological data is an important reason why hydrological research on the Congo Basin has not progressed at the same rate as hydrological research in the Amazon Basin and Europe (Alsdorf et al. 2016).

In October 2020, the first flux tower in the Congo Basin rainforest was installed at the Yangambi Reserve (ICOS 2020). This tower is now delivering data on biosphere-atmosphere greenhouse gas exchange using eddy covariance techniques. Additionally, radiation, meteorological and soil sensors installed at the site are providing a full energy and water balance for the rainforest (Congoflux 2020). The continuous in situ data now provide a promising route for understanding interactions between the land surface and the

atmosphere diurnally. However, the flux tower will need to remain in operation for many years before information on the climatological seasonal cycle of evaporation can be obtained. Also, as the Congo Basin has heterogeneous vegetation, further flux towers will need to be installed across the basin to examine how the climatological seasonal cycle of evaporation varies regionally from observed data.

As long-term in situ records of evaporation and its controls are unavailable for the Congo Basin, this thesis will need to research the dynamics controlling the climatological seasonal cycle of evaporation in the basin using alternative contemporary data sources. GCMs will be used for initial exploratory research on evaporation and its components, and reanalyses will be used to research what drives these components for the reason set out in Section 1.1. However, as there is a wide spread in GCM and reanalysis output for hydrological variables in the Congo Basin (Washington et al. 2013; Hua et al. 2019), it is necessary to validate GCMs and reanalyses before they are used to confirm that they provide a trustworthy source of data. GCM and reanalysis data for evaporation will therefore be compared against the LandFlux-EVAL evaporation benchmark product (Mueller et al. 2013). A justification for using LandFlux-EVAL for the basin will be provided in Chapter 2. Data from GCMs and reanalyses that perform well against LandFlux-EVAL for credible reasons will then be used to improve understanding of the dynamics controlling the climatological seasonal cycle of Congo Basin evaporation, thereby answering Research Question 1.

In order to reveal information from the reanalysis data on these dynamics, the following approach will be used. The dynamics controlling each component of evaporation will be determined by comparing each component to hydroclimatic variables. Plausible dynamics

controlling the evaporation will then be defined as the collective of the dynamics controlling the individual components. Finally, these dynamics will be assessed against the Budyko framework, and confidence will be achieved if changes in soil moisture or solar radiation appear to cause evaporation to change in the reanalysis in accordance with this framework. However, if evaporation and its components are affected by variables other than soil moisture and solar radiation, then to achieve confidence in the derived dynamics, they will be assessed for realism against evidence from the literature.

1.5 Congo Basin evaporation in land surface models

As there is a lack of agreement between contemporary reanalyses on their simulation of hydrological variables in the basin (Maidment et al. 2015; Hua et al. 2019), it is necessary to validate reanalyses against evaporation reference data before they can be used to improve understanding of the dynamics controlling the seasonal cycle of basin evaporation. However, as the basin has a wide diversity of land cover types, it may not be possible to achieve good agreement between evaporation from contemporary reanalyses and from LandFlux-EVAL for the whole Congo Basin. This is because LSMs included in reanalyses have been shown to overestimate evaporation in areas of high LAI in the past (Wang and Eltahir 2000; Wang et al. 2006).

As high LAI typically occurs in areas of high-intensity convective rainfall, errors in convective parameterisations in atmospheric models could generate too much input rainfall, thereby contributing to the overestimation in evaporation (Pathak et al. 2019; James et al. 2020). Additionally, errors in older version LSMs have been shown to

contribute to overestimates in evaporation because these models tend to generate too much evaporation per unit of rainfall (Pitman 1991). It is feasible that biases of this kind could remain in the LSMs of contemporary reanalyses, which would preclude agreement with LandFlux-EVAL. Where there is a lack of agreement, then evaporation dynamics cannot be understood using reanalyses.

1.5.1 Errors in the partitioning of evaporation into its components

Many LSMs overestimate evaporation in the Congo Basin because they produce too little transpiration and too much canopy evaporation. Wei et al. (2017) reviewed estimates of the ratio of transpiration to evaporation on a global scale from multiple sources, including satellite data, reanalyses, and isotopic measurements. They found a mean estimate for the Congo Basin of 0.6-0.7 (Figure 1.11). However, using CMIP5 models, Berg and Sheffield (2019) found a multimodel mean ratio of 0.4-0.5, thereby showing that the LSMs in most CMIP5 models underestimate transpiration in the basin compared to the estimates of Wei et al. (2017).

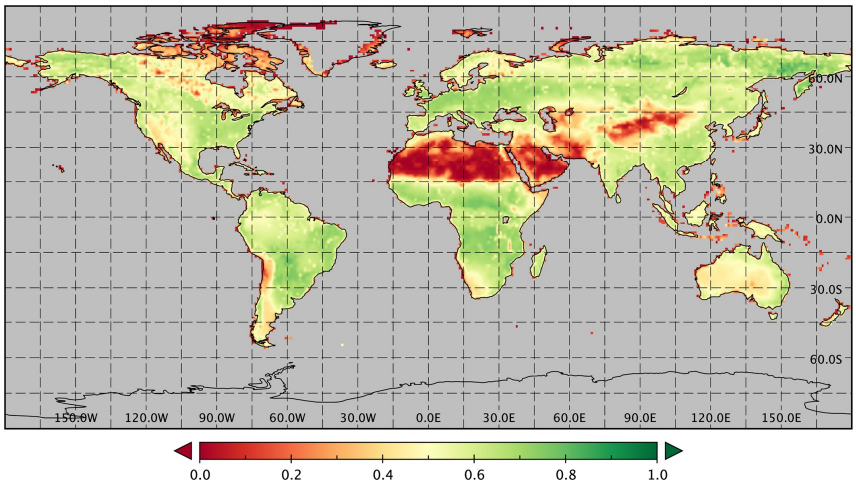


Figure 1.11 Ensemble mean of the global ratio of transpiration to evaporation (dimensionless) from 108 different data sets. Source: Wei et al. (2017)

Similarly, Miralles et al. (2010) provided global-scale estimates of the percentage of canopy interception loss. This is the amount of rainfall intercepted by the plant canopy and returned to the atmosphere through canopy evaporation. Their estimates were obtained by driving an analytical model with observations. The data revealed an interception loss of between 200-250 mm $year^{-1}$ (0.5-0.6 mm day^{-1}) for the Congo Basin (Figure 1.12). However, Berg and Sheffield (2019) found a multimodel mean interception loss of approximately 1.0 mm day^{-1} in the CMIP5 models. Therefore, the authors showed that the LSMs in most CMIP5 models overestimate canopy interception loss in the basin compared to the estimates from Miralles et al. (2010). These LSMs therefore evaporate too much water from the canopy into the atmosphere.

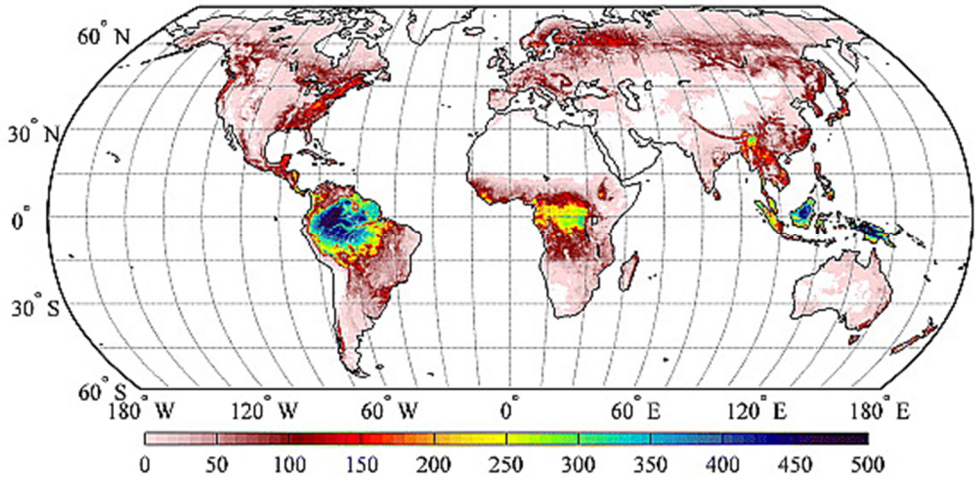


Figure 1.12 Global canopy interception loss derived from an analytical model. Units of mm $year^{-1}$. Source: Miralles et al. (2010)

An erroneous partitioning of evaporation into transpiration and canopy evaporation causes overestimates in evaporation because the resistances which act on these two components are different. The following equations are commonly used in LSMs to calculate transpiration (E_t) and canopy evaporation (E_c). Further details on the terms of these equations are included in Chapter 3.

$$E_{\mathrm{t}} = F_{\mathrm{dry}}\,\rho\,\frac{qsat(T_{\mathrm{s}})-q_{\mathrm{a}}}{r_{\mathrm{a}}+r_{\mathrm{c}}} \quad (1.1)$$

$$E_{\mathrm{c}} = F_{\mathrm{wet}}\,\rho\,\frac{qsat(T_{\mathrm{s}})-q_{\mathrm{a}}}{r_{\mathrm{a}}} \quad (1.2)$$

Equation 1.1 shows that the rate of transpiration is influenced by both aerodynamic resistance (r_a) and a canopy resistance associated with stomatal closure (r_c). In contrast, equation 1.2 shows that the rate of canopy evaporation is influenced by aerodynamic resistance only. Therefore, transpiration is a slower process than canopy evaporation, because it is affected by two resistance terms, while canopy evaporation is only affected by one. As the two evaporation processes operate at different speeds, an LSM which produces an unrealistically low fraction of transpiration and an unrealistically high fraction of canopy evaporation will overestimate the total evaporation. Previous studies have analysed the causes of this erroneous partitioning globally, but it remains unclear why contemporary LSMs produce too little transpiration and too much canopy evaporation in the Congo Basin.

Some studies have discussed potential reasons why LSMs underestimate transpiration. As LAI is the primary driver of transpiration (Lian et al. 2018), an assumption could be that underestimates in LAI are responsible for underestimates in transpiration. However, evaluations of vegetation density have found that LSMs typically overestimate LAI (Anav et al. 2013; Mahowald et al. 2016), which implies that biases in LAI are unlikely to be responsible for underestimates in transpiration. Lian et al. (2018) confirmed this by running a machine learning model using model-driven LAI in a control run and observed LAI in an experimental run. They found that correcting the LAI to match observations

did not correct the transpiration. Therefore, they suggested that underestimates in transpiration must be due to biases in other processes that affect the evaporation partitioning, rather than biases in the magnitude of the vegetation density.

Fatichi and Pappas (2017) argued that a possible reason for the underestimates in transpiration in LSMs could be an erroneous parameterisation of the hydraulic conductivity of the topsoil layer. This parameterisation might not permit enough rainfall through the soil pores to reach plant roots for transpiration. Studies have also suggested that many LSMs misrepresent lateral water flow within the soil, meaning that incoming rainfall is not redistributed correctly beneath the ground (Maxwell and Condon 2016; Chang et al. 2018). This could restrict water availability for plant growth in some areas and contributes to underestimates in transpiration. Neglect of diffuse radiation could also contribute to the underestimates in transpiration by reducing the light availability for plant growth (Mercado et al. 2009).

Overestimates in canopy evaporation have also been cited as an important reason why transpiration is underestimated in LSMs. Lawrence et al. (2007) argued that a high canopy evaporation rate means that much of the atmospheric demand for evaporation is satisfied by canopy evaporation, which suppresses transpiration. This poses the question as to why there is too much canopy evaporation.

Overestimates in the rainfall supplied to the LSM could generate overestimates in canopy water storage and therefore the rate of canopy evaporation. However, LSMs themselves may have weaknesses which also contribute to the overestimates in canopy evaporation.

An important error could be the absence of sub-grid rainfall parameterisations in contemporary LSMs. Grid boxes in atmospheric models typically have spatial resolutions of approximately 1° x 1°, which means that atmospheric models cannot represent convective rain cells occurring on fine spatial scales. Atmospheric models at coarse resolutions produce rainfall uniformly over the entire grid box area in the form of drizzle, which means that rainfall intensity on the grid-box average is underestimated. Many LSMs do not correct this error in the input rainfall. As a result, canopy throughfall is too low, canopy interception is too high, too much water is stored on the canopy, and too much water is evaporated from the canopy. Therefore, the atmospheric demand for evaporation is satisfied by high canopy evaporation, resulting in low transpiration. As canopy evaporation is a faster process than transpiration, evaporation is overestimated.

Wang and Eltahir (2000) showed in West Africa that this error in the evaporation partitioning extends into the atmosphere. The easily accessible water on the canopy favours a more humid environment, while the increased wetness of the canopy reduces leaf temperature, which reduces sensible heat flux and cools the atmosphere. This causes too many low-level clouds, which alter solar radiation, impacting the atmospheric circulation and the distribution of rainfall. Therefore, errors in the evaporation partitioning change the biosphere-atmosphere equilibrium and cause errors in rainfall amount. Pitman (1991) argued that errors generated by failing to represent rainfall intensity on sub-grid scales have serious implications for the use of GCMs in studying interactions between the land surface and the atmosphere. Wang et al. (2006) suggested that biases in evaporation associated with the lack of sub-grid rainfall could be highest in areas of high LAI such as the Central African and Amazon rainforests and lower in regions of low LAI such as Europe.

1.5.2 Identifying how to improve reanalysis evaporation

As previously discussed, the LSMs included in older version LSMs have been shown to overestimate evaporation in areas of high LAI. Although contemporary reanalyses now include improved convective parameterisations (Hersbach et al. 2020) or use corrected precipitation (Reichle et al. 2017) in their atmospheric models, it is plausible that substantial errors in the LSMs themselves could remain in contemporary reanalyses (Fisher and Koven 2020). This indicates that it may not be possible to achieve a good agreement between contemporary reanalysis products and LandFlux-EVAL evaporation for the whole basin. Therefore, this thesis also seeks to identify possible ways to bring reanalyses into good agreement with LandFlux-EVAL, for the part(s) of the basin where this is needed. The focus will be on identifying how to improve the LSMs in the reanalyses. Some studies have discussed how this could be achieved.

Aloysius et al. (2016) argued that some models will perform better than others in the basin because they contain more realistic parameterisations. The authors suggested that detailed investigations of how model algorithms represent physical processes are necessary to highlight the strengths that some models have in simulating hydrological variables. Some LSMs may contain parameterisations that credibly alter the partitioning of evaporation to bring evaporation into good agreement with reference data. Fisher and Koven (2020) argued that there is a need to identify why some LSMs produce evaporation realistically. This information could then be used by developers whose LSMs do not produce evaporation realistically, to upgrade their LSMs and improve the realism of their evaporation output.

Therefore, to identify possible ways to improve reanalyses and answer Research Question 2, the approach this thesis will take is to document the parameterisations that are used to produce evaporation in contemporary LSMs included in a wide range of CMIP5 GCMs. The research will then identify the parameterisations which are present in GCMs that perform well for evaporation in the basin, but absent in GCMs that perform less well for evaporation in the basin. Although both GCMs and reanalyses contain LSMs, the decision to use GCMs for this exercise is due to the greater number of GCMs with available data.

This approach aims to identify information connected with good LSM performance that could guide developers whose GCMs and reanalyses do not perform well for evaporation. Where evaporation dynamics cannot be discovered from reanalyses due to there being no agreement with LandFlux-EVAL, improving reanalysis LSMs could resolve this lack of agreement and allow data from the reanalyses to be used to advance understanding of the dynamics controlling the seasonal cycle of Congo Basin evaporation in future work.

1.6 Thesis format

The results chapters of this thesis take the form of academic papers. The minimum requirement for a DPhil thesis is that three papers are submitted to peer-reviewed journals. This thesis includes three papers, two of which have been published and one of which has been submitted. Statements of authorship are included at the start of each paper.

Published

Crowhurst DM, Dadson SJ, Washington R (2020) Evaluation of Evaporation Climatology for the Congo Basin Wet Seasons in 11 Global Climate Models. J Geophys Res Atmos 125:e2019JD030619. https://doi.org/10.1029/2019JD030619

Crowhurst D, Dadson S, Peng J, Washington R (2021) Contrasting controls on Congo Basin evaporation at the two rainfall peaks. Clim Dyn 56:1609-1624. https://doi.org/10.1007/s00382-020-05547-1

Submitted

Crowhurst D, Dadson S, Washington R (2021) Understanding the dynamics controlling the seasonal cycle of Congo Basin evaporation using a regional approach. Clim Dyn.

2 Data and methods

2.1 Introduction

This thesis uses two reference data sets, eleven CMIP5 model data sets and four reanalysis data sets. Section 2.2 provides a brief overview of the data sets used and justifies their inclusion in the thesis. Section 2.3 details the key methods used to analyse the data.

2.2 Data

2.2.1 Reference data sets

Table 2.1 summarises the reference data sets used within this thesis. These are CHIRPS2 for rainfall (Funk et al. 2015) and LandFlux-EVAL for evaporation (Mueller et al. 2013).

Table 2.1 Reference data sets

Data Set	Type	Spatial Resolution	Temporal Resolution	Period Available
CHIRPS2 Rainfall	Satellite/gauge	0.05° x 0.05°	Monthly	1981-present
LandFlux-EVAL Evaporation	Synthesis product	1° x 1°	Monthly	1989-2005

The thesis uses CHIRPS2 as a credible point of reference for Congo Basin rainfall for two reasons. Firstly, CHIRPS2 performed well over the basin in a recent validation exercise carried out by Nicholson et al. (2019). These authors compared satellite rainfall estimates over central Equatorial Africa to the NIC131-Gridded rainfall data set, which was derived using a spatial reconstruction method applied to gauge data (Nicholson et al. 2018b). The main finding of their validation exercise was that several rainfall products show excellent agreement with NIC131-Gridded, including CHIRPS2. The authors also argued that CHIRPS2 stands out as probably the best monthly satellite product to use in the central Congo Basin. Secondly, CHIRPS2 has a high spatial resolution of 0.05° x 0.05°, which enables this dataset to accurately quantify rainfall delivered to the Congo by MCSs. These reasons provide a strong justification for using CHIRPS2 to study Congo Basin rainfall in this thesis.

The thesis uses LandFlux-EVAL as a credible point of reference for Congo Basin evaporation for three reasons. Firstly, LandFlux-EVAL is a global benchmark synthesis product that merges information from a range of LSMs, satellite products and reanalyses. Therefore, LandFlux-EVAL averages over inter-product variations to produce a best guess estimate of evaporation against which evaporation products can be effectively compared. Trambauer et al. (2014) recommended that all remotely sensed evaporation data sets used in their study should be compared with the LandFlux-EVAL evaporation benchmark product when assessing the performance of these data sets over Africa. Secondly, Miralles et al. (2016) argued that because there are large discrepancies in how different products produce their evaporation, caution is needed when using estimates of evaporation in isolation and relying on a data set based on one evaporation algorithm could lead to an inaccurate comparison against models. They pointed out that in the basin

rainforest, the virtual total of the evaporation in the Global Land Evaporation Amsterdam Model (GLEAM) product (Martens et al. 2017) comes from transpiration, while in the Moderate Resolution Imaging Spectroradiometer (MODIS) product (Running and Zhao 2015), soil evaporation is the dominant component. Therefore, as LandFlux-EVAL is a synthesis data product, the use of LandFlux-EVAL avoids prioritising one evaporation algorithm in isolation. Thirdly, during this thesis research, a water budget evaluation of various evaporation products for the African continent showed that LandFlux-EVAL performs well in all major African basins (Weerasinghe et al. 2020). This study noted that LandFlux-EVAL reproduces evaporation effectively regardless of its coarse resolution. This combination of factors is a strong justification for using LandFlux-EVAL as a reference point for basin evaporation, despite the caveat that it has not been validated against in situ data from within the basin due to the lack of historical flux tower data.

2.2.2 CMIP5 models

This thesis uses data from CMIP5 models to provide initial insights on the seasonal cycle of Congo Basin evaporation, and to investigate LSM parameterisations. The primary aim of the Coupled Model Intercomparison Project is to discover why GCMs developed by different modelling centres produce different outcomes in historical and future climate experiments, given that they have a standard set of input forcings (Taylor et al. 2012). CMIP5 model data are freely available online from the Program for Climate Model Diagnosis and Intercomparison data portal (https://pcmdi.llnl.gov/mips/cmip5/). Approximately 40 models contribute to CMIP5 from over 20 modelling centres around the world. Compared to previous model versions, for example CMIP3 models, CMIP5 models generally have a higher spatial resolution, and some CMIP5 earth system models

now incorporate interactive prognostic aerosol, chemistry and dynamic vegetation components. In 2018, during the research for this thesis, the first model data from the sixth phase of the Coupled Model Intercomparison Project (CMIP6) became available (Eyring et al. 2016). These models have improved physics and higher spatial resolutions. However, CMIP6 is still in progress, and many centres have not yet submitted data. At the beginning of this thesis research, CMIP6 data were insufficient to enable a detailed analysis of evaporation and its components across a spectrum of models. Therefore, the decision was taken to use CMIP5 data to sample as wide a range of GCMs as possible.

Monthly data from CMIP5 GCMs participating in the Atmospheric Model Intercomparison Project (AMIP) experiment are used in this thesis. Observed sea surface temperature (SST) data are prescribed to the AMIP models (Hurrell et al. 2008). The advantage of this approach for studying the historical climate of the Congo Basin is that SST biases which erroneously affect modelled Congo Basin hydrology, as identified by Creese and Washington (2018), are eliminated from the model data.

GCMs selected for use are presented in Chapter 3. Model selection is based on the availability of data for evaporation and its three components. As some models are from the same modelling centre, only one model from each centre with the finest spatial resolution was selected. This avoids introducing biases towards models with similar LSMs when ensemble means are taken. Individual models are presented in native resolution, but models are interpolated to a 1° x 1° grid before calculating ensemble means or composites. As differences arising from initial conditions are negligible when considering long-term climatology (Munday and Washington 2017), only the first ensemble member (r1i1p1) is used for each model.

2.2.3 Reanalysis data sets

Reanalysis data products assimilate observations with a numerical model to generate a dynamically consistent, gridded global estimate of the state of the climate system. Reanalyses are used in this thesis to investigate drivers of evaporation rather than GCMs because reanalyses have an observational constraint on the model evolution. Therefore, reanalyses are more likely to realistically represent controls on evaporation such as radiation and soil moisture. Table 2.2 summarises the reanalyses used within this thesis.

Table 2.2 Reanalysis data sets

Data Set	Spatial Resolution	Temporal Resolution	Period Available
CFSR	0.25 x 0.25	Monthly	1979-present
ERA5-Land	0.1 x 0.1	Monthly	1981-present
MERRA-2	0.5 x 0.625	Monthly	1980-present
NCEP-2	2.5 x 2.5	Monthly	1979-present

In the Congo Basin, reanalyses differ widely in their representation of the climate system (Washington et al. 2013; Hua et al. 2019). Therefore, it is important to validate reanalyses against reference data, to obtain confidence that the reanalysis is deriving the dynamics controlling evaporation realistically. Three criteria are established to select reanalyses for validation against LandFlux-EVAL evaporation: (1) the reanalysis is the latest available version of its type, (2) the reanalysis is independent of LandFlux-EVAL, which allows for a fair comparison to be made, and (3) the reanalysis produces data for evaporation, its three components, and a wide range of controls, including soil moisture and solar radiation. To the knowledge of the authors, ERA5-Land (Hersbach et al. 2020) and MERRA-2 (Gelaro et al. 2017) are the only reanalyses that meet these criteria. It could be argued that the reanalyses are not truly independent of LandFlux-EVAL as both

reanalyses and LandFlux-EVAL are constrained by observations, which could suggest that a caveat is needed. However, it is important to note that ERA5-Land and MERRA-2 are not included in LandFlux-EVAL. Additionally, both reanalyses produce evaporation using revised LSMs compared to previous versions included in LandFlux-EVAL. The ERA5-Land reanalysis now contains monthly vegetation maps from MODIS and MERRA-2 uses precipitation corrections. Therefore, it is plausible to argue that both reanalyses produce evaporation independently from LandFlux-EVAL.

2.3 Methods

2.3.1 Seasonal cycles

Seasonal cycles are produced from the data sets in two steps. Firstly, the mean value across the domain is calculated for each month and year. Secondly, monthly mean values are calculated from the data by averaging across a specified climatological period. The seasonal cycle is then defined as the evolution of the monthly mean value throughout the year. In this thesis, seasonal cycles are plotted for the full calendar year, for example from January to January, to ensure that the entire cycle is covered. For brevity, spatial distributions are plotted at the key turning points of the seasonal cycle.

2.3.2 GCM and reanalysis evaluation

In this thesis, GCMs and reanalyses are evaluated to assess their performance. GCMs are evaluated against CHIRPS2 rainfall and LandFlux-EVAL evaporation in Chapter 3, and reanalyses are evaluated against LandFlux-EVAL evaporation in Chapters 4 and 5. Ritter

and Munoz-Carpena (2013) argued that using a single metric to evaluate the performance of a model or reanalysis could lead to an incorrect verification. For example, root mean square error (RMSE) alone indicates the goodness of fit but does not indicate whether a model or reanalysis reproduces reference data realistically for a good reason. Therefore, Chapters 3, 4 and 5 use multiple evaluation exercises to assess the performance of the GCMs and reanalyses beyond just the RMSE alone. Five different types of exercise are undertaken across the results chapters, and each chapter uses at least two of these, dependent upon context-specific factors. The five exercises are as follows:

1. Quantitatively comparing the seasonal cycle from a GCM or reanalysis against the seasonal cycle from reference data using the RMSE equation:

$$\text{RMSE} = \sqrt{\frac{\sum_{i=1}^{n}(x_i - \hat{x}_i)^2}{n}} \tag{2.1}$$

where x is the monthly mean value as predicted by the GCM or reanalysis, $\hat{x}$ is the monthly mean value from the reference data, and n is the number of months in the year. For each month, the difference between the model data and the reference data is calculated, and the result is squared. The mean of the twelve months is then calculated, and the square root is taken to determine the RMSE. Lower RMSE values indicate a superior quantitative fit to the reference data.

2. Qualitatively comparing the seasonal cycle from a GCM or reanalysis against the seasonal cycle from reference data.

3. Qualitatively comparing the similarity between the shape of the spatial distribution from a GCM or reanalysis and the shape of the spatial distribution from reference data.

4. Qualitatively comparing the similarity between the values of the spatial distribution from a GCM or reanalysis and the values of the spatial distribution from reference data.

5. Quantitatively analysing the partitioning of evaporation into its components from a GCM or reanalysis. A reasonably high proportion of transpiration and low proportion of canopy evaporation would be an additional indicator that the GCM or reanalysis is producing evaporation realistically.

3 Evaluation of evaporation climatology for the Congo Basin wet seasons in 11 global climate models

David M. Crowhurst[1], Simon J. Dadson[1], and Richard Washington[1]

[1]School of Geography and the Environment, University of Oxford, Oxford, UK

Submitted 12/03/2019, Accepted 31/01/2020, Published 03/02/2020, Issue 22/03/2020

Journal of Geophysical Research: Atmospheres, 125, e2019JD030619

https://doi.org/10.1029/2019JD030619

Authorship declaration

David Crowhurst conducted all of the analysis and wrote this paper. Simon Dadson and Richard Washington contributed to the planning of the methodology and the interpretation of the results and commented on and edited the manuscript during preparation and revision.

Abstract

Across the Congo, there is a wide spread in rainfall in the two wet seasons in Coupled Model Intercomparison Project 5 global climate models (GCMs). As the Congo is believed to be a moisture recycling hot spot, the evaporation of excess water from the land surface in some models could be amplifying the model spread in rainfall. This chapter performs an exploratory process-based evaluation of Congo Basin evaporation in 11 Coupled Model Intercomparison Project 5 GCMs that took part in the Atmospheric Model Intercomparison Project. Our aims are to improve scientific understanding about Congo evaporation, and to determine whether there are opportunities to improve how models produce Congo evaporation. Climatologically, we find that models with "realistic" rainfall simulate higher rainfall in November, the peak of the second wet season, than March, the peak of the first. However, models with "realistic" evaporation simulate lower evaporation in November than March, because these models suppress the transpiration component of the evaporation in November relative to March. In both wet seasons, subgrid rainfall schemes make these models simulate a credible ratio of transpiration to canopy evaporation, and cause them to generate evaporation in a more realistic manner. We therefore trust how these models produce evaporation in the wet seasons, and argue that lower transpiration is likely to explain why evaporation is lower in November than March in reality. We also suggest that using subgrid rainfall schemes in all GCMs could improve how models produce Congo evaporation during the wet seasons. This might reduce the model spread in Congo rainfall.

3.1 Introduction

The Congo Basin is one of three major global hot spots of convective rainfall (Webster 1983). Congo climate is of critical global importance, as latent heat release drives the large-scale tropical and subtropical circulation, delivering heat and moisture poleward (Jury and Mpeta 2009). Regionally, Congo climate is important given the sensitivity of agriculture to rainfall (Sonwa et al. 2017). Furthermore, the Congo Basin rainforests and the peatlands beneath them are a particularly large store of carbon (Dargie et al. 2017; Xu et al. 2017), and the release of carbon due to either deforestation or peatland decomposition is a significant threat (Dargie et al. 2018). Unfortunately, there is currently a wide spread in global climate model (GCM) simulations of Congo Basin rainfall amount and distribution during the two wet seasons, which have peak rainfall in March and November (Haensler et al. 2013).

As the models differ vastly in their simulation of present-day wet season rainfall, credibility in model projections of future rainfall is undermined. This problem is hampering the development of adaptation strategies for the Congo Basin, which are required to lessen vulnerability to changes in rainfall (Bele et al. 2015). In addition, it is not yet possible to work out whether the Congo Basin will have water stress during the wet seasons (Zhou et al. 2014). To resolve this, it is essential to establish whether some models produce realistic and credible simulations of Congo Basin rainfall in the wet seasons, as these models are more likely to have trustworthy projections. In addition, if certain model schemes are responsible for improving model rainfall, these schemes could be used more widely to reduce the model spread.

Washington et al. (2013) were the first to identify the wide spread in rainfall amount and distribution in the Congo Basin wet seasons in coupled GCMs from the fifth phase of the Coupled Model Intercomparison Project (CMIP5). Building upon this, Creese and Washington (2016) suggested that an observational campaign at key Congo Basin boundaries could help to constrain the spread in model rainfall. Furthermore, Creese and Washington (2018) argued that models with large sea surface temperature (SST) biases in the Gulf of Guinea produce more evaporation from the ocean, enhanced local convection, and higher rainfall in the western Congo Basin during the September-October-November rainy season. Their results questioned the credibility of Congo Basin rainfall produced by models with large Atlantic SST biases.

Nevertheless, in CMIP5 models participating in the Atmospheric Model Intercomparison Project (AMIP) experiment, where observed SST is prescribed and SST biases cannot account for model differences in rainfall, there is still a wide spread in rainfall amount during the two wet seasons in the Congo Basin. A potential reason for the remaining spread is that errors in model land surface schemes could cause models to generate divergent evaporation from the land surface in response to a unit of rainfall. As evidence from moisture tagging algorithms indicates that the Congo Basin is a hot spot of moisture recycling (Pokam et al. 2012; Dyer et al. 2017), it is possible that the release of excess water vapor from the land surface through evaporation (often referred to as “evapotranspiration”) in some models could be amplifying the model spread in Congo Basin rainfall.

3.1.1 Process-based evaluation of Congo Basin evaporation

This chapter performs an exploratory process-based evaluation of Congo Basin evaporation for a selection of CMIP5 GCMs which took part in AMIP. Process-based evaluation methods establish whether models reproduce reference data well (with "realism"), using a physically credible set of processes (James et al. 2018). The purpose of this evaluation is twofold. The first is to improve scientific understanding about the annual cycle of evaporation and its three components, canopy evaporation, transpiration, and soil evaporation, in the Congo Basin. If some models realistically simulate evaporation against reference data, and partition evaporation into its components using credible processes, this would strengthen the trustworthiness of their evaporation partitioning. The three components of evaporation produced by these models could then provide some information about why the annual cycle has the characteristics that it does, in the absence of in situ data for these components in the Congo Basin.

The second purpose is to identify methods to improve how Congo Basin evaporation is generated in the GCMs. Certain GCMs might contain favourable schemes within their land surface models (LSMs) which credibly alter the partitioning of evaporation to bring evaporation into good agreement with reference data. If some GCMs contain favourable schemes, while others do not, this would present an opportunity to improve how models simulate Congo Basin evaporation, by using favourable schemes more widely. This might contribute to reducing the model differences in Congo Basin rainfall in the wet seasons.

3.1.2 Aims

This chapter aims to answer the following questions:

1. How is evaporation partitioned into its components in the Congo Basin in GCMs with more “realistic” evaporation, and what can this tell us about the evaporation?

2. Are there opportunities to improve the realism of Congo Basin evaporation across GCMs?

In section 3.2, we describe the data and methods used. In section 3.3, we compare the annual cycle of evaporation produced by a range of GCMs against reference data, and establish what defines the annual cycle for models which have more realistic evaporation than others.

In section 3.4, we determine how evaporation is partitioned into its three components in these models, and assess the credibility of the processes which do this. If the evaporation is plausibly produced, we will be able to use the model evaporation partitioning to gain some useful information about the characteristics of the evaporation. In section 3.5, we discuss the results, and in section 3.6, we conclude.

3.2 Data and methods

3.2.1 Domain

The Congo Basin domain is defined as 14°S to 4°N, 18°E to 29°E (Figure 3.1). Although the Congo Basin has evergreen rainforests to the north and deciduous savannah to the south (Yan et al. 2017), we select the whole Congo Basin to complement previous process-based rainfall (Creese and Washington 2018) and water vapor transport (Pokam et al. 2012) analyses. No study has done the same for evaporation. By considering the entire Congo Basin, the current exploratory chapter begins to improve knowledge about evaporation and its three components for the region as a whole.

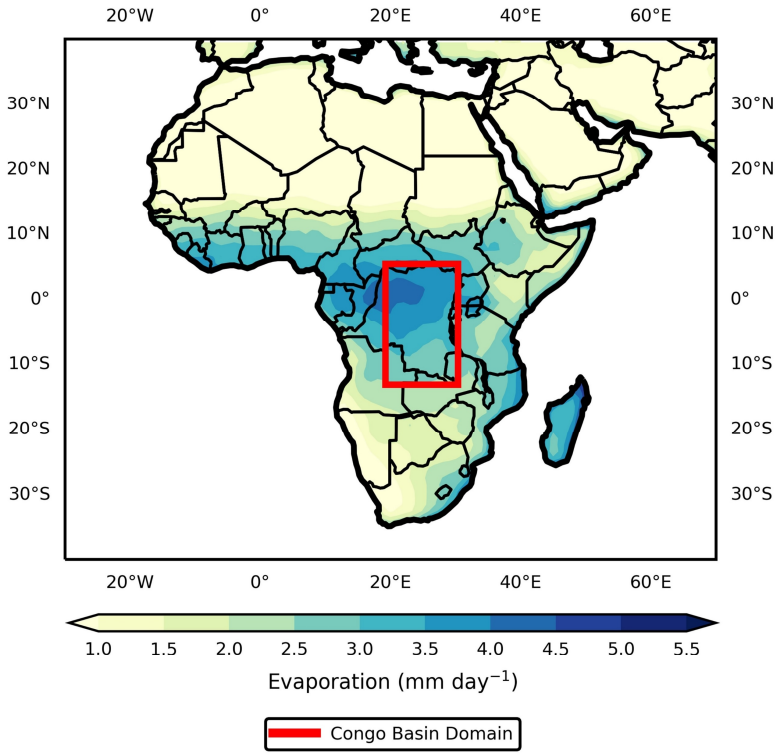


Figure 3.1 Thirty-year mean (1979–2008) evaporation across the African continent (mm day^{-1}), from a composite mean of the 11 AMIP models used in this chapter. Congo Basin domain used in this chapter (14°S to 4°N, 18°E to 29°E) is shown by a red box

3.2.2 AGCMs

This chapter focuses on monthly thirty-year mean (1979–2008) atmosphere-only global climate model (AGCM) simulations from the AMIP component of CMIP5 (Taylor et al. 2012). AMIP simulations are preferred instead of direct output from CMIP5, because observed SST in AMIP is prescribed, which removes SST biases that could erroneously impact upon Congo Basin hydrology (Richter et al. 2016). Nevertheless, AMIP runs should be treated with some caution, because fluxes of water and energy from the ocean to the atmosphere are also dependent on the correct specification of the atmosphere (Zhou et al. 2018). Although evaporation data are available across all AMIP models, data for the three components are only available from 17 AMIP models. Some of these models are from the same centre, so an ensemble mean might contain biases toward models with similar LSMs. For each centre, we therefore retain one AMIP model, selecting the model with the lowest grid spacing. This constrains our analysis to 11 AMIP models.

LSMs embedded within GCMs calculate the three components of evaporation in each grid box in response to meteorological and hydrological inputs, and sum the components to obtain total evaporation (Pitman 2003). For equations commonly used in GCMs to calculate each evaporation component, see Appendix A. Table 3.1 also provides details about the equations used to calculate each evaporation component within the LSMs of the 11 AMIP models selected. Data from individual AGCMs are presented in native resolution, and the models are regridded using bilinear interpolation to a common 1° × 1° grid before the ensemble mean is calculated. Comparison between models at native and regridded resolution shows that regridding does not noticeably alter the model output.

Table 3.1 AGCMs used and details about their evaporation components

Model	Grid Spacing	LSM	Canopy Evaporation	Transpiration	Soil Evaporation
bcc-csm1-1-m (Wu et al. 2014)	1.1° × 1.1°	Community Land Model 3 (CLM3) (Oleson et al. 2004) plus AVIM2 Dynamic Vegetation (Ji et al. 2008)	Equation 3.1, with additional leaf boundary layer resistance	Equation 3.2	Equation 3.3
BNU-ESM (Ji et al. 2014)	2.8° × 2.8°	Common Land Model (CoLM) (Dai et al. 2003) plus LPJ Dynamic Vegetation (Sitch et al. 2003)	Equation 3.1	Minimum of atmospheric demand and water supply	Equation 3.3
CanAM4 (Von Salzen et al. 2013)	2.8° × 2.8°	CLASS v2.7 (Verseghy 2000)	Equation 3.1	Equation 3.2	Equation 3.3, with adjustments to account for soil water gradients based on Deardorff equations
CNRM-CM5 (Voldoire et al. 2013)	1.4° × 1.4°	ISBA v3.0 (Decharme and Douville 2007)	Equation 3.1, with sub-grid rainfall used in calculating canopy water storage	Equation 3.2	Equation 3.3, with humidity at the ground estimated from surface soil moisture
GFDL-HIRAM-C360 (Zhao et al. 2009)	0.3° × 0.3°	LM3.0 (Milly et al. 2014) plus LM3V Dynamic Vegetation (Shevliakova et al. 2009)	Equation 3.1	Equation 3.2	Equation 3.3
GISS-E2-R (Schmidt et al. 2014)	2.5° × 2.0°	GISS 2-LS (Schmidt et al. 2006) plus Ent TBM Dynamic Vegetation (Kim et al. 2015)	Equation 3.1, with sub-grid rainfall used in calculating canopy water storage	Equation 3.2	Equation 3.3

inmcm4 (Volodin et al. 2010)	2.0° × 1.5°	1D Model (Volodin and Lykosov 1998)	Equation 3.1, except that an 'intercepted rainfall', equal to half of the rainfall rate, is used in calculating canopy water storage	Equation 3.2, except that F_{dry} is function of soil moisture and soil temperature	Equation 3.3, plus Jacquemin and Noilhan (1990) equation to account for soil water gradients
IPSL-CM5A-MR (Dufresne et al. 2013)	2.5° × 1.25°	ORCHIDEE (Krinner et al. 2005)	Equation 3.1, with additional leaf boundary layer resistance	Equation 3.2	Minimum of atmospheric demand, and water supply from the top soil layer
MIROC5 (Watanabe et al. 2010)	1.4° × 1.4°	MATSIRO (Takata et al. 2003)	Equation 3.1, with rainfall occurring in a fraction of the grid cell for canopy water storage (no probability distribution)	Equation 3.2	Equation 3.3, with adjustments to account for soil water gradients based on a modified surface roughness length
MRI-AGCM3-2S (Mizuta et al. 2012)	0.2° × 0.2°	Hydrology, Atmosphere and Land Model (Hosaka 2011)	Equation 3.1, with additional leaf boundary layer resistance	Equation 3.2	Equation 3.3
NorESM1-M (Bentsen et al. 2013)	2.5° × 1.9°	Community Land Model 4 (CLM4) (Oleson et al. 2010)	Equation 3.1, with additional leaf boundary layer resistance	Equation 3.2	Alpha and beta methods (the latter models diffusion of water vapour through the soil)

3.2.3 Reference data sets

In this chapter, rainfall from each of the 11 AMIP models is compared to the Climate Hazards Group InfraRed Precipitation with Station data v 2.0 (CHIRPS2) (Funk et al. 2015). Evaporation from each of the 11 AMIP models is then compared to LandFlux-EVAL (Mueller et al. 2013). Further details on these data sets are provided in Table 3.2.

Table 3.2 Reference data sets used in this chapter

Dataset	Grid Spacing	Further Details
CHIRPS v2.0 Rainfall (Funk et al. 2015)	0.05° × 0.05°	High resolution, quasi-global rainfall dataset which merges satellite imagery with in situ station data to produce a gridded rainfall record.
LandFlux-EVAL Evaporation (Mueller et al. 2013)	1.0° × 1.0°	Synthesis product based on a total of 14 remote sensing products, LSMs, reanalyses, diagnostic estimates and flux tower measurements. All datasets are interpolated onto a common grid before merging.

The use of CHIRPS2 in the current chapter as a reference point is justified for the following two reasons. First, CHIRPS2 has the best agreement of 10 satellite and gauge rainfall products, against a new, gridded, gauge-based rainfall data set ("NIC131-Gridded") in the Congo Basin (Nicholson et al. 2019). Second, CHIRPS2 has a high spatial resolution of 0.05° × 0.05°, which enables CHIRPS2 to accurately quantify rainfall delivered to the Congo by mesoscale convective systems (Funk et al. 2015). Conversely, to our knowledge, no evaporation products have been validated in the Congo, because no flux towers are installed (Sjöström et al. 2013), and no trustworthy, long-term ground observations are available for evaporation. However, there are satellite products, evaporation models and synthesis estimates of evaporation, as presented by Trambauer et al. (2014). Unlike rainfall, for which Washington et al. (2013) show that there is a wide spread between several products in the Congo Basin, Trambauer et al. (2014) show in their Figure 7 that there is excellent consistency among several evaporation products for the magnitude of the annual cycle of evaporation in the Congo Basin. Although the potential exists for a systematic bias across all products, the consistency across multiple products suggests it is more probable than not that the choice of evaporation data set will not substantially affect results. LandFlux-EVAL, a synthesis data set which merges evaporation from a range of LSMs, satellite products and reanalyses, was selected to

avoid prioritizing one evaporation algorithm in isolation (Miralles et al. 2016). In addition, the annual cycle from LandFlux-EVAL in the Congo, presented in the current chapter, compares favourably to the annual cycles presented by Trambauer et al. (2014). Furthermore, LandFlux-EVAL is believed to be a "best guess" estimate of evaporation (Peng et al. 2016), and has been used to evaluate CMIP5 models in previous studies (Mueller and Seneviratne 2014). The above points strongly support using LandFlux-EVAL as an evaporation reference. To begin our research on model evaporation in an understudied region, the current chapter uses LandFlux-EVAL as a best guess estimate, notwithstanding the caveat that the lack of validation in the Congo poses. Nevertheless, it may be possible to validate the data set in the near future if flux towers are installed.

3.2.4 Methods

3.2.4.1 Root mean square error analysis

For each of the 11 models, we first calculate the root mean square error (RMSE) for the annual cycle of rainfall against CHIRPS2, and second calculate the RMSE for the annual cycle of evaporation against LandFlux-EVAL (Table 3.3). Following the RMSE equation, for each month we calculate the difference between the model and the reference data and square the result. We then calculate the mean of the twelve months and take the square root to determine the RMSE. After ranking the 11 models from smallest to largest RMSE, a rainfall composite mean is taken across models with rainfall ranks from 1 to 4 ('Realistic Rainfall'), and rainfall ranks from 7 to 11 ('Unrealistic Rainfall'). An evaporation composite mean is then taken across models with rainfall and evaporation ranks from 1 to 4 ('Realistic Evaporation'), and rainfall and evaporation ranks from 7 to

11 (‘Unrealistic Evaporation’). The latter is done because models with realistic evaporation must have realistic rainfall. Table 3.4 lists the models included within each model composite.

Table 3.3 AGCM rankings for 30-year mean (1979-2008) annual cycles of rainfall and evaporation in the Congo Basin (14°S to 4°N, 18°E to 29°E). CHIRPS2 rainfall (1981-2008) and LandFlux-EVAL evaporation (1989-2005) are used as reference datasets

AMIP Model	Rainfall RMSE	Rainfall Rank	Evaporation RMSE	Evaporation Rank
CNRM-CM5	0.676	1	0.248	1
GFDL-HIRAM-C360	0.787	2	0.776	8
inmcm4	0.863	3	1.237	11
GISS-E2-R	1.014	4	0.460	3
bcc-csm1-1-m	1.035	5	0.525	5
MRI-AGCM3-2S	1.390	6	0.712	7
CanAM4	1.414	7	0.309	2
MIROC5	2.782	8	1.029	9
NorESM1-M	2.901	9	0.612	6
IPSL-CM5A-MR	2.989	10	0.501	4
BNU-ESM	3.375	11	1.052	10

Table 3.4 Models selected for the composites analysed within this chapter

Composite	Unrealistic Rainfall	Realistic Rainfall	Unrealistic Evaporation	Realistic Evaporation
Models Selected	BNU-ESM IPSL-CM5A-MR MIROC5 NorESM1-M	CNRM-CM5 GFDL-HIRAM-C360 GISS-E2-R inmcm4	BNU-ESM MIROC5	CNRM-CM5 GISS-E2-R

3.2.4.2 Process-based evaluation

In this chapter we perform a process-based evaluation of the model evaporation, by assessing the credibility of the processes which partition evaporation into its three components. If the models with more realistic evaporation complete this partitioning in a credible way, the three components of evaporation they produce could justifiably provide us with useful information about the character of the annual cycle of total evaporation. In addition, if specific model schemes enable some models to simulate evaporation more realistically for good reasons, it might be possible to argue that these schemes should be used in all models, to improve how models simulate Congo Basin evaporation. The advantage of this might be a narrowing of the model spread in wet season rainfall.

3.3 Annual cycles of rainfall and evaporation in the Congo Basin

Figure 3.2a shows that the annual cycle of rainfall is bimodal in most models, with two wet seasons and two drier seasons. The model ensemble mean has 6.35 mm day^{-1} less rainfall in July, the trough of the summer dry season, than March, the peak of the first wet season. In addition, the ensemble mean has 0.43 mm day^{-1} more rainfall in November, the peak of the second wet season, than March, the peak of the first. The largest intermodel differences occur in wet months (e.g. March, standard deviation 2.08, and November, standard deviation 2.10), but the smallest intermodel differences occur in drier months (e.g. July, standard deviation 0.60). It is also interesting to note that most models overestimate CHIRPS2 rainfall in the two wet seasons, but not in the summer dry season. Conversely, Figure 3.2b shows that the annual cycle of evaporation in most models has a

decline in evaporation between March and July, but recovery between July and November. The model ensemble mean has 2.10 mm day^{-1} less evaporation in July than March and 0.29 mm day^{-1} less evaporation in November than March. In contrast to rainfall, the spread in evaporation between models is very small throughout the annual cycle. For example, standard deviations are 0.39 in March, 0.43 in July, and 0.44 in November. Nevertheless, Figure 3.2b also shows that the majority of models overestimate LandFlux-EVAL evaporation in the two wet seasons, but not in the summer dry season.

Table 3.3 describes the RMSE ranking of the individual models for both rainfall and evaporation (see section 3.2 for a description of the methodology). CNRM-CM5 and GISS-E2-R have small errors for both rainfall and evaporation, while BNU-ESM and MIROC5 have large errors for both rainfall and evaporation. However, models with small errors for rainfall do not always have small errors for evaporation, and vice versa. For example, GFDL-HIRAM-C360 and inmcm4 have small errors for rainfall, but large errors for evaporation. This could be because these two models have errors in their land surface schemes which convert rainfall to evaporation, or because they have errors in other important variables which are required to produce evaporation, such as solar radiation. Conversely, CanAM4 and IPSL-CM5A-MR have large errors for rainfall but small errors for evaporation. As these two models have too much rainfall, interception and re-evaporation from the canopy might be too large. The effect would be to suppress transpiration from plant stomata, as the atmospheric demand for evaporation would be erroneously satisfied (Lawrence et al. 2007). These two models might produce a realistic amount of evaporation, but for the incorrect reason, because their ratio of canopy evaporation to transpiration could be incorrect (Wang and Eltahir 2000).

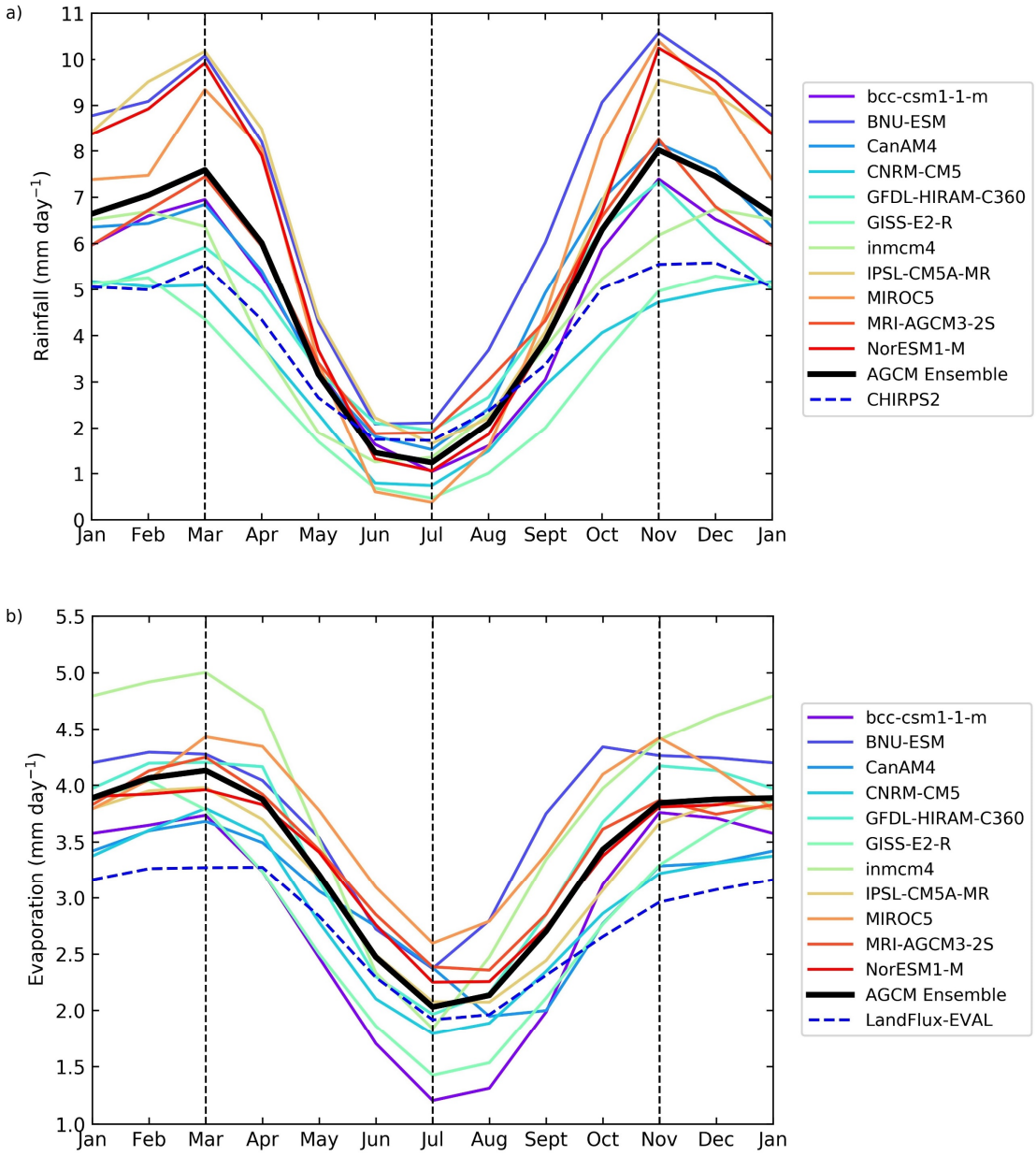


Figure 3.2 Thirty-year mean (1979–2008) annual cycles of **a** rainfall (mm day^{-1}) and **b** evaporation (mm day^{-1}) in the Congo Basin (14°S to 4°N, 18°E to 29°E), from 11 AMIP models, and their ensemble mean. CHIRPS2 rainfall (1981–2008) and LandFlux-EVAL evaporation (1989–2005) are used as reference data sets

Figure 3.3 shows the spatial distribution of evaporation at the turning points of the evaporation annual cycle.

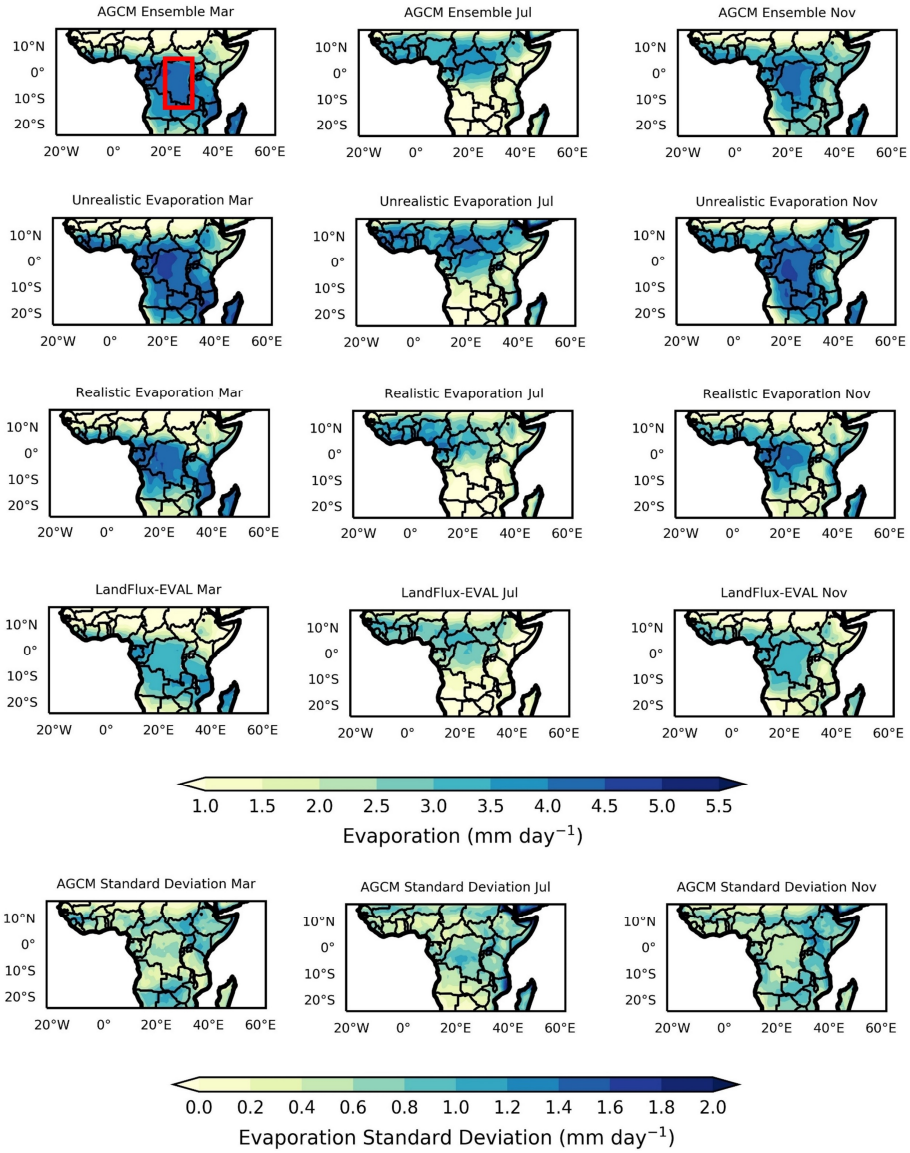


Figure 3.3 Thirty-year mean (1979–2008) evaporation (mm day^{-1}) for March, July, and November, from the AGCM ensemble mean, models with unrealistic evaporation, models with realistic evaporation, and LandFlux-EVAL. AGCM standard deviations are also included. Domain analysed in this chapter (14°S to 4°N, 18°E to 29°E) is shown by a red box in the first panel

In March, the band of peak evaporation in the model ensemble mean is in the centre of the basin. Evaporation rates are highest in the composite of models with “unrealistic” evaporation, lower in the composite of models with “realistic” evaporation, and lower

still in LandFlux-EVAL. By July, the band of peak evaporation has migrated to the north in the model ensemble mean. This band is strong in models with unrealistic evaporation, not as strong in models with realistic evaporation, and in between these two in LandFlux-EVAL. By November, the band of peak evaporation in the model ensemble mean has migrated back southward. Once more, evaporation rates are highest in models with unrealistic evaporation, lower in models with realistic evaporation, and lower still in LandFlux-EVAL. AGCM standard deviations are small throughout the year.

Figure 3.4a shows that rainfall is 3.81 mm day^{-1} lower in March, 0.04 mm day^{-1} lower in July and 3.78 mm day^{-1} lower in November in models with realistic rainfall compared to unrealistic rainfall. The reduction in rainfall during the wet seasons causes greater coherence between the annual cycle of rainfall in the models and CHIRPS2, with an RMSE of 0.56 for models with realistic rainfall as compared to 2.99 for models with unrealistic rainfall. Models with realistic rainfall also simulate less rainfall in July than March (−4.97 mm day^{-1}), and more rainfall in November than March (+0.29 mm day^{-1}). The latter is consistent with Jackson et al. (2009), who argued that the presence of the southern component of the African Easterly Jet in boreal autumn increases the frequency of mesoscale convective systems in the second wet season, which increases rainfall.

Conversely, Figure 3.4b shows that evaporation is 0.45 mm day^{-1} lower in March, 0.84 mm day^{-1} lower in July and 0.97 mm day^{-1} lower in November in models with realistic evaporation compared to models with unrealistic evaporation. This causes greater coherence between the annual cycle of evaporation in models and LandFlux-EVAL, with an RMSE of 0.38 for models with realistic evaporation as compared to 1.01 for models

with unrealistic evaporation. In addition, models with realistic evaporation simulate less evaporation in July than March (−2.23 mm day^{-1}), and importantly, less evaporation in November than March (−0.55 mm day^{-1}).

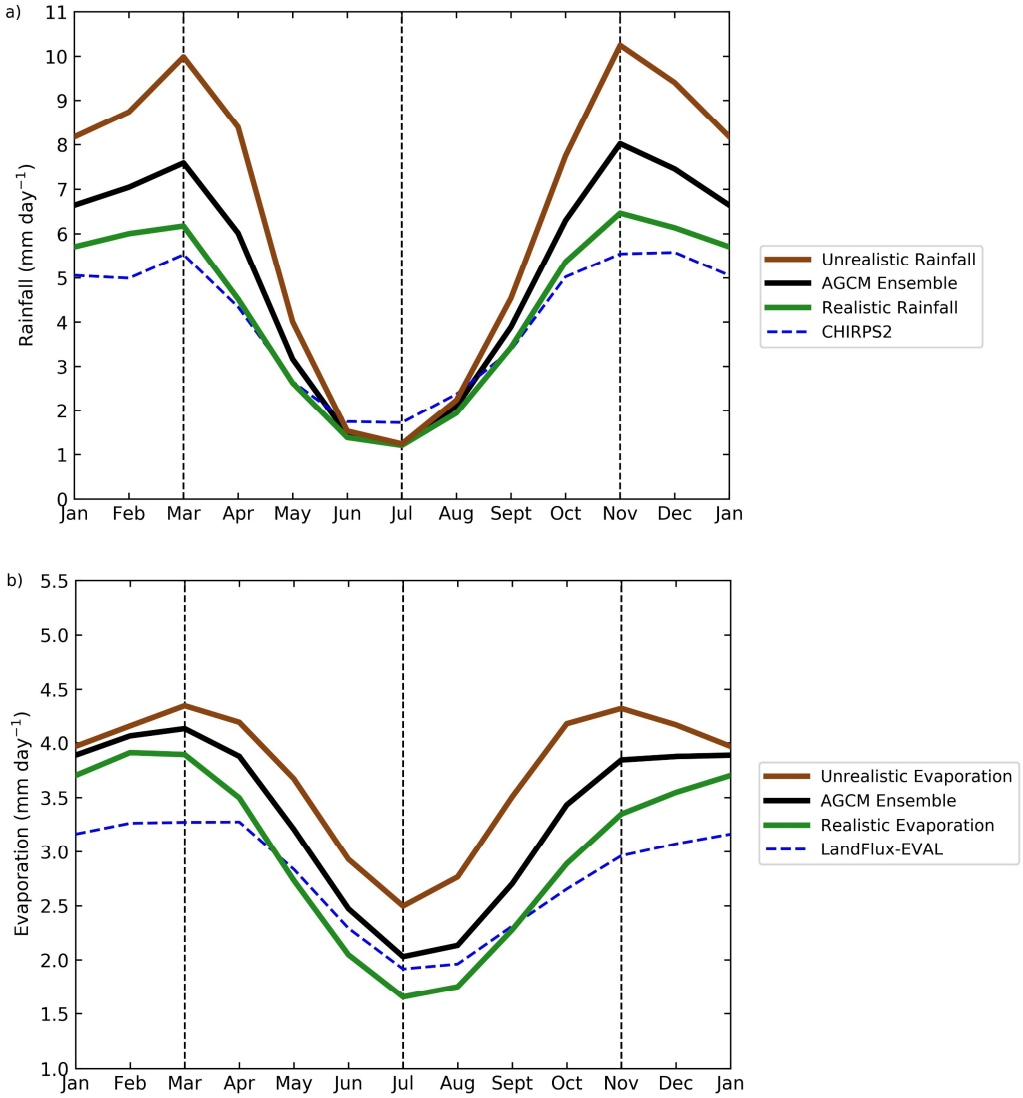


Figure 3.4 Thirty-year mean (1979–2008) annual cycles of **a** rainfall (mm day^{-1}) and **b** evaporation (mm day^{-1}) in the Congo Basin (14°S to 4°N, 18°E to 29°E). Rainfall annual cycles are from models with unrealistic rainfall, the AGCM ensemble mean, and models with realistic rainfall. Evaporation annual cycles are from models with unrealistic evaporation, the AGCM ensemble mean, and models with realistic evaporation. CHIRPS2 rainfall and LandFlux-EVAL evaporation are used as reference data sets

The above analysis highlights two important characteristics about the annual cycle of evaporation in the Congo Basin. First, the realistic models and reference data show that evaporation is lower in the summer dry season than the first wet season. Second, the realistic models and reference data show that evaporation is lower in the second wet season than the first, despite higher rainfall in the second. Both of these characteristics are, to our knowledge, not understood. The former is consistent with a plausible positive feedback (Seneviratne et al. 2010), whereby lower rainfall during the summer dry season would result in lower soil moisture, which would reduce evaporation. However, the latter is not consistent with a positive feedback. Instead, higher rainfall in November corresponds with lower evaporation in November. The latter suggests that the wet seasons have very different climatological characteristics, which are worthy of exploration.

An analysis to attribute what is causing lower evaporation in November than March would require splitting the Congo into the northern rainforest and southern savannah, and is beyond the scope of this chapter. However, it might still be possible to obtain some useful information about this feature from the evaporation partitioning, to aid a future attribution. In the next section, we focus our process-based evaluation on the two wet seasons. We examine the credibility of the processes which partition evaporation into its three components in models with realistic evaporation in March and November. If the processes are credible, we will be able to obtain information from the evaporation partitioning regarding the negative evaporation difference between March and November. In addition, we might be able to suggest whether certain schemes should be used in more models to improve evaporation during the wet seasons specifically. As the Congo Basin is believed to be a hot spot of moisture recycling during the wet seasons (Dyer et al. 2017), this might help to constrain the model spread in rainfall during the two wet seasons.

3.4 Evaporation partitioning in the Congo Basin wet seasons

3.4.1 Canopy evaporation

Table 3.1 shows that models with realistic evaporation (CNRM-CM5 and GISS-E2-R) use subgrid rainfall schemes in their land surface components. These approaches follow Eltahir and Bras (1993) to correct the "GCM drizzle" problem, whereby intense convective rainfall at scales below the grid box can only be represented as grid box average rainfall of lower intensity. Subgrid rainfall schemes modify the fractional coverage of rainfall in each grid box, and distribute rainfall intensity according to a probability density function. Physically, the action of these schemes is to increase canopy throughfall, reduce canopy water storage, and reduce canopy evaporation.

Conversely, models with unrealistic evaporation (BNU-ESM and MIROC5) do not use subgrid rainfall schemes. As a result, the canopy is more easily able to intercept the low intensity rainfall, and the models simulate low canopy throughfall, high canopy water storage, and high canopy evaporation.

Subgrid rainfall schemes offer an explanation for why canopy evaporation is 1.12 mm day^{-1} lower in March and 1.10 mm day^{-1} lower in November in models with realistic evaporation than in models with unrealistic evaporation, as shown in Figure 3.5. Nevertheless, canopy evaporation in models with realistic evaporation occurs at a similar rate in both March and November.

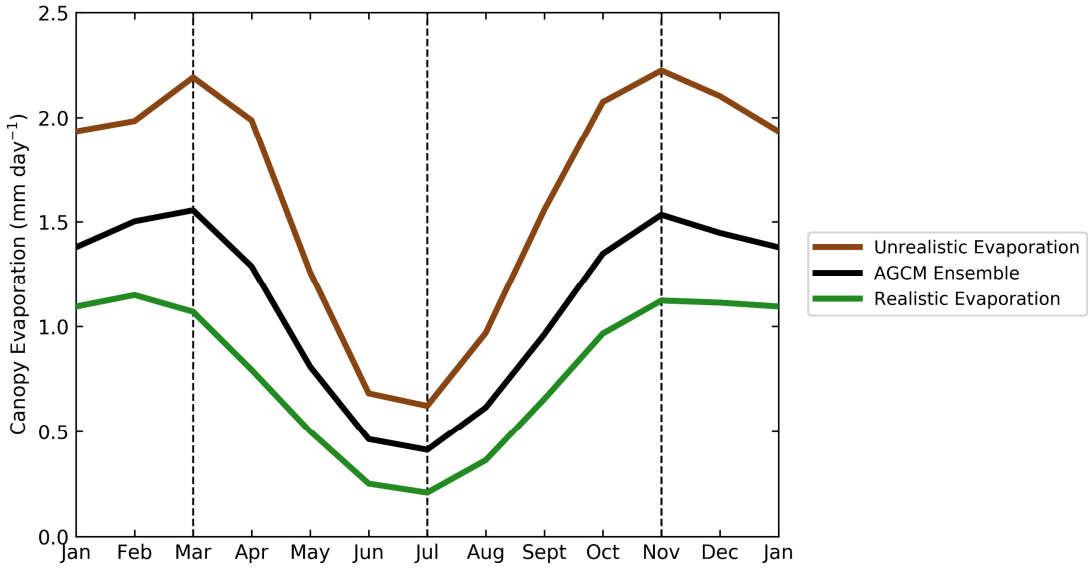


Figure 3.5 Thirty-year mean (1979–2008) annual cycle of canopy evaporation (mm day^{-1}) in the Congo Basin (14°S to 4°N, 18°E to 29°E) from models with unrealistic total evaporation, the AGCM ensemble mean, and models with realistic total evaporation

3.4.2 Transpiration

Figure 3.6 shows that transpiration is 0.85 mm day^{-1} higher in March and 0.32 mm day^{-1} higher in November in models with realistic evaporation than in models with unrealistic evaporation. As the models with realistic evaporation contain subgrid rainfall schemes, canopy evaporation is decreased in these models relative to models with unrealistic evaporation. This means that the atmospheric demand for evaporation is not satisfied, so transpiration increases in March and November (Lawrence et al. 2007). However, the increase in transpiration is less than the decrease in canopy evaporation, because transpiration is typically calculated with reference to canopy resistances (Equation 3.2). As a result, total evaporation is realistically brought down into better agreement with

LandFlux-EVAL, as shown by Figure 3.4b. In addition, the ratio of transpiration to total evaporation increases during the wet seasons, and these models are credibly brought into agreement with studies which suggest that transpiration in the Congo should be a larger component of evaporation than most models simulate (Lian et al. 2018). Subgrid rainfall schemes therefore cause the models to simulate evaporation in a realistic manner in the wet seasons, by credibly adjusting down the fraction of canopy evaporation and adjusting up the fraction of transpiration. However, Figure 3.6 also shows that when the fraction of transpiration is high in models with realistic evaporation, transpiration is suppressed by 0.62 mm day^{-1} in November relative to March. To date, it is unclear why, at a time when there is more rainfall in the Congo, models with realistic evaporation suggest that less transpiration is released from the vegetation.

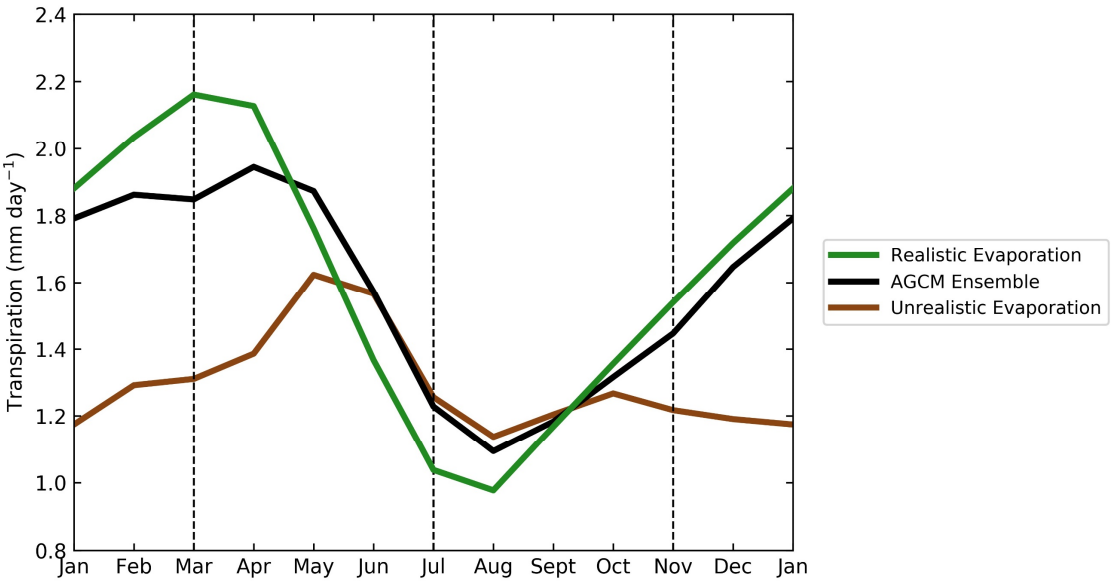


Figure 3.6 Thirty-year mean (1979–2008) annual cycle of transpiration (mm day^{-1}) in the Congo Basin (14°S to 4°N, 18°E to 29°E) from models with realistic total evaporation, the AGCM ensemble mean, and models with unrealistic total evaporation

3.4.3 Soil evaporation

Figure 3.7 shows that soil evaporation is 0.16 mm day^{-1} lower in March and 0.15 mm day^{-1} lower in November in models with realistic evaporation as compared to models with unrealistic evaporation. Soil evaporation in models with realistic evaporation is therefore a small fraction of the total evaporation in the wet seasons. In addition, soil evaporation in models with realistic evaporation occurs at a similar rate in both March and November. However, the above characteristics of soil evaporation are not believable improvements. This is because there is no credible reason which explains why soil evaporation is lower in the models with realistic evaporation compared to others.

Nevertheless, four models from the set of 11 (as detailed in Table 3.1) include a scheme which plausibly decreases specific humidity in the top soil layer to account for soil water gradients (Jacquemin and Noilhan 1990). This scheme is not considered by any of the other models, and is distributed across models, rather than being solely associated with models that have realistic evaporation. Figure 3.7 shows that in a composite of the models with this credible scheme for soil evaporation (CanAM4, CNRM-CM5, inmcm4 and MIROC5), the models have 0.21 and 0.38 mm day^{-1} less soil evaporation in March and November respectively than the model ensemble mean. In addition, the difference in soil evaporation between March and November is −0.02 mm day^{-1}. This allows us to argue with more confidence that soil evaporation might be lower in reality than most models suggest, and is not likely to differ substantially between March and November.

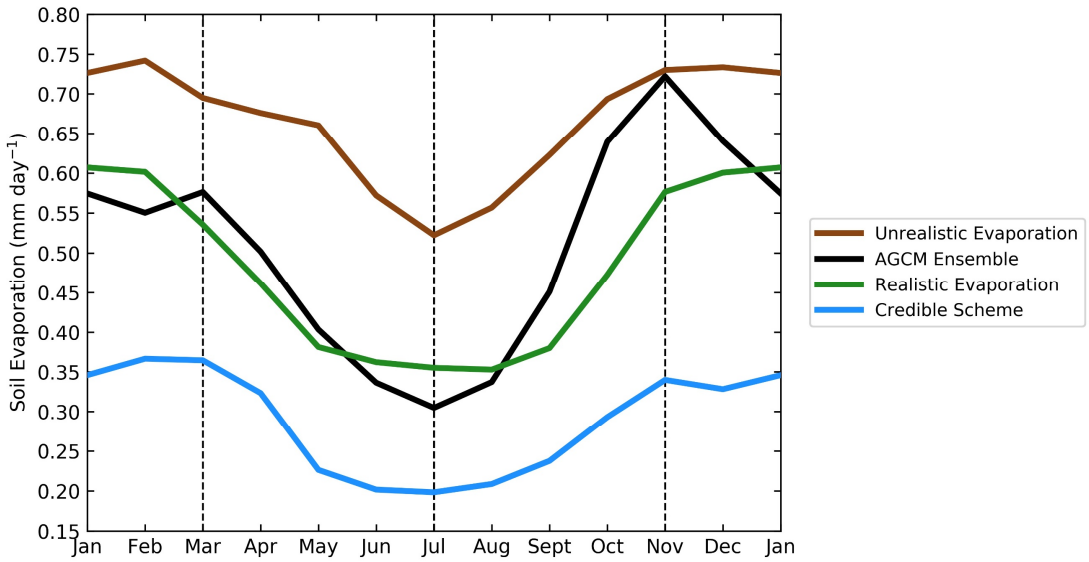


Figure 3.7 Thirty-year mean (1979–2008) annual cycle of soil evaporation (mm day^{-1}) in the Congo Basin (14°S to 4°N, 18°E to 29°E) from models with unrealistic total evaporation, the AGCM ensemble mean, models with realistic total evaporation, and models which contain a credible scheme for soil evaporation (refer to section 3.4.3)

3.5 Discussion

Models with realistic evaporation include sub-grid rainfall schemes in their land surface components. During wet seasons, these schemes credibly decrease canopy evaporation, which causes increased transpiration to satisfy the atmospheric demand for evaporation. The upward adjustment in transpiration is plausible, as the transpiration is brought into agreement with studies which suggest that there is a high ratio of transpiration to total evaporation in the Congo Basin (Wei et al. 2017). In addition, the downward adjustment in canopy evaporation is greater than the upward increase in transpiration in both March and November, because canopy resistance terms cap the increase in transpiration. This reduces total evaporation in both March and November to more realistic values, which

are comparable with LandFlux-EVAL (Figure 3.4b), and suggests that models with more realistic evaporation, that have sub-grid rainfall schemes, are producing evaporation in a more credible and realistic manner during the wet seasons.

Table 3.5 shows that in models with unrealistic evaporation, the differences in the three evaporation components between March and November are very small. This explains why evaporation does not notably change in these models between March and November (-0.02 mm day^{-1}). Table 3.5 also shows that in models with realistic evaporation, the climatological difference between March and November is -0.62 mm day^{-1} for transpiration, +0.05 mm day^{-1} for canopy evaporation, and +0.04 mm day^{-1} for soil evaporation. Therefore, importantly, Table 3.5 shows that the suppression of the transpiration component in November relative to March is almost fully responsible for the 0.55 mm day^{-1} lower evaporation in November than March in these models.

Table 3.5 30-year mean (1979-2008) difference in total evaporation and its components in the Congo Basin (14°S to 4°N, 18°E to 29°E) between March and November, from model composites with unrealistic and realistic evaporation. Units are mm day^{-1}

	Δ Total Evaporation	**Δ Canopy Evaporation**	**Δ Transpiration**	**Δ Soil Evaporation**
Difference between March and November (Unrealistic Evaporation)	-0.02	+0.03	-0.10	+0.04
Difference between March and November (Realistic Evaporation)	-0.55	+0.05	-0.62	+0.04

In models with sub-grid rainfall, because total evaporation is more realistic, and because transpiration and canopy evaporation are more realistically partitioned, we argue that the lower transpiration in November than March, and similar canopy evaporation in November and March, are likely to be trustworthy differences. In addition, a composite of models containing a credible scheme for soil evaporation shows no substantial difference in soil evaporation between November and March (Figure 3.7), which suggests that a negligible difference in soil evaporation is also likely to be trustworthy. We therefore argue that climatologically, lower transpiration is likely to explain why evaporation is lower in November than March in reality. However, as stated in Section 3.4, it is not clear why, when there is more rainfall in the Congo Basin in November, models with realistic evaporation suggest that there is less transpiration from the vegetation. Further research is therefore needed to investigate what factors might be responsible.

As sub-grid rainfall schemes enable models to simulate evaporation with increased realism during the wet seasons, by making plausible adjustments to the ratio of transpiration to canopy evaporation, we suggest that using sub-grid rainfall schemes in the land surface components of all GCMs could improve how models produce evaporation from the Congo Basin during the wet seasons. This might also have benefits for how models simulate the wider hydrological cycle of the region. Creese et al. (2019b) suggested that improving how models represent the two African Easterly Jets could reduce the model spread in Congo Basin wet season rainfall. Additionally, given that the Congo is a potential hotspot of moisture recycling, it is possible that using sub-grid rainfall schemes in all GCMs to improve how models represent Congo Basin evaporation during both wet seasons could further reduce the model spread in wet season rainfall.

3.6 Conclusions

In this chapter, we performed a process-based evaluation of the evaporation climatology for the Congo Basin wet seasons in eleven CMIP5 models contributing to AMIP. The key findings are:

1. GCMs with realistic rainfall in the Congo simulate higher rainfall in November, the peak of the second wet season, than March, the peak of the first, on the climatological average.

2. GCMs with realistic evaporation in the Congo simulate lower evaporation in November than March, because these models suppress transpiration.

3. In both wet seasons, sub-grid rainfall schemes in the GCMs with realistic evaporation make the models simulate a credible ratio of transpiration to canopy evaporation, and cause them to bring evaporation down into better agreement with LandFlux-EVAL reference data.

4. As a result, we broadly trust how evaporation is produced in the two wet seasons in the models with realistic evaporation, and argue that lower transpiration is likely to explain why evaporation is lower in November than March in reality.

5. In addition, we suggest that using sub-grid rainfall schemes in the land surface components of all GCMs could improve how the models produce Congo Basin evaporation during both wet seasons.

It is unclear why there would be less transpiration in November than March across the Congo Basin, when more rainfall is delivered to the Congo Basin in November. The processes controlling the lower November transpiration are likely to be crucial in explaining why the annual cycle of evaporation on the domain-wide average varies as it does. A follow up attribution analysis, in preparation by the authors, therefore aims to investigate what factors might be responsible. In addition, it is still unclear why models and reference data have lower evaporation in the summer dry season than the first wet season, and the authors are considering researching this in future.

As the Congo Basin is believed to be a hotspot of moisture recycling, using sub-grid rainfall schemes to improve how models produce Congo evaporation could lead to improvements in how models generate Congo rainfall. If implemented across models, this might lead to a narrowing of the large model spread in wet season rainfall in the Congo Basin. Further research is needed to confirm this hypothesis, and to examine whether using sub-grid rainfall schemes might provide hydrological benefits for other regions too. If the benefits are widespread, then consideration should be given to including these schemes as standard in the next generation of GCMs (Pitman 1991).

Acknowledgements

David Crowhurst is supported by the UK Natural Environment Research Council (NERC) through a Doctoral Training Partnership (grant NE/L002612/1). Richard Washington is supported by the NERC-Department for International Development (DfID)-funded Improving Model Processes for African Climate (IMPALA) project (grant NE/M017206/1), as part of the Future Climate for Africa (FCFA) programme (http://www.futureclimateafrica.org/project/impala/). AGCM data used in this chapter were downloaded from the Earth System Grid Federation (ESGF), at https:// pcmdi.llnl.gov/. CHIRPS2 data were downloaded from the Climate Hazards Group (ftp://ftp.chg.ucsb.edu/pub/org/chg/products/CHIRPS-2.0/, accessed 21 January 2020). This chapter uses the LandFlux-EVAL merged benchmark synthesis products of ETH Zurich produced under the aegis of the Global Energy and Water Exchanges (GEWEX) and Integrated Land-Ecosystem Atmosphere Process Study (ILEAPS) projects (http://www.iac.ethz.ch/url/research/LandFlux-EVAL/). The authors acknowledge the helpful inputs of Amy Creese, Ellen Dyer and Jian Peng in preparing the manuscript. We also thank the Editor and one anonymous reviewer, whose comments helped us to considerably improve the quality of the manuscript.

Appendix A

A.1 Canopy evaporation

LSMs typically incorporate an equation which considers a balance between rainfall, canopy evaporation and canopy throughfall in the previous time step to predict canopy water storage. LSMs then use leaf area index (the one-sided leaf area per unit ground area), which is either prescribed from satellite data (e.g. Running et al. (2017)), or predicted using a dynamic vegetation model (Yu et al. 2016), to calculate the fraction of wet foliage.

This is then typically used to scale potential evaporation, or the amount of evaporation that would occur if the water supply were sufficient, to an estimate of the current evaporation of water from the canopy store, as follows:

$$E_{\mathrm{c}} = F_{\mathrm{wet}}\,\rho\,\frac{qsat(T_{\mathrm{s}})-q_{\mathrm{a}}}{r_{\mathrm{a}}} \qquad (3.1)$$

where F_{wet} is the fraction of wet foliage, ρ is the density of air, $qsat(T_{\mathrm{s}})$ is the saturation specific humidity at near-surface air temperature T_{s}, q_{a} is the atmospheric specific humidity, and r_{a} is an aerodynamic resistance, which depends on a drag coefficient and on wind speed.

A.2 Transpiration

To calculate transpiration (or the flux of water vapour from plant stomata into the atmosphere), LSMs typically scale potential evaporation by the fraction of dry foliage, as follows:

$$E_{\mathrm{t}} = F_{\mathrm{dry}}\, \rho\, \frac{qsat(T_{\mathrm{s}}) - q_{\mathrm{a}}}{r_{\mathrm{a}} + r_{\mathrm{c}}} \tag{3.2}$$

where the equation uses F_{dry} (the fraction of dry foliage, equal to 1 minus F_{wet}), and an additional term r_c, the canopy resistance to transpiration. This defines the balance between the desire to close stomata to minimise transpiration, and open stomata to take in CO_2 (the 'stomatal conductance'), scaled up to the canopy leaf area (Damour et al. 2010). The canopy leaf area controls the number of stomata, and sets upper limits on plant transpiration (Jarvis and McNaughton 1986).

A.3 Soil evaporation

'Alpha' methods are typically used to calculate soil evaporation in LSMs. An equation for the alpha method is of the following form (Mahfouf et al. 1995):

$$E_{\mathrm{b}} = \rho\, \frac{\alpha\, qsat(T_{\mathrm{g}}) - q_{\mathrm{a}}}{r_{\mathrm{a}}} \tag{3.3}$$

where $qsat(T_g)$ is the saturation specific humidity at ground surface temperature T_g, and alpha is a coefficient which scales down this humidity to an estimate of the actual specific humidity of the upper soil layer. Note that T_g is used rather than T_s, because this allows for shortwave radiation to control the soil evaporation. In forest regions, a high leaf area reduces shortwave radiation penetrating to the ground surface, reduces T_g and reduces soil evaporation (Wang and Liu 2007). In many LSMs, alpha is defined by the thermodynamic relationship of Philip (1957), which depends on the soil matrix potential. This defines the maximum amount of water that can be retained in the soil, and is typically related to properties such as soil pore size (Whalley et al. 2013).

4 Contrasting controls on Congo Basin evaporation at the two rainfall peaks

David Crowhurst[1], Simon Dadson[1], Jian Peng[1,2] and Richard Washington[1]

[1]School of Geography and the Environment, University of Oxford, OX1 3QY, UK

[2]Department of Remote Sensing, Helmholtz Centre for Environmental Research, 04318, Leipzig, Germany

Submitted 07/05/2020, Accepted 17/11/2020, Published 05/12/2020, Issue 03/03/2021

Climate Dynamics, 56, 1609-1624

https://doi.org/10.1007/s00382-020-05547-1

Authorship declaration

David Crowhurst conducted all of the analysis and wrote this paper. Simon Dadson, Jian Peng and Richard Washington contributed to the planning of the methodology and the interpretation of the results and commented on and edited the manuscript during preparation and revision.

Abstract

Evaporation is a crucial driver of Congo Basin climate, but the dynamics controlling the seasonality of basin evaporation are not well understood. This chapter aims to discover why evaporation on the basin-wide average is lower at the November rainfall peak than the March rainfall peak, despite similar rainfall. Using 16-year mean LandFlux-EVAL data, we find that evaporation is lower in November than March in the rainforest and the eastern savannah. The ERA5-Land reanalysis, which effectively reproduces this pattern, shows that transpiration is the main component responsible for lower evaporation in these regions. Using ERA5-Land, we find the following contrasting controls on transpiration, and therefore evaporation, at the two rainfall peaks: (a) In the northern rainforest, there is lower leaf area index (LAI) in November, which is plausibly driven by lower surface downward shortwave radiation (DSR), and lower vapour pressure deficit (VPD) in November, which is plausibly driven by lower sensible heat flux that results from lower net radiation. The combination of lower LAI and VPD explains lower transpiration, and therefore lower evaporation, in November. (b) In the southern rainforest, and in the north-eastern savannah, there is lower LAI in November, which is plausibly driven by lower surface DSR, and this explains lower transpiration, and therefore lower evaporation, in November. (c) In the south-eastern savannah, there is lower LAI in November, which is plausibly driven by lower volumetric water content (VWC), and this explains lower transpiration, and therefore lower evaporation, in November. Collectively, these contrasting controls at the two rainfall peaks provide a plausible explanation for why the basin-wide average evaporation is lower in November than March.

4.1 Introduction

The Congo Basin is one of the most convectively active regions of the world, receiving around 1500 to 2000 mm of rainfall per year (Dezfuli 2017). Over 60% of the rainfall occurs during the wet seasons (Hua et al. 2019), and the basin-wide average seasonal cycle has two rainfall peaks, one in March and the other in November, as discussed in Chapter 3. Approximately 75% of the rainfall is delivered by mesoscale convective systems (Jackson et al. 2009), which are contiguous areas of cold cloud that exceed 25,000 km^2 in size (Taylor et al. 2018). A maximum of thunderstorm activity occurs over the eastern Congo Basin, and this region has one of the highest rainfall totals in the tropics, with an average of 10 mm day^{-1} delivered during boreal winter (Sandjon et al. 2012). Knowledge of the processes that affect Congo Basin rainfall and its future change is desirable for adaptation planning (Nicholson 2018a), as the basin region has a population of more than 75 million people, the majority of whom rely on subsistence agriculture for food and income (Samba and Nganga 2012).

An important factor that affects the seasonality of Congo Basin rainfall which has received little research attention is evaporation from the land surface (Alsdorf et al. 2016). Evaporation is the sum of canopy evaporation, soil evaporation and transpiration (Lawrence et al. 2007). The land surface of the basin, which transitions from a tropical rainforest in the northern half to a deciduous savannah in the southern half, features continually high evaporation throughout the year. This is believed to make a substantial contribution to local rainfall, as evident in high recycling ratios for the basin (Dyer et al. 2017; Sori et al. 2017).

Despite the importance of evaporation for Congo Basin climate, the broad-scale dynamics controlling the seasonality of basin evaporation are not well understood. Knowledge of what controls the present-day seasonality of basin evaporation would provide a point of reference with which to compare climate and ecosystem models. This evaluation would determine whether these models produce the correct seasonality of evaporation for the right reasons (Maeda et al. 2017; Adole et al. 2019). Additionally, without a robust understanding of controls on the present-day seasonality, it is difficult to analyse whether model projections of shifts in the seasonality of Congo Basin evaporation are trustworthy (Berg and Sheffield 2019).

4.1.1 Lower evaporation in November than March in the Congo Basin

Previous studies suggest that although rainfall is likely to be an important control on the seasonal cycle of evaporation in Tropical Africa, other factors could additionally modulate this cycle. For example, in a small region north-west of the basin, Gond et al. (2013) discussed possible controls on the seasonal cycle of enhanced vegetation index (EVI), a variable closely related to evaporation. They argued that the seasonal cycle of EVI is primarily controlled by rainfall, but that light availability is an important secondary control. In this same region, Philippon et al. (2016) argued that there is higher rainfall in the September-October-November (SON) wet season than the March-April-May (MAM) wet season, but lower EVI in SON than MAM. This suggests that factors other than rainfall could modulate EVI during SON.

Results from Chapter 3 showed that averaged across the Congo Basin, the best performing global climate models (GCMs) with low root mean square errors (RMSEs) against CHIRPS2 rainfall (Funk et al. 2015) have slightly higher rainfall at the November rainfall peak than the March rainfall peak. While this agrees with several studies (Haensler et al. 2013; Washington et al. 2013; Creese and Washington 2016), and several reanalyses (Figure 4.1a, Table 4.1), the CHIRPS2 data set, which has the best agreement of 10 satellite and gauge rainfall products against the NIC131-Gridded rainfall dataset in the Congo Basin (Nicholson et al. 2019), has a similar amount of rainfall at the two peaks (Figure 4.1a, Table 4.1). This suggests that rainfall amounts on the basin-wide average are similar in March and November. Results from Chapter 3 also showed that the best performing GCMs with low RMSEs against LandFlux-EVAL evaporation reference data (Mueller et al. 2013) have lower evaporation in November than March on the basin-wide average, which agrees with several reanalyses (Figure 4.1b, Table 4.1).

Similar rainfall amounts in March and November suggest that lower water availability is not the cause of lower evaporation in November than March. This similar rainfall also suggests that cloud cover is similar and that lower energy availability is not the cause of lower evaporation either. It therefore remains unclear why evaporation on the basin-wide average is lower at the November rainfall peak than the March rainfall peak, despite similar amounts of rainfall in an equatorial climate. An understanding of the dynamics controlling the seasonality of basin evaporation will only be achieved when factors controlling this difference are revealed.

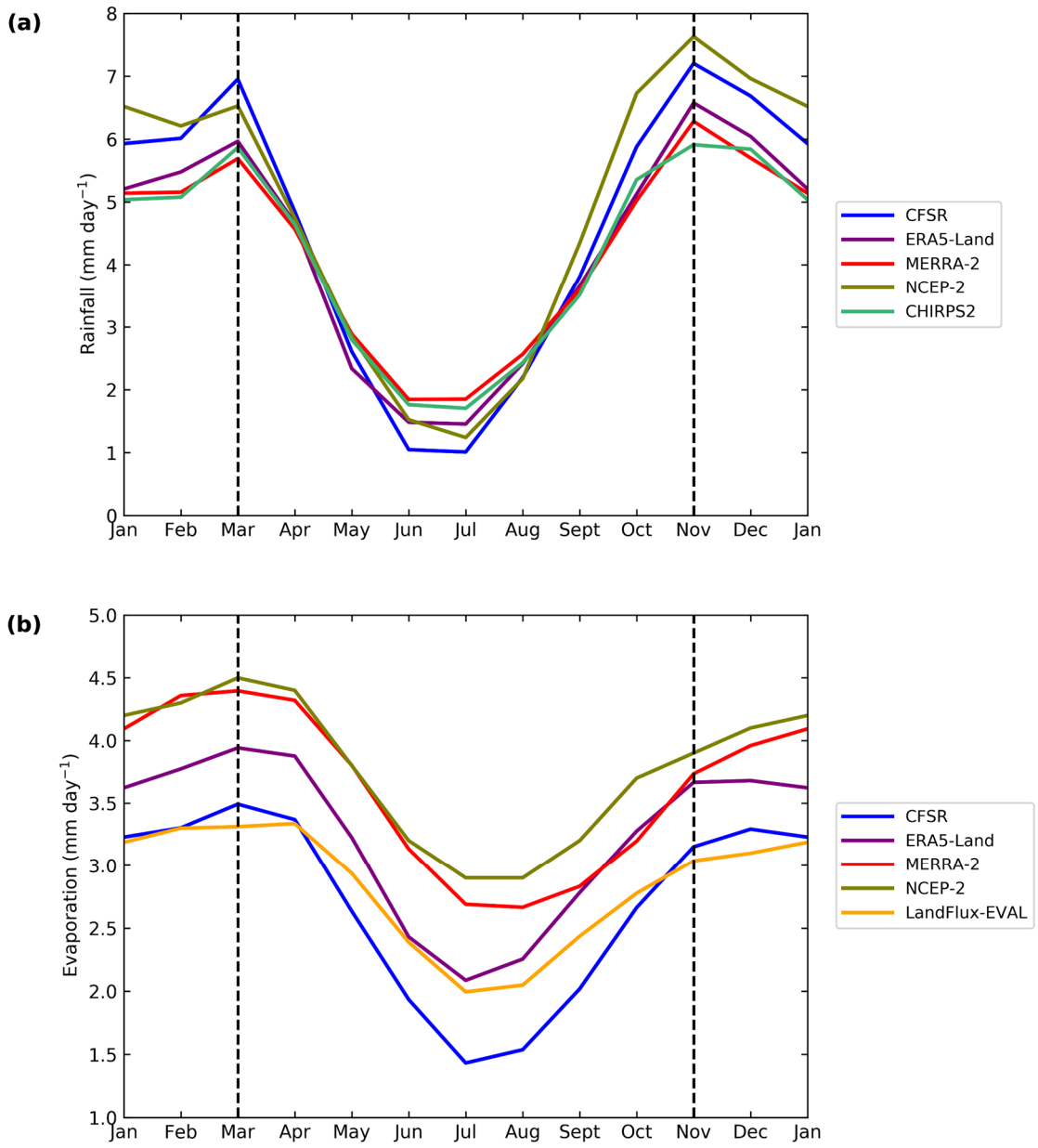


Figure 4.1 Sixteen-year mean (1989-2005) seasonal cycles of **a** rainfall (mm day^{-1}) and **b** evaporation (mm day^{-1}) averaged over the Congo Basin (14°S to 4°N, 18°E to 30°E), from four reanalyses, CFSR (Saha et al. 2010), ERA5-Land (Hersbach et al. 2020), MERRA-2 (Gelaro et al. 2017) and NCEP-2 (Kanamitsu et al. 2002), and two reference data sets, CHIRPS2 rainfall (Funk et al. 2015) and LandFlux-EVAL evaporation (Mueller et al. 2013)

Table 4.1 November minus March rainfall (mm day^{-1}) and evaporation (mm day^{-1}), averaged over the Congo Basin (14°S to 4°N, 18°E to 30°E) from four reanalysis data sets and two reference data sets

Data Set	Data Set Type	November minus March Rainfall (mm day^{-1})	November minus March Evaporation (mm day^{-1})
CFSR (Saha et al. 2010)	Reanalysis	+0.25	-0.34
ERA5-Land (Hersbach et al. 2020)	Reanalysis	+0.61	-0.33
MERRA-2 (Gelaro et al. 2017)	Reanalysis	+0.59	-0.66
NCEP-2 (Kanamitsu et al. 2002)	Reanalysis	+1.10	-0.53
CHIRPS2 Rainfall (Funk et al. 2015) and LandFlux-EVAL Evaporation (Mueller et al. 2013)	Reference	+0.04	-0.35

As evaporation is the sum of three components, a fluctuation in any of these components will cause evaporation to fluctuate (Fisher et al. 2017; Berg and Sheffield 2019). To find out why evaporation is lower in November than March on the basin-wide average, and to begin understanding the controls on the seasonal cycle of basin evaporation, this chapter will first need to identify where in the basin evaporation is lower in November than March, and then discover which evaporation components are responsible in these regions separately. Chapter 3 showed that on the basin-wide average, the best performing GCMs have similar canopy evaporation and soil evaporation in March and November, but lower transpiration in November than March. It was therefore argued that lower transpiration is likely to explain why evaporation is lower in November than March on the basin-wide

average. This result suggests that where evaporation is lower within the basin, lower transpiration could be responsible, although this needs to be verified. Once the relevant evaporation components are identified regionally, we can then establish contrasting controls on these components at the two rainfall peaks, which cause the components to be reduced in November, and therefore cause the evaporation to be lower in November than March in the identified regions. Collectively, these contrasting controls provide the explanation for why evaporation is lower at the November rainfall peak than the March rainfall peak on the basin-wide average.

4.1.2 Aims

To move towards a physical understanding of why Congo Basin evaporation on the basin-wide average is lower at the November rainfall peak than the March rainfall peak, despite similar amounts of rainfall in an equatorial climate, this chapter aims to:

1. Identify where in the basin lower evaporation in November than March occurs.

2. Discover which evaporation components are responsible for lower evaporation in November than March in the identified regions.

3. Establish contrasting controls on the evaporation components at the two rainfall peaks, which cause the evaporation components to be reduced in November, and therefore cause the evaporation to be lower in November than March in the identified regions.

4.2 Data and methods

4.2.1 Domain and evaporation reference data

The studied domain for the Congo Basin is 14°S to 4°N, 18°E to 30°E (Figure 4.2), which covers the evergreen tropical rainforests in the northern half, and the deciduous savannah in the southern half (see Figure 2 from Yan et al. (2017)).

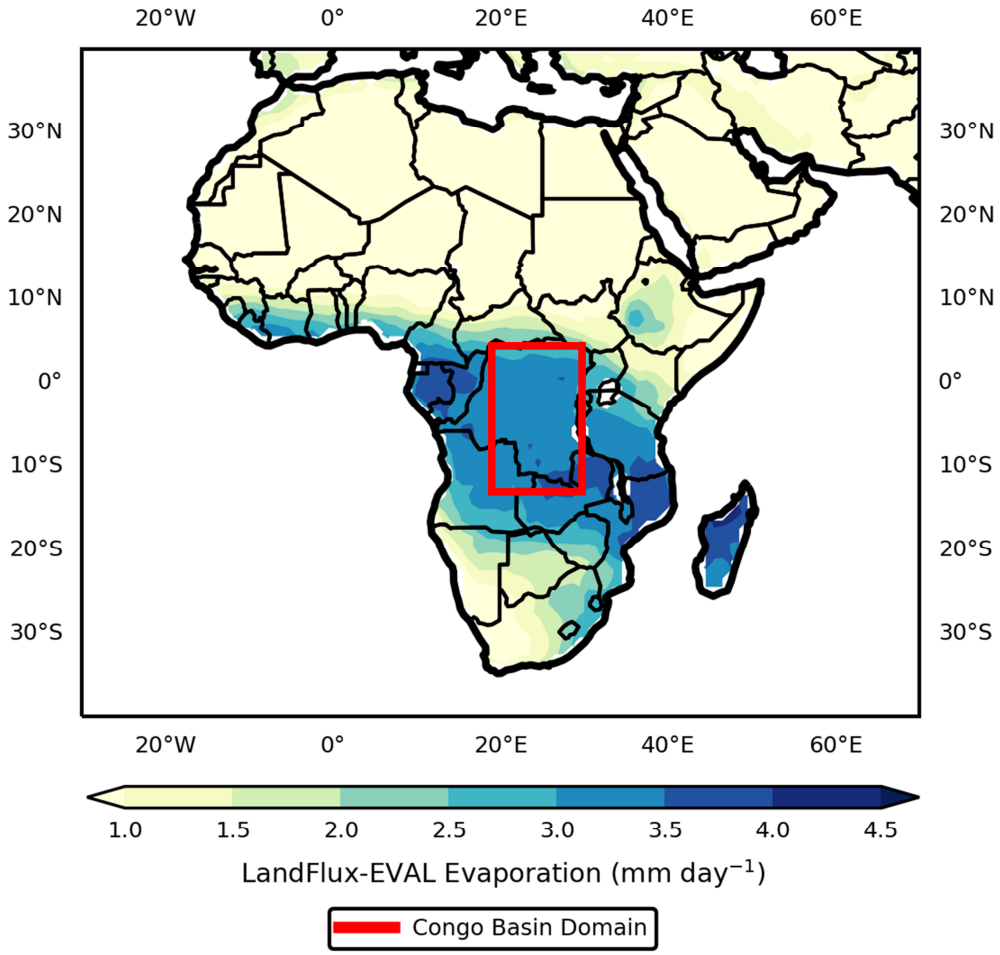


Figure 4.2 Sixteen-year mean (1989-2005) evaporation across Africa (mm day^{-1}) from the LandFlux-EVAL synthesis data set. Congo Basin domain used in this chapter (14°S to 4°N, 18°E to 30°E) is shown with a red box

All data sets are averaged over 1989-2005 to produce monthly climatologies. We use LandFlux-EVAL (Mueller et al. 2013) to identify spatially where in the domain lower evaporation in November than March occurs. The main reasons for using LandFlux-EVAL in the absence of in-situ evaporation observations are that LandFlux-EVAL performed well across the African continent in a water budget evaluation (Weerasinghe et al. 2020), compares favourably against several other products in the basin (Trambauer et al. 2014), and is an ensemble product that does not prioritize use of one algorithm alone (Miralles et al. 2016). Further details are available in Chapter 3.

4.2.2 Reanalysis data

The LandFlux-EVAL evaporation product does not have data available for the three evaporation components. Therefore, we use a reanalysis which does produce this data to discover which evaporation components are responsible for lower evaporation in November than March within the basin. Reanalyses assimilate observations with a numerical model to generate a dynamically consistent, gridded estimate of the climate system (Parker 2016). They are useful tools that can help understand climate dynamics in data-scarce parts of the world (Hua et al. 2019).

However, as there is little agreement between reanalyses on their simulation of the hydrological cycle in the Congo Basin (Washington et al. 2013; Maidment et al. 2015), it is necessary to find a reanalysis which effectively reproduces the evaporation difference between March and November from LandFlux-EVAL. Good agreement would indicate that a reanalysis is deriving the evaporation difference using a realistic set of processes.

This would allow us to trust how the reanalysis partitions the evaporation difference into its three components, and then use this reanalysis to establish reasons why specific evaporation components are lower in November than March in the different regions of the basin.

We use three criteria to determine whether a reanalysis is suitable for evaluation against LandFlux-EVAL: (1) the reanalysis is the latest version available of its type, (2) the reanalysis is fully independent from LandFlux-EVAL, which allows for a fair comparison, and (3) data for evaporation, its three components, and a variety of evaporation drivers are available from the reanalysis. To the knowledge of the authors, ERA5-Land and MERRA-2 are the only reanalyses that meet these criteria (Mueller et al. 2013; Schwingshackl et al. 2017). Further details on LandFlux-EVAL and the two reanalyses to be evaluated are described in Table 4.2.

Table 4.2 Further details on LandFlux-EVAL and the reanalyses evaluated in this chapter. Monthly climatologies are produced by averaging over 1989-2005

Data Set	Spatial Resolution	Temporal Resolution	Available Periods	Land Surface Model
LandFlux-EVAL (Mueller et al. 2013)	1.0° x 1.0°	Monthly	1989-2005	LandFlux-EVAL Synthesis Algorithm (Mueller et al. 2013)
MERRA-2 (Gelaro et al. 2017)	0.5° x 0.625°	Monthly	1980-2008	MERRA-2 Catchment Model (Reichle et al. 2017)
ERA5-Land (Hersbach et al. 2020)	0.1° x 0.1°	Monthly	1981-2020	CH-TESSEL (Balsamo et al. 2009)

4.2.3 Methods

We first produce a climatological November minus March evaporation difference map for LandFlux-EVAL by calculating the spatial distribution of LandFlux-EVAL evaporation for March and November for the studied domain, and subtracting the March distribution from the November distribution. The resulting difference map allows us to identify the regions of the basin with lower evaporation in November than March. We then produce a November minus March evaporation difference map for the ERA5-Land and MERRA-2 reanalyses, and select the reanalysis which most effectively reproduces LandFlux-EVAL.

Using the selected reanalysis, we produce November minus March difference maps for canopy evaporation, soil evaporation and transpiration, and discover which of the evaporation components are responsible for lower evaporation in November than March in the basin regions identified from LandFlux-EVAL. We then produce November minus March difference maps for a range of possible controls on these particular components. This allows us to determine contrasting controls which cause these components to be reduced in November, and therefore cause evaporation to be lower in November than March in the basin regions identified from LandFlux-EVAL. Methods used to derive each of the controls are listed in Appendix B.

The robustness of the difference between the March and November values is assessed on each difference map using the double-sided Students *t*-test. Stippling indicates where the mean difference between March and November is statistically significant ($p < 0.05$).

4.3 Lower evaporation in November than March

4.3.1 Regions

Figure 4.3a shows the November minus March evaporation difference map produced by LandFlux-EVAL.

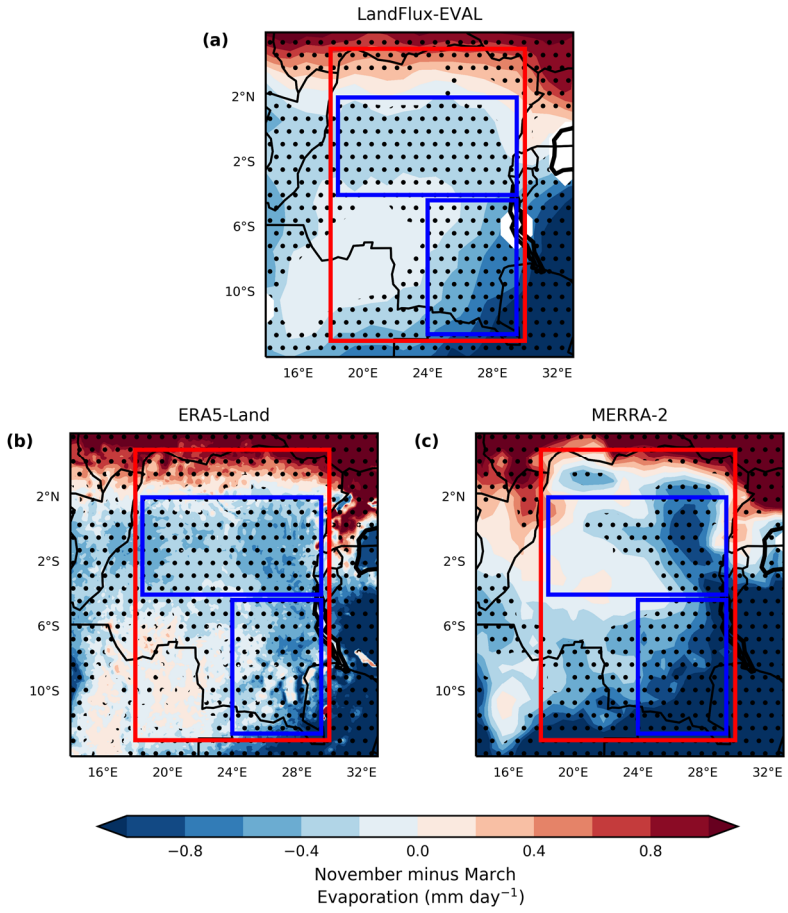


Figure 4.3 16-year mean (1989-2005) November minus March evaporation (mm day^{-1}) difference maps from **a** LandFlux-EVAL, **b** ERA5-Land, and **c** MERRA-2. The domain used in this chapter (14°S to 4°N, 18°E to 30°E) is shown with a red box. Sub-domains are shown with blue boxes and indicate the two regions in LandFlux-EVAL where evaporation is lower in November than March: (1) the rainforest, and (2) the eastern savannah. Dots are grid points where the difference between March and November is statistically significant ($p<0.05$)

There is lower evaporation in November than March in two regions: (1) the rainforest, with coordinates 4°S to 2°N, 18°E to 30°E and a regional mean difference of -0.25 mm day^{-1}, and (2) the eastern savannah, with coordinates 14°S to 4°S, 24°E to 30°E and a regional mean difference of -0.60 mm day^{-1}. As the processes controlling evaporation might be influenced by vegetation type, we analyse these two regions separately in the rest of the chapter.

4.3.2 ERA5-Land v MERRA-2

We now discuss whether ERA5-Land or MERRA-2 should be used to discover which components are responsible for lower evaporation in November than March in the rainforest and the eastern savannah. Figure 4.3b shows the November minus March evaporation difference map produced by ERA5-Land. This reanalysis does effectively reproduce the pattern of lower evaporation in November than March in the rainforest and the eastern savannah that is evident in LandFlux-EVAL (Figure 4.3a). Even though in the eastern rainforest (coordinates 4°S to 2°N, 24°E to 30°E), regional mean evaporation in ERA5-Land is 0.45 mm day^{-1} lower in November than March, as opposed to 0.30 mm day^{-1} for LandFlux-EVAL, this small discrepancy is too insignificant to rule out ERA5-Land as a preferred reanalysis.

Figure 4.3c shows the November minus March evaporation difference map produced by MERRA-2. This reanalysis does not effectively reproduce the pattern of lower evaporation in November than March in the rainforest and the eastern savannah evident in LandFlux-EVAL (Figure 4.3a). In the eastern rainforest (coordinates 4°S to 2°N, 24°E

to 30°E), regional mean evaporation in MERRA-2 is 0.80 mm day^{-1} lower in November than March, as opposed to 0.30 mm day^{-1} for LandFlux-EVAL. In the eastern savannah, regional mean evaporation in MERRA-2 is 0.90 mm day^{-1} lower in November than March, as opposed to 0.60 mm day^{-1} for LandFlux-EVAL. These two discrepancies rule out the further use of MERRA-2 in this chapter.

The good agreement between LandFlux-EVAL and ERA5-Land suggests that the ERA5-Land reanalysis is deriving the evaporation difference between March and November using a realistic set of processes. Therefore, we use ERA5-Land data to discover the evaporation components responsible for lower evaporation in November than March in the rainforest and the eastern savannah.

4.3.3 Rainforest

Figure 4.4 shows the November minus March canopy evaporation (Figure 4.4a), soil evaporation (Figure 4.4b), and transpiration (Figure 4.4c), difference maps produced by the ERA5-Land reanalysis. In the rainforest, regional mean evaporation in ERA5-Land is 0.35 mm day^{-1} lower in November than March (Figure 4.3b). This is partitioned into 0.26 mm day^{-1} higher canopy evaporation (Figure 4.4a), 0.02 mm day^{-1} lower soil evaporation (Figure 4.4b) and 0.59 mm day^{-1} lower transpiration (Figure 4.4c). In ERA5-Land, lower transpiration is 97% responsible for lower evaporation in November than March, with 3% explained by lower soil evaporation. On the regional mean, transpiration is therefore the main component responsible for lower evaporation in November than March in the rainforest. However, higher canopy evaporation in November than March offsets lower transpiration, thereby reducing the amplitude of the evaporation difference.

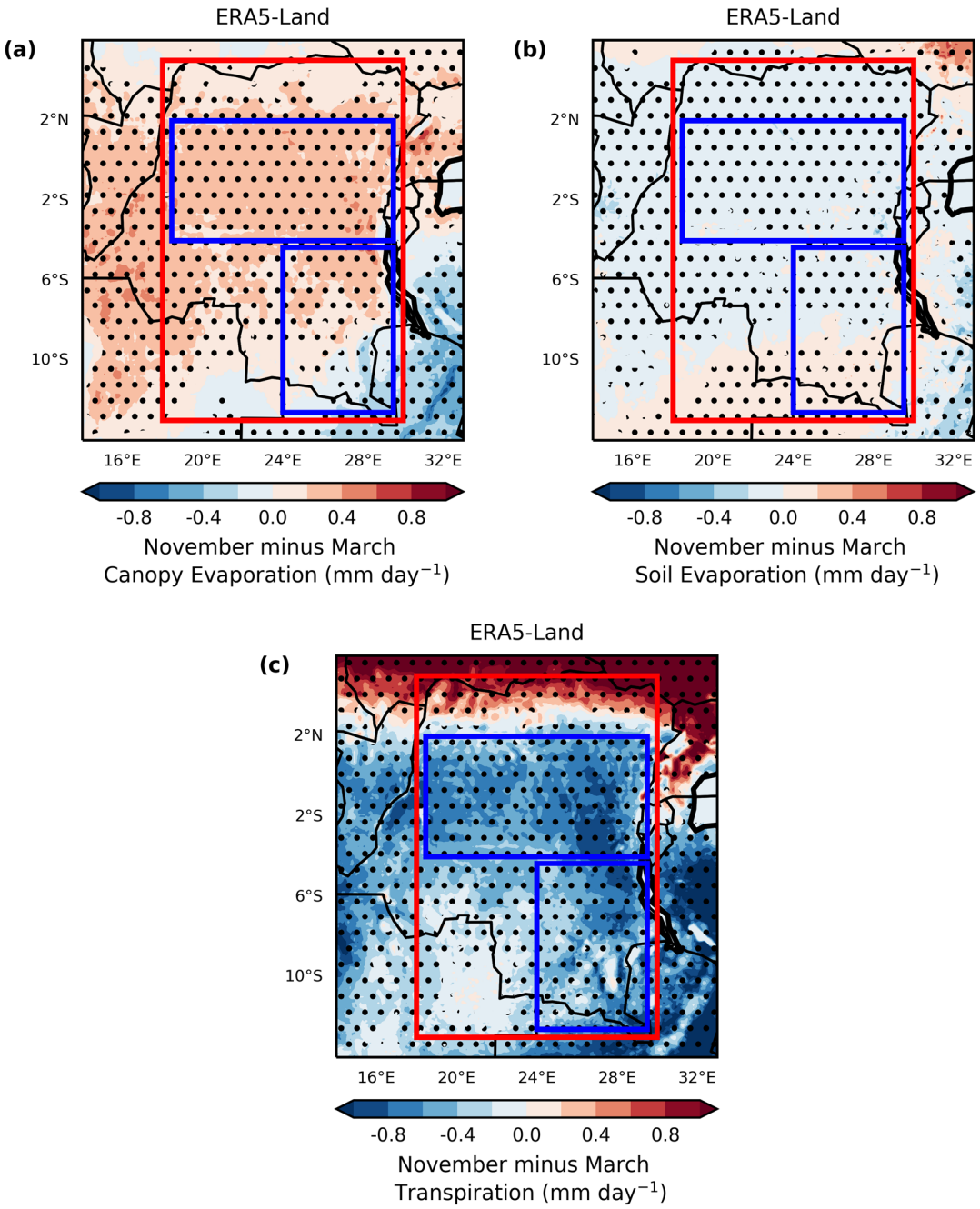


Figure 4.4 Sixteen-year mean (1989-2005) **a** November minus March canopy evaporation (mm day^{-1}), **b** November minus March soil evaporation (mm day^{-1}), and **c** November minus March transpiration (mm day^{-1}), difference maps from ERA5-Land. Domains are as for Figure 4.3. Dots are grid points where the difference between March and November is statistically significant ($p<0.05$)

At every grid point within the rainforest, Figure 4.4 shows that lower transpiration is almost fully responsible for lower evaporation in November than March, with soil evaporation explaining the very small remainder. There are some hotspots where the transpiration difference between March and November is much larger than the regional mean. The most prominent is at the 2°S, 28°E coordinate, where transpiration is 0.85 mm day^{-1} lower in November than March.

4.3.4 Eastern savannah

In the eastern savannah, regional mean evaporation in ERA5-Land is 0.53 mm day^{-1} lower in November than March (Figure 4.3b). This is partitioned into 0.02 mm day^{-1} higher canopy evaporation (Figure 4.4a), 0.01 mm day^{-1} higher soil evaporation (Figure 4.4b) and 0.57 mm day^{-1} lower transpiration (Figure 4.4c). On the regional mean, transpiration is therefore the only component responsible for lower evaporation in November than March in the eastern savannah. An interesting observation is that the offsetting of lower transpiration in November by higher canopy evaporation does not occur in the eastern savannah. This explains why the evaporation difference between the March and November months is larger in the eastern savannah (-0.53 mm day^{-1}) than in the rainforest (-0.35 mm day^{-1}) on the regional mean.

Figure 4.4 shows that the partitioning of the evaporation difference into its components varies within the eastern savannah. In the north-eastern savannah, coordinates 9°S to 4°S, 24°E to 30°E, regional mean evaporation in ERA5-Land is 0.37 mm day^{-1} lower in November than March (Figure 4.3b), because canopy evaporation is 0.16 mm day^{-1}

higher, soil evaporation is 0.02 mm day^{-1} lower and transpiration is 0.51 mm day^{-1} lower (Figure 4.4). Lower transpiration is therefore responsible for 96% of the lower evaporation in November than March, with 4% explained by lower soil evaporation. In the south-eastern savannah, coordinates 14°S to 9°S, 24°E to 30°E, regional mean evaporation in ERA5-Land is 0.66 mm day^{-1} lower in November than March (Figure 4.3b) because canopy evaporation is 0.12 mm day^{-1} lower, soil evaporation is 0.03 mm day^{-1} higher and transpiration is 0.57 mm day^{-1} lower (Figure 4.4). Lower transpiration is therefore responsible for 83% of the lower evaporation in November than March, with 17% explained by lower canopy evaporation.

4.4 Contrasting controls on transpiration at the two rainfall peaks

As transpiration is largely responsible for the lower evaporation, we now use ERA5-Land to establish contrasting controls on transpiration at the two rainfall peaks of March and November. These cause transpiration to be reduced in November, and therefore lower the evaporation in November compared to March in the rainforest and the eastern savannah. Collectively, these contrasting controls provide an explanation for why evaporation is lower in November than March on the basin-wide average. To establish these contrasting controls, we produce November minus March difference maps for possible controls on the lower transpiration, and then discuss whether the contrasts in these controls are sufficient to explain the lower transpiration. If they are sufficient, we suggest what causes these controls to differ between March and November.

4.4.1 Leaf area index (LAI) and vapour pressure deficit (VPD)

Although several drivers interact to control transpiration variability, studies confirm that leaf area index (LAI), or the one-sided leaf area per unit ground area, is the main control on transpiration at a global scale (Lian et al. 2018). Lower LAI typically means that there are fewer stomata, which results in lower water supply through transpiration (Wei et al. 2017). Another variable which may contribute to the lower transpiration is lower vapour pressure deficit (VPD), defined as the atmospheric demand that provides the driving force for transpiration (Massmann et al. 2019). Given that VPD is believed to have implications for land surface processes in the Amazon (Barkhordarian et al. 2019), VPD could also be important in the Congo. Lower VPD typically means that the atmospheric demand for evaporation is lower, and so less water moves through the stem and transpires through the stomata (Bonal et al. 2016).

Figure 4.5 shows the November minus March LAI (Figure 4.5a) and VPD (Figure 4.5b) difference maps produced by ERA5-Land. The derivation of LAI is presented in Appendix B.1, and the derivation of VPD is presented in Appendix B.2. It should be noted that LAI variables are prescribed in ERA5-Land from the MODIS Collection 5 satellite product (Boussetta et al. 2013). In the rainforest, there are variations in the LAI and VPD differences between the northern and southern rainforest, while in the eastern savannah, there is variation in the VPD difference between the north-eastern and south-eastern savannah. We therefore sub-divide the two regions of lower evaporation into their northern and southern halves, as indicated on Figure 4.5, and analyse these four sub-domains separately.

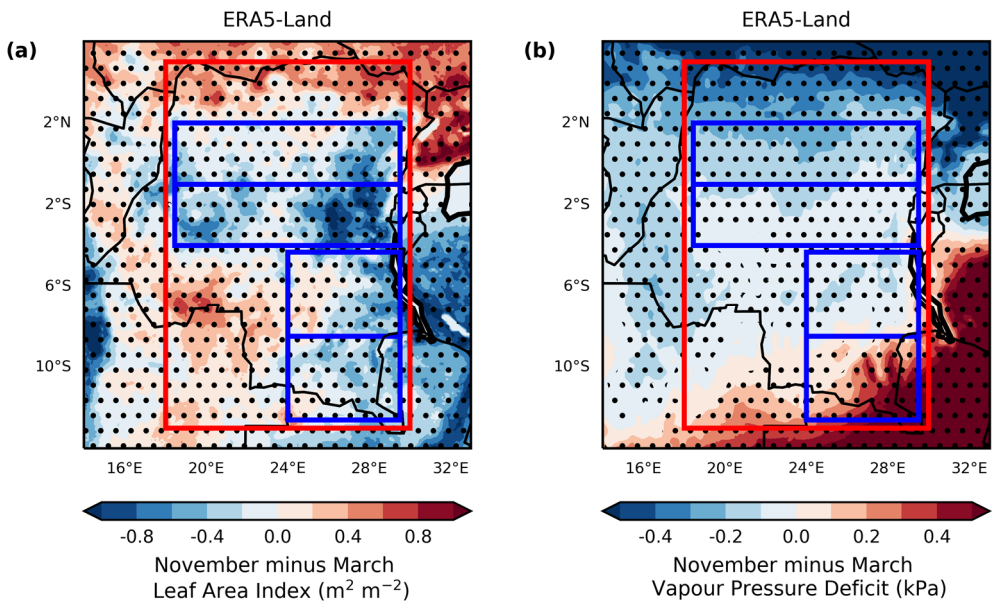


Figure 4.5 Sixteen-year mean (1989-2005) **a** November minus March LAI (m^2 m^{-2}), and **b** November minus March VPD (kPa), difference maps from ERA5-Land. Domains are as for Figure 4.3, with additional sub-division into the northern rainforest, southern rainforest, north-eastern savannah and south-eastern savannah. Dots are grid points where the difference between March and November is statistically significant ($p<0.05$)

The differences in VPD between March and November in the southern rainforest (-0.06 kPa) and the north-eastern savannah (-0.02 kPa) are very small (Figure 4.5b) and do not contribute to the lower transpiration in November than March. Lower LAI alone is therefore likely to explain the lower November transpiration in these parts of the basin (Figure 4.5a). In the southern rainforest, where VPD is not an important control, the ΔLAI/ΔTranspiration ratio is approximately 1.0. This indicates that where LAI is 1 unit lower, transpiration is 1 mm day^{-1} lower. As the northern rainforest and southern rainforest are of identical vegetation type, the ΔLAI/ΔTranspiration ratio of 1.0 applies to the northern rainforest too. Figure 4.5a shows that there is 0.18 m^2 m^{-2} lower LAI in November than March in the northern rainforest, which implies that there should be 0.18 mm day^{-1} lower transpiration in November than March. However, transpiration is 0.46

mm day^{-1} lower in November than March (Figure 4.4c). This indicates that another variable further lowers the transpiration difference in the northern rainforest. In this region, VPD is 0.17 kPa lower in November than March (Figure 4.5b), and the combination of 0.18 m^2 m^{-2} lower LAI and 0.17 kPa lower VPD offers a full explanation for 0.46 mm day^{-1} lower transpiration in November than March in ERA5-Land.

In the south-eastern savannah, VPD is 0.39 kPa higher in November than March (Figure 4.5b). This causes higher evaporative demand, which should theoretically lead to higher transpiration. However, the down-regulation of transpiration in November compared to March suggests that the effect of the lower LAI (Figure 4.5a) outweighs the effect of the higher VPD (Figure 4.5b), and that the lower LAI explains the lower transpiration.

4.4.2 Lower LAI in November than March

In the natural environment, LAI is controlled by soil moisture and surface solar radiation (Cowling and Field 2003; Myneni et al. 2007). We therefore calculate November minus March difference maps for soil moisture and solar radiation from ERA5-Land, and assess whether lower water or light availability is likely to drive lower LAI in November than March in the four sub-domains. Since LAI is prescribed from the MODIS satellite in ERA5-Land, the soil moisture and solar radiation produced by ERA5-Land do not drive LAI in ERA5-Land. Therefore, it is not possible to make causal statements regarding drivers of LAI in ERA5-Land, and this is a caveat on our interpretation.

The measure of soil moisture we use is one metre volumetric water content (VWC), which is the percentage of wet soil mass compared to total soil mass. The derivation of one metre VWC from ERA5-Land data is presented in Appendix B.3. Figure 4.6 shows the November minus March VWC difference map produced by ERA5-Land (Figure 4.6a), as well as water budget diagrams for the four parts of the basin (Figure 4.6b, c, d, e). These diagrams allow us to determine why VWC differs between March and November in ERA5-Land.

The measure of solar radiation we use is surface downward shortwave radiation (DSR). This variable is available directly from ERA5-Land. November minus March difference maps are presented for surface DSR (Figure 4.7a) as well as the decomposition into its three components: (1) top-of-atmosphere (TOA) DSR (Figure 4.7b) + (2) the reduction in surface DSR due to cloud cover (‘cloud forcing’) (Figure 4.7c) + (3) the reduction in surface DSR due to atmospheric absorption (‘atmospheric forcing’) (Figure 4.7d). The derivation of these components from ERA5-Land is presented in Appendix B.4. These maps allow us to determine why surface DSR differs between March and November.

4.4.2.1 Northern rainforest

In the northern rainforest, VWC is 7% higher in November than March, with values of 35% in March and 42% in November (Figure 4.6a). Higher VWC in November than March occurs due to soil moisture accumulation between March and May and between July and November, which outweighs soil moisture depletion between May and July (Figure 4.6b). Higher water availability in November than March cannot explain why LAI is lower in November than March. The typical field capacity of the clay soil in the basin is between 45% and 55%, so the soil in November is close to saturation (Van Engelen et al. 2013) and water availability is not a control on leaf growth. Instead, light availability is a plausible control on the growth of leaves as the soil moisture content is high. There is 26 W m^{-2} lower surface DSR in November than March (Figure 4.7a). This is the sum of 18 W m^{-2} less TOA DSR (Figure 4.7b), 12 W m^{-2} less surface DSR due to higher cloud cover (Figure 4.7c), and 4 W m^{-2} more surface DSR due to lower atmospheric absorption (Figure 4.7d). Therefore, lower surface DSR, caused by lower TOA DSR and higher cloud cover, is a plausible explanation for why LAI is 0.18 m^2 m^{-2} lower in November than March (Figure 4.5a).

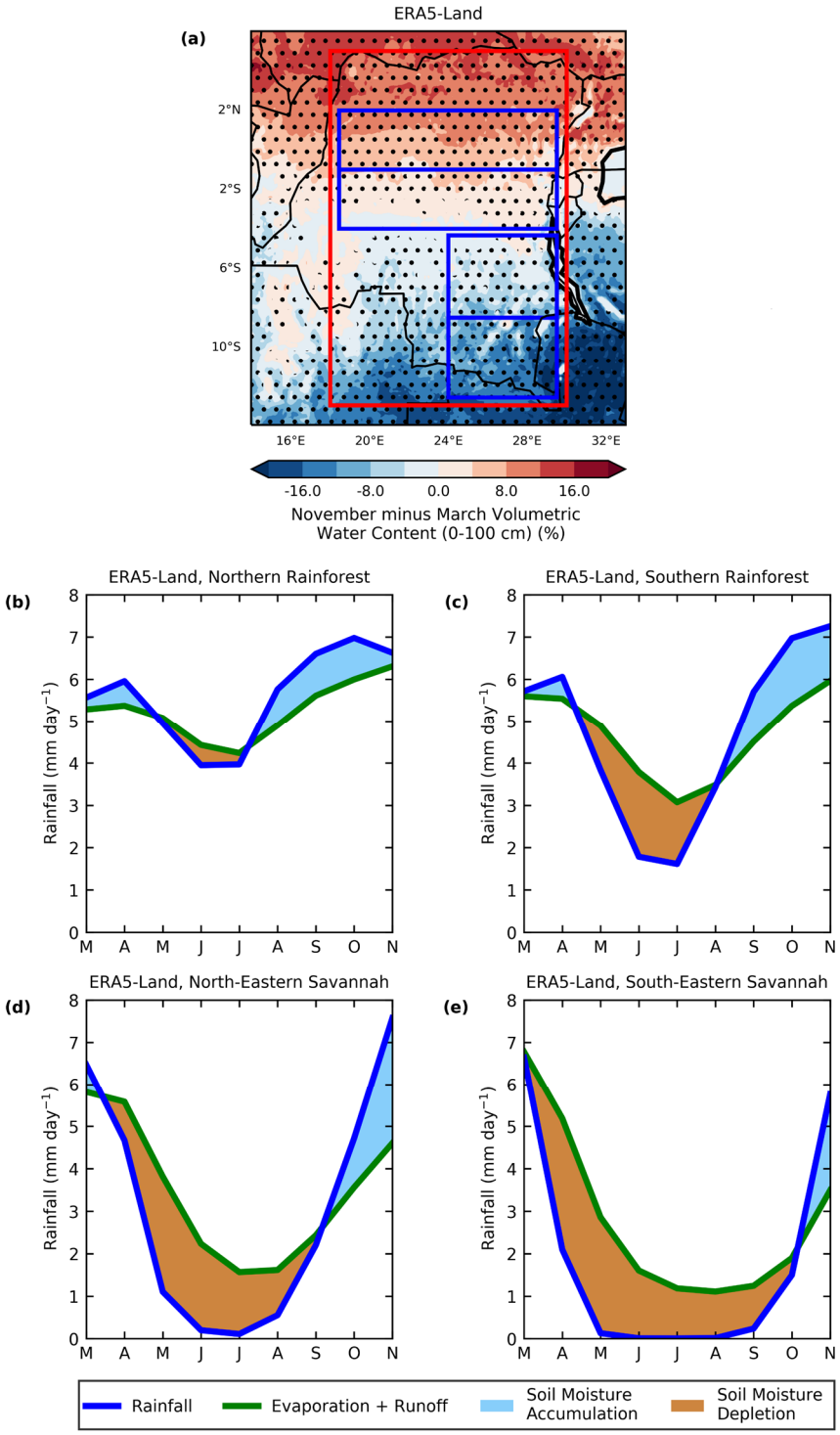


Figure 4.6 a Sixteen-year mean (1989-2005) November minus March VWC (%) difference map from ERA5-Land, where domains are as for Figure 4.5, and dots are grid points where the difference between March and November is statistically significant ($p<0.05$). **b-e** Sixteen-year mean (1989-2005) water budget diagrams from ERA5-Land for **b** the northern rainforest, **c** the southern rainforest, **d** the north-eastern savannah, and **e** the south-eastern savannah

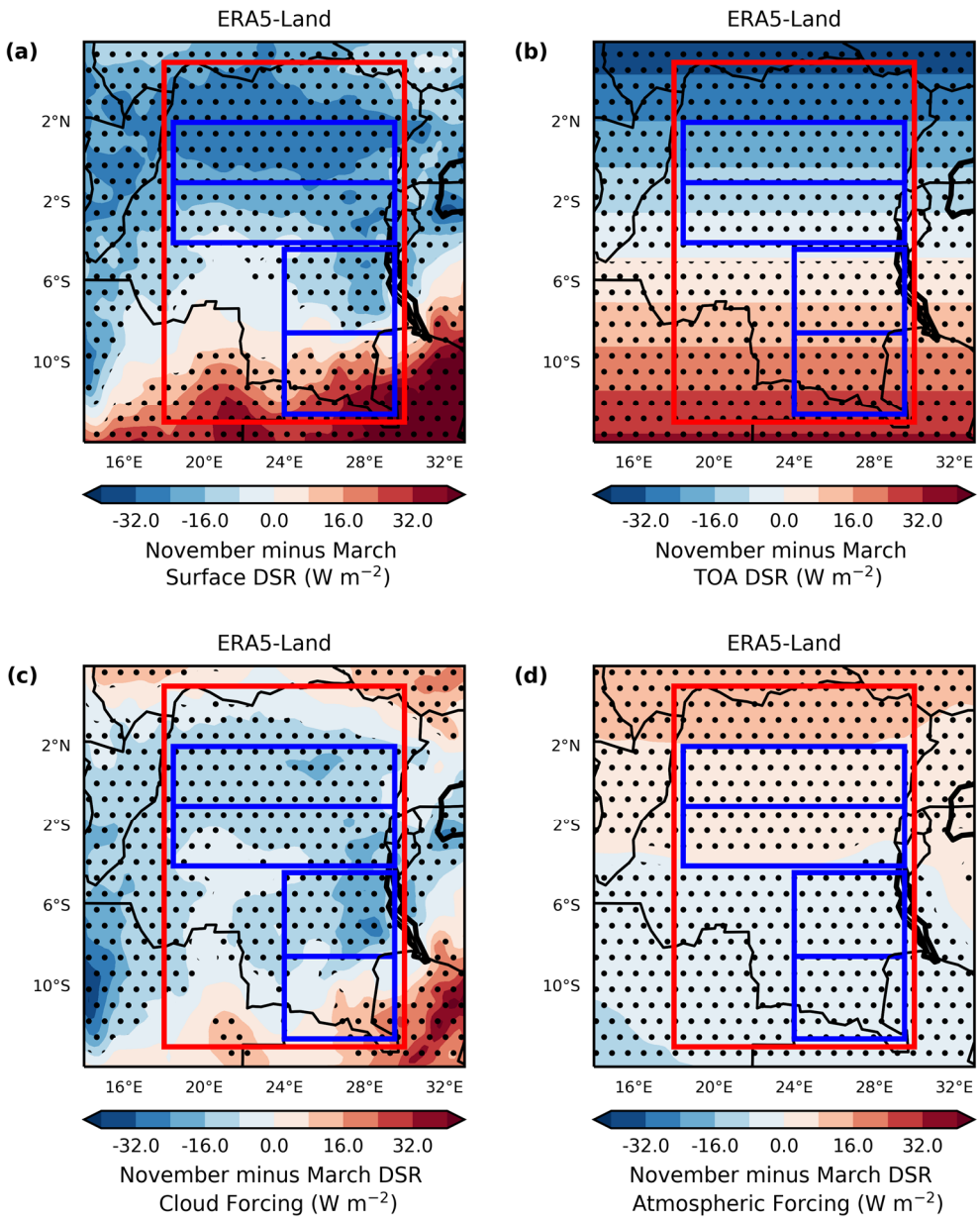


Figure 4.7 16-year mean (1989-2005) **a** November minus March surface DSR (W m^{-2}), **b** November minus March top-of-atmosphere DSR (W m^{-2}), **c** November minus March cloud forcing (W m^{-2}), and **d** November minus March atmospheric forcing (W m^{-2}), difference maps from ERA5-Land. Domains are as for Figure 4.5. Dots are grid points where the difference between March and November is statistically significant ($p<0.05$). Figure 4.7a is equal to Figure 4.7b + Figure 4.7c + Figure 4.7d

4.4.2.2 Southern rainforest

In the southern rainforest, VWC is 4% higher in November than March, with values of 37% in March and 41% in November (Figure 4.6a). The lower percentage difference in the southern rainforest compared to the northern rainforest is due to a larger soil moisture depletion between May and August (Figure 4.6c). Higher water availability in November than March cannot explain why LAI is lower in November than March. The soil is close to saturation in November, and light availability is therefore a plausible control on LAI. There is 17 W m^{-2} lower surface DSR in November than March (Figure 4.7a). This is the sum of 8 W m^{-2} less TOA DSR (Figure 4.7b), 10 W m^{-2} less surface DSR due to higher cloud cover (Figure 4.7c), and 1 W m^{-2} more surface DSR due to lower atmospheric absorption (Figure 4.7d). Therefore, the lower surface DSR, caused by lower TOA DSR and higher cloud cover, is a plausible explanation for why LAI is 0.55 m^2 m^{-2} lower in November than March (Figure 4.5a). This effect is particularly strong at 2°S, 28°E (Figure 4.4c, Figure 4.5a) and this may be due to the influence of mesoscale convective systems, which develop in the afternoon in November and block incoming sunlight. This hotspot is not present in March (Jackson et al. 2009; Hart et al. 2019).

4.4.2.3 North-eastern savannah

In the north-eastern savannah, VWC is 4% lower in November than March, with values of 41% in March and 37% in November (Figure 4.6a). Lower VWC occurs due to soil moisture depletion between March and September, outweighing accumulation between September and November (Figure 4.6d). Although lower VWC does covary with lower

LAI, the soil is close to saturation in November, and light availability is still a plausible control on LAI. There is 10 W m^{-2} lower surface DSR in November than March (Figure 4.7a). This is the sum of 8 W m^{-2} higher TOA DSR (Figure 4.7b), 15 W m^{-2} less DSR due to higher cloud cover (Figure 4.7c), and 3 W m^{-2} less DSR due to higher atmospheric absorption (Figure 4.7d). Therefore lower surface DSR, caused by higher cloud cover, plausibly explains why LAI is 0.35 m^2 m^{-2} lower in November than March (Figure 4.5a).

4.4.2.4 South-eastern savannah

In the south-eastern savannah, VWC is 15% lower in November than March, with values of 42% in March and 27% in November (Figure 4.6a). This occurs because a large soil moisture depletion between March and October outweighs a small recovery in soil moisture between October and November (Figure 4.6e). There is 25 W m^{-2} higher surface DSR in November than March (Figure 4.7a). This is the sum of 25 W m^{-2} higher TOA DSR (Figure 4.7b), 5 W m^{-2} less DSR due to higher cloud cover (Figure 4.7c), and 5 W m^{-2} more DSR due to lower atmospheric absorption (Figure 4.7d). However, higher light availability cannot cause lower LAI in November than March. Instead, lower VWC in November, driven by soil moisture depletion between March and October, is a plausible explanation for why LAI is 0.44 m^2 m^{-2} lower in November than March (Figure 4.5a).

4.4.3 Lower VPD in November than March in the northern rainforest

As lower VPD contributes to lower transpiration in the northern rainforest, we investigate the factors that cause lower VPD in this region. VPD is defined as the saturated vapour pressure (SVP) minus the actual vapour pressure (AVP). SVP is a function of air

temperature, while AVP is a function of specific humidity. SVP is 0.23 kPa lower and AVP is 0.06 kPa lower in November than March in the northern rainforest. This indicates that lower VPD in November than March is predominately a result of lower temperature rather than lower humidity.

Table 4.3 shows differences in the surface energy budget between March and November in the northern rainforest. Surface net radiation is 15 W m^{-2} lower in November than March, meaning that less net radiation is absorbed by the leaves at the top of the rainforest canopy. These leaves release 6 W m^{-2} less sensible heat flux, which explains why the near-surface atmosphere is 1.15°C cooler. This in turn explains why SVP is 0.23 kPa lower in November.

Table 4.3 Sixteen-year mean (1989-2005) November minus March surface energy budget averaged over the northern rainforest (2°S to 1°N, 18°E to 30°E) from ERA5-Land

Downward Flux	**November minus March Value (W m^{-2})**	**Upward Flux**	**November minus March Value (W m^{-2})**
Net Radiation (NR)	-15.21	Sensible Heat Flux (SHF)	-5.47
Ground Heat Flux (G)	-0.41	Latent Heat Flux (LHF)	-9.33
Total (NR - G)	-14.80	Total (SHF + LHF)	-14.80

As described in Sections 4.4.1 and 4.4.2, lower surface DSR is a plausible driver of the lower LAI, which in turn lowers transpiration in the northern rainforest. This lower transpiration means that specific humidity and AVP are lower, which causes higher VPD (as SVP - (-AVP) = + VPD). However, as described in the previous paragraph, lower

surface net radiation causes lower sensible heat flux from the leaves, which in turn lowers the near-surface air temperature, SVP and VPD. The net result is that VPD is lower in November than March, and this further lowers the transpiration difference to its final value of -0.46 mm day^{-1} (Figure 4.4c). The lower transpiration means that latent heat flux is 9 W m^{-2} lower in November than March (Table 4.3), and the energy budget therefore maintains its balance in November. This is because the lower net radiation in November balances the lower sensible heat flux and lower latent heat flux.

4.5 Summary and discussion

Using LandFlux-EVAL, this chapter has found that evaporation is lower in November than March in two regions of the basin, the rainforest and the eastern savannah. To determine which components are responsible for the lower evaporation in these regions, ERA5-Land was used because it effectively reproduces the pattern of lower evaporation in November than March evident in LandFlux-EVAL.

The good agreement between LandFlux-EVAL and ERA5-Land suggests that ERA5-Land is deriving the evaporation difference between March and November using a realistic set of processes. Therefore, using ERA5-Land, this chapter has found that the transpiration component of evaporation is the main component responsible for lower evaporation in November than March in these two regions.

4.5.1 Contrasting controls on Congo Basin evaporation at the two rainfall peaks

We used ERA5-Land to establish contrasting controls on transpiration at the two rainfall peaks. These contrasting controls cause transpiration to be reduced in November, and therefore lower the evaporation in November compared to March in the rainforest and the eastern savannah. To determine these contrasting controls, we produced November minus March difference maps for possible controls on the lower transpiration, discussed whether the contrasts in these controls are sufficient to explain the lower transpiration, and suggested what causes these controls to differ between March and November. Although many drivers affect transpiration, this chapter has analysed supply (LAI) and demand (VPD) controls which are recognised globally as two of the most important (Lian et al. 2018; Barkhordarian et al. 2019). The regional variations in these contrasting controls are summarised below and visualised in Figure 4.8.

(1) In the northern rainforest, there is lower LAI in November than March. This is plausibly driven by lower surface DSR in November, which is a response to lower TOA DSR and higher cloud cover. Additionally, there is lower VPD in November than March. This is driven by lower net radiation in November. As less net radiation is absorbed by the leaves, the leaves emit less sensible heat. The result is a cooler near-surface air temperature, lower SVP and VPD. The combination of lower LAI and VPD explains lower transpiration, and therefore lower evaporation, in November than March.

(2) In the southern rainforest, there is lower LAI in November. This is plausibly driven by lower surface DSR in November, which is a response to lower TOA DSR and higher cloud cover. The difference in VPD between March and November is very small and not

sufficient to cause lower transpiration. The lower LAI alone explains lower transpiration, and therefore lower evaporation, in November than March. LAI and transpiration are much lower in November than March at 2°S, 28°E, and this is likely to reflect the influence of mesoscale convective systems that develop in the afternoon in November but not in March (Jackson et al. 2009; Hart et al. 2019). These storms block DSR and plausibly suppress LAI, transpiration, and therefore evaporation.

(3) In the north-eastern savannah, there is lower LAI in November. This is plausibly driven by lower surface DSR in November, which is a response to higher cloud cover. The difference in VPD between March and November is not sufficient to cause lower transpiration. The lower LAI alone explains lower transpiration, and therefore lower evaporation, in November than March.

(4) In the south-eastern savannah, there is lower LAI in November. This is plausibly driven by lower VWC, which occurs because a large soil moisture depletion between March and October outweighs a small soil moisture recovery between October and November. VPD is higher in November, and should cause higher transpiration, but this effect is overwhelmed by lower LAI, which explains lower transpiration, and therefore lower evaporation, in November than March.

Collectively, these contrasting controls on evaporation at the two rainfall peaks provide a plausible explanation for why the basin-wide average evaporation is lower in November than March.

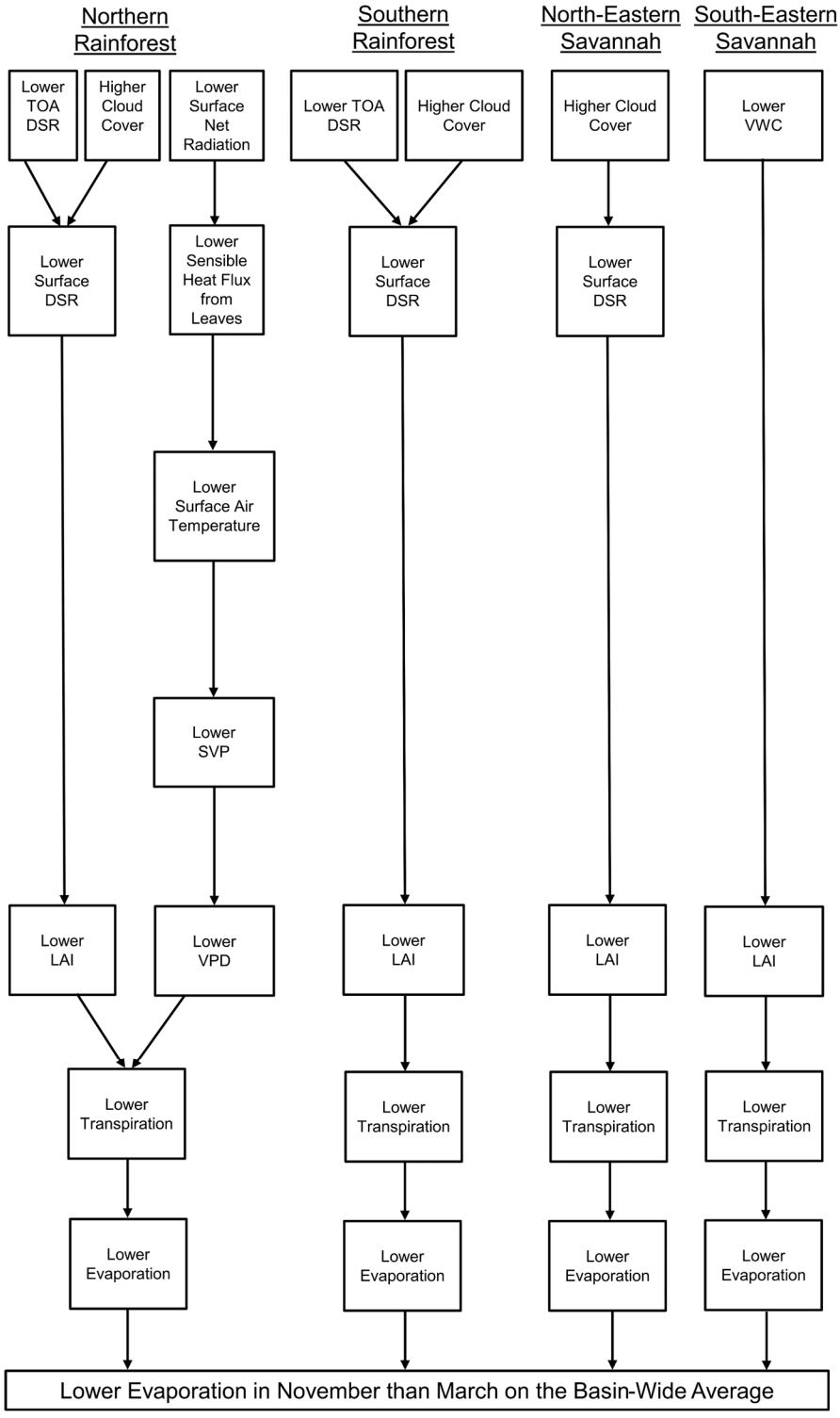


Figure 4.8 Flow chart showing contrasting controls on evaporation at the two rainfall peaks in the four sub-domains around the basin. The results in each sub-domain are consistent with the Budyko framework for evaporation. The collective of these contrasting controls provides a plausible explanation for why there is lower evaporation in November than March on the basin-wide average

4.5.2 Consistency with the Budyko framework

We have confidence in our results that explain why evaporation is lower at the November rainfall peak than the March rainfall peak in each of the four sub-domains. This is because the results are consistent with the Budyko framework, which defines how evaporation typically varies as a function of VWC and surface DSR (Budyko 1961). This framework contains three evaporation regimes: (1) dry regimes, where VWC is too low for evaporation to occur, (2) wet regimes, where VWC is plentiful and evaporation varies in response to changes in surface DSR (energy availability), and (3) transition zones between wet and dry regimes, where evaporation varies in response to changes in VWC (water availability) (Figure 5 from Seneviratne et al. 2010).

The Budyko framework states that if evaporation is lower in one month than another when both months have a wet regime, then lower surface DSR must be the reason why evaporation is lower. Our findings agree with this for the northern rainforest, the southern rainforest and the north-eastern savannah, as VWC is plentiful in both March and November, and lower surface DSR is a plausible driver of lower LAI, transpiration and therefore evaporation in November than March. The Budyko framework also states that if evaporation is lower in one month than another, when the first month has a wet regime and the second has a transition regime, then lower VWC must be the reason why evaporation is lower. Our findings agree with this for the south-eastern savannah, as VWC is plentiful in March but moderate in November, and lower VWC is a plausible driver of lower LAI, transpiration and therefore evaporation in November than March.

4.6 Conclusions

In this chapter, we have developed an understanding of why Congo Basin evaporation is lower at the November rainfall peak than the March rainfall peak on the basin-wide average, despite similar amounts of rainfall in an equatorial climate. The key findings are:

1. LandFlux-EVAL data show that evaporation is lower in November than March in the rainforest and the eastern savannah (Figure 4.3a).

2. The ERA5-Land reanalysis, which effectively reproduces the pattern of lower evaporation in November than March in LandFlux-EVAL, shows that transpiration is the main component of evaporation responsible for lower evaporation in November than March in the rainforest and the eastern savannah (Figure 4.4c).

3. Using ERA5-Land, we find the following contrasting controls on transpiration, and therefore evaporation, at the two rainfall peaks in the rainforest and the eastern savannah:

(a) In the northern rainforest, there is lower LAI in November, which is plausibly driven by lower surface DSR. Additionally, there is lower VPD in November, which is plausibly driven by lower sensible heat flux from the leaves at the top of the canopy, that results from lower surface net radiation. The combination of lower LAI and VPD explains lower transpiration, and therefore lower evaporation, in November compared to March (Section 4.4).

(b) In the southern rainforest, and in the north-eastern savannah, there is lower LAI in November, which is plausibly driven by lower surface DSR. This lower LAI alone explains lower transpiration, and therefore lower evaporation, in November compared to March (Section 4.4).

(c) In the south-eastern savannah, there is lower LAI in November, which is plausibly driven by lower VWC. This lower LAI alone explains lower transpiration, and therefore lower evaporation, in November compared to March (Section 4.4).

4. Collectively, these contrasting controls on evaporation at the two rainfall peaks in the four sub-domains around the basin provide a plausible explanation for why there is lower transpiration, and therefore lower evaporation, at the November rainfall peak than the March rainfall peak on the basin-wide average. We have confidence in our results for the four sub-domains, because these results are consistent with the Budyko framework for evaporation.

Only by considering lower evaporation in November than March on the basin-wide average as the collective of contrasting controls on evaporation in specific basin regions were we able to move towards a physical understanding of the mechanisms that control the imbalance in evaporation between the two rainfall peaks. Therefore, to understand what controls the full seasonal cycle of evaporation on the basin-wide average, a regional approach is also needed. The following chapter begins this regional research.

Acknowledgements

CHIRPS2 data were downloaded from the Climate Hazards Group website (https://data.chc.ucsb.edu/products//CHIRPS-2.0/global_monthly/netcdf/, accessed on 8 November 2020). This chapter uses the LandFlux-EVAL merged benchmark synthesis products of ETH Zurich produced under the aegis of the Global Energy and Water Exchanges (GEWEX) and Integrated Land-Ecosystem Atmosphere Process Study (ILEAPS) projects (http://www.iac.ethz.ch/url/research/LandFlux-EVAL/). The authors acknowledge the data providers for the reanalysis data sets used in this chapter (see Table 4.1). David Crowhurst is funded by the U.K. Natural Environment Research Council (NERC) through the Doctoral Training Partnership in Environmental Research (Grant NE/L002612/1). Richard Washington is partly supported by the NERC-Department for International Development (DfID) Uncertainty reduction in Models For Understanding deveLopment Applications (UMFULA) project (Grant NE/M020207/1). We thank the advice from two anonymous reviewers, whose comments helped us to considerably improve the quality of the manuscript.

Appendix B

B.1 LAI

Total LAI is derived from ERA5-Land as the sum of LAI from low vegetation and LAI from high vegetation. As detailed in Section 4.4.1, monthly LAI values are prescribed in ERA5-Land using data from MODIS Collection 5 (Boussetta et al. 2013).

B.2 VPD

We use near-surface air temperature and near-surface dew point temperature from ERA5-Land to calculate VPD. The Tetens approximation is used to calculate SVP as follows:

$$e_s(T) = 6.112 \exp\left(\frac{17.67T}{T+237.3}\right) \quad (4.1)$$

where $e_s(T)$ is the SVP (hPa), and T is the near-surface air temperature (°C).

The Magnus approximation is then used to calculate relative humidity as follows:

$$RH = 100 \exp\left(\frac{17.625 \times 243.04 \times (T_d - T)}{(243.04 + T_d)(243.04 + T)}\right) \quad (4.2)$$

where RH is the relative humidity (%) and T_d is the dew point temperature (°C).

AVP is then calculated as follows:

$$e = \frac{RH}{100}\, e_s(T) \tag{4.3}$$

where e is the AVP (hPa). Finally, VPD is calculated as follows:

$$VPD = \frac{e_s(T)}{10} - \frac{e}{10} \tag{4.4}$$

where kPa is the unit.

B.3 VWC

VWC is available for 0-7 cm, 7-28 cm, and 28-100 cm layers in ERA5-Land. We therefore calculate one metre VWC as the weighted mean of the VWC from these layers.

B.4 Surface DSR

Surface DSR is equal to (1) TOA DSR + (2) the reduction in surface DSR due to cloud cover ('cloud forcing') + (3) the reduction in surface DSR due to atmospheric absorption ('atmospheric forcing'). (1) is available directly from ERA5-Land. (2) is calculated as surface DSR with cloud ('average sky') minus surface DSR without cloud ('clear sky'). As surface DSR = (1) + (2) + (3), (3) is calculated as surface DSR - (1) - (2).

5 Understanding the dynamics controlling the seasonal cycle of Congo Basin evaporation using a regional approach

David Crowhurst[1], Simon Dadson[1], and Richard Washington[1]

[1]School of Geography and the Environment, University of Oxford, Oxford, UK

Submitted 28/04/2021

Climate Dynamics

Authorship declaration

David Crowhurst conducted all of the analysis and wrote this paper. Simon Dadson and Richard Washington contributed to the planning of the methodology and the interpretation of the results and commented on and edited the manuscript during preparation and revision.

Abstract

The seasonal cycle of Congo Basin evaporation on the basin-wide average is not well understood. As evaporation differs substantially between the basin's rainforest and savannah, this chapter aims to achieve a complete understanding of the dynamics controlling this cycle using a regional approach. Collectively, the previously researched dynamics on why evaporation is suppressed at the November rainfall peak relative to the March rainfall peak, and the dynamics controlling the seasonal cycles of evaporation in the rainforest and savannah, will explain what controls the seasonal cycle of evaporation on the basin-wide average. Therefore, we seek to derive dynamics controlling the seasonal cycles of evaporation in the rainforest and savannah. We find that the ERA5-Land reanalysis effectively reproduces evaporation from LandFlux-EVAL data in the savannah only. Therefore, we derive the following plausible dynamics from ERA5-Land controlling the savannah's seasonal cycle of evaporation: Between November and March, an increase in surface downward shortwave radiation (DSR) explains an increase in LAI, transpiration and evaporation. Between March and April, the effects of a decrease in rainfall and an increase in surface DSR offset one another, leading to stable evaporation. Between April and July, a decrease in rainfall explains why evaporation falls. Between July and November, early green-up and an increase in rainfall explain why evaporation recovers. Using sub-grid rainfall in the land surface model of the next version of ERA5-Land could bring this reanalysis into good agreement with LandFlux-EVAL in the rainforest, allowing it to be used to derive the dynamics controlling the seasonal cycle of evaporation here.

5.1 Introduction

The Congo Basin is the second-largest river basin in the world and supports one of the major tropical rainforest biomes (Gond et al. 2013). However, the basin's climate remains understudied relative to the size and global influence of the region (Alsdorf et al. 2016). Knowledge of the processes that influence basin climate and its future change is desirable, as approximately 70% of the population is reliant on rain-fed agriculture for food and income (Sonwa et al. 2017).

The seasonal cycle of basin rainfall depends on the evolution of several factors, including the north-south migration of the rain belt (Nicholson 2018a), wind convergence (Creese and Washington 2016), regional and global circulation (Cook et al. 2020), mesoscale convective systems (Raghavendra et al. 2018; Taylor et al. 2018; Alber et al. 2021), topography (Dezfuli et al. 2015), and jet dynamics (Nicholson and Dezfuli 2013; Kuete et al. 2020). The seasonal cycle of basin evaporation is also an important control on the seasonal cycle of basin rainfall through moisture recycling (Pokam et al. 2012; Dyer et al. 2017; Sori et al. 2017). Research to begin developing an understanding of the seasonal cycle of basin evaporation has been carried out in Chapters 3 and 4 of this thesis and by Burnett et al. (2020), and to further this understanding more research is required.

This research could enhance knowledge on the climate system of the Congo Basin and contribute to the development of a theoretical framework on hydrological science and land-atmosphere coupling for the basin (Ndehedehe et al. 2018). An improved understanding of the dynamics controlling the seasonal cycle of basin evaporation could

also provide a baseline against which global climate models (GCMs) could be evaluated (Guan et al. 2015). Rainfall depends on many variables beyond just the atmospheric circulation, including evaporation, convection and topography (Taguela et al. 2020; Tamoffo et al. 2020). Several studies suggest that the basin has high recycling ratios, with between 25-50% of the moisture for rainfall derived from local evaporation (Dyer et al. 2017; Sori et al. 2017). Therefore, as basin evaporation contributes substantially to basin rainfall, evaluating GCM evaporation against known evaporation dynamics could increase confidence in GCM simulations of basin rainfall (Nicholson 2018a). Only once confidence in rainfall simulations is achieved for a GCM will it be possible to trust its future projections of basin rainfall (Creese and Washington 2018; Creese et al. 2019a). Gaining confidence in model projections of rainfall is vital for adaptation planning in a basin with a population heavily reliant on subsistence farming (Sonwa et al. 2020).

Before evaluating models to establish whether they effectively reproduce basin evaporation, the dynamics controlling the seasonal cycle of evaporation on the basin-wide average need to be characterised. Therefore, in this chapter, we focus on understanding these evaporation dynamics to provide an essential baseline for evaluating models.

5.1.1 Background

Ndehedehe et al. (2018) made efforts to understand the dynamics controlling the seasonal cycle of evaporation in Sub-Saharan Africa. They argued that evaporation might be controlled by temperature in densely vegetated regions, but in less densely vegetated regions, evaporation might be controlled by available soil moisture. For the Congo Basin

alone, a more detailed exploratory analysis on the seasonal cycle of evaporation was performed in Chapter 3 using eleven GCMs and the LandFlux-EVAL evaporation benchmark synthesis product (Mueller et al. 2013). From these data sets, the seasonal cycle of evaporation was plotted on the basin-wide average in Figure 3.2b. Evaporation in LandFlux-EVAL was shown to increase from January to its one peak in March, remain at its peak between March and April, decrease from April to a trough in July, and then recover between July and January. Figure 3.2 also showed that evaporation is suppressed at the November rainfall peak relative to the March rainfall peak. This feature occurs in most GCMs and in LandFlux-EVAL, despite similar rainfall at the two rainfall peaks in CHIRPS2 (Funk et al. 2015).

As part of the exploratory analysis in Chapter 3, the seasonal cycles of the three components of evaporation, being transpiration, canopy evaporation and soil evaporation, were plotted from a composite of GCMs with a low root mean square error (RMSE) against LandFlux-EVAL evaporation. On the basin-wide average, the lower evaporation in November than March in these GCMs was shown to be caused by lower transpiration in November. A key conclusion of this chapter was that lower transpiration is likely to explain why evaporation is lower in November than March in reality. Burnett et al. (2020) argued that a plausible explanation for this difference in transpiration, and therefore evaporation, on the basin-wide average is lower net radiation in November, which allows for higher water use efficiency. In addition, these authors argued that depleted terrestrial water stores in November limit the water available for transpiration.

However, Burnett et al. (2020) recognised that studying evaporation on the basin-wide average has limitations because it averages over spatial variations in the drivers of evaporation across the two main ecoregions of the basin. These are the evergreen rainforest to the north and the deciduous savannah to the south (Matsuyama et al. 1994), which may affect the seasonal cycle in different ways.

To further understand the difference in evaporation between the two rainfall peaks, Chapter 4 analysed the causes of this difference regionally by establishing contrasting controls on the evaporation components in March and November in the regions of lower evaporation using the ERA5-Land reanalysis. By understanding the difference as the collective of contrasting controls in separate regions, this chapter considered spatial variations important for understanding the difference on the basin-wide average.

Chapter 4 showed that lower surface downward shortwave radiation (DSR) in November is a plausible driver of lower leaf area index (LAI), transpiration and therefore evaporation in the northern rainforest, southern rainforest, and north-eastern savannah. It also showed that lower soil moisture in November is a plausible driver of lower LAI, transpiration and therefore evaporation in the south-eastern savannah. Confidence was achieved in the results for all four sub-domains because the results were consistent with the Budyko framework, which defines how evaporation varies in response to changes in soil moisture and solar radiation. The argument was made that collectively, these contrasting controls on evaporation at the two rainfall peaks provide a plausible explanation for why basin-wide average evaporation is lower at the November rainfall peak than the March rainfall peak.

A regional approach is needed to expand beyond the peaks and achieve a complete understanding of the dynamics controlling the seasonal cycle of evaporation, but this time based on land cover type. This is because evaporation differs substantially between the evergreen rainforest, which covers the northern half of the basin, and the deciduous savannah, which covers the southern half of the basin. Collectively, the previously researched dynamics on why evaporation is suppressed at the November rainfall peak relative to the March rainfall peak, and the dynamics controlling the seasonal cycles of evaporation in the basin's rainforest and savannah, will explain what controls the seasonal cycle of Congo Basin evaporation on the basin-wide average.

5.1.2 Aims

To achieve a complete understanding of the dynamics controlling the seasonal cycle of Congo Basin evaporation on the basin-wide average using a regional approach, this chapter aims to:

1. Plot the seasonal cycles of evaporation for the rainforest and the savannah.

2. Derive plausible dynamics that control each of these cycles.

5.2 Data and methods

5.2.1 Ecoregions

The studied domain for the Congo Basin is 14°S to 4°N, 18°E to 30°E, which is consistent with the domain used in Chapters 3 and 4. In the present chapter, we divide the domain into its two ecoregions based upon the land cover type. These are shown in Figure 5.1: the evergreen rainforest to the north (5°S to 4°N, 18°E to 30°E), and the deciduous savannah to the south (14°S to 5°S, 18°E to 30°E).

5.2.2 Evaporation reference data

We plot seasonal cycles of evaporation for each ecoregion from the LandFlux-EVAL evaporation benchmark synthesis product. This product merges evaporation from various data sets, including satellite products, land surface models (LSMs) and reanalyses, to produce global evaporation estimates at a 1° x 1° resolution (Mueller and Seneviratne 2014). Following Chapters 3 and 4, the reasons for selecting LandFlux-EVAL for the Congo Basin are: (1) the product performed well in a water budget evaluation across the African continent regardless of its relatively coarse resolution (Weerasinghe et al. 2020), (2) the seasonal cycle of basin-wide average evaporation from LandFlux-EVAL compares favourably with seasonal cycles from a range of other products for the Congo Basin specifically (Trambauer et al. 2014), and (3) LandFlux-EVAL is a synthesis product that does not prioritise the use of one evaporation algorithm (Miralles et al. 2016).

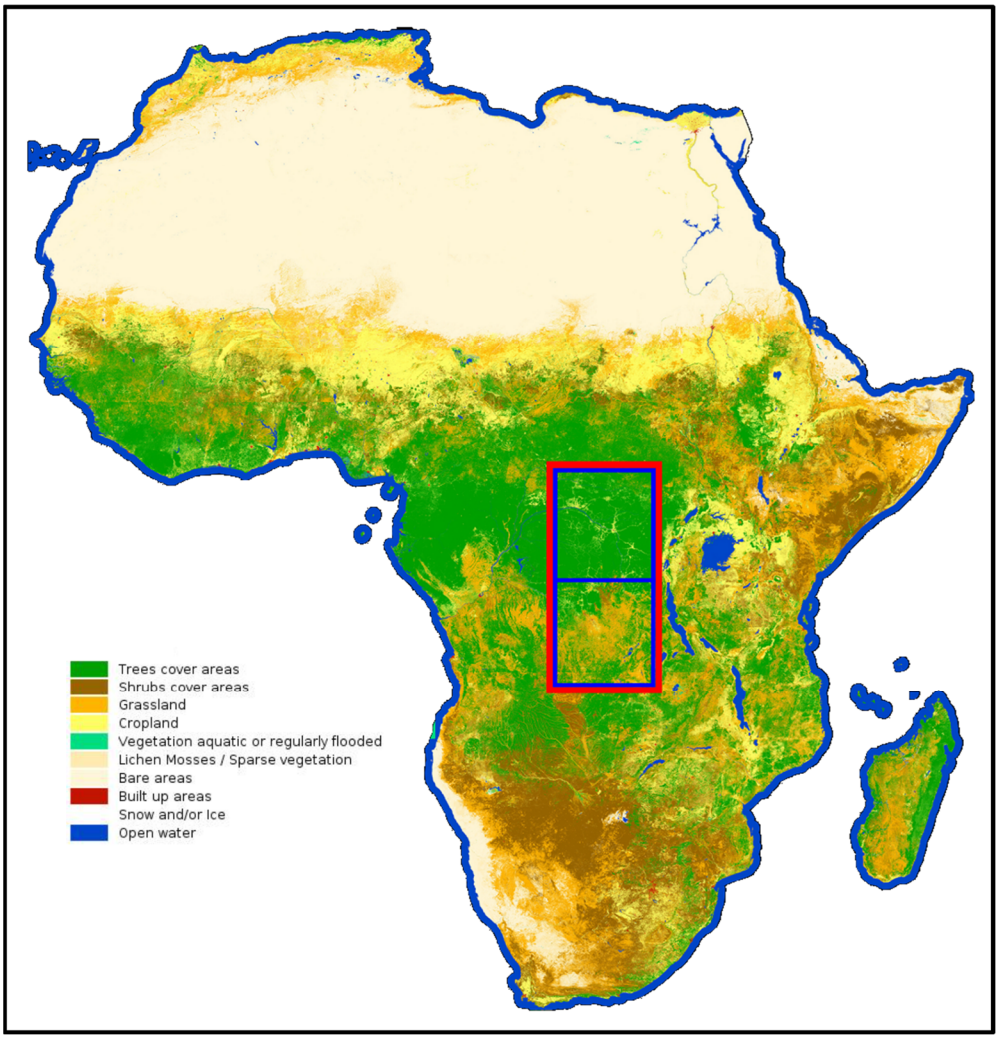


Figure 5.1 Land cover map for Africa. Data are sourced from the European Space Agency Climate Change Initiative Land Cover map (2017). The Congo Basin domain used in this chapter (14°S to 4°N, 18°E to 30°E) is shown with a red box. Sub-domains in blue indicate the two ecoregions analysed: the rainforest to the north (5°S to 4°N, 18°E to 30°E), and the savannah to the south (14°S to 5°S, 18°E to 30°E)

5.2.3 Reanalysis data

This chapter aims to use reanalysis data to derive plausible dynamics that control the seasonal cycles of evaporation in the rainforest and the savannah. If the seasonal cycle from a reanalysis compares favourably with LandFlux-EVAL data for an ecoregion, this provides confidence that the LSM in the reanalysis is deriving the seasonal cycle of evaporation realistically. This would allow us to justify using further data from this reanalysis to derive a plausible explanation for why the seasonal cycle of evaporation in each of these ecoregions has the shape that it does.

Following Chapter 4, we use the following criteria to determine whether a reanalysis is suitable for evaluation against LandFlux-EVAL: (1) the reanalysis must be the latest version released, (2) the reanalysis must be independent of LandFlux-EVAL, and (3) the reanalysis must produce data for evaporation, its three components, and a variety of evaporation drivers. To the knowledge of the authors, ERA5-Land (Hersbach et al. 2020) and MERRA-2 (Gelaro et al. 2017) are the only reanalyses that meet these criteria. Table 4.2 of Chapter 4 provides details on documentation, resolution and available time periods for LandFlux-EVAL and the two reanalyses.

5.2.4 Methods

We plot the 16-year mean (1989-2005) seasonal cycle of evaporation for the rainforest and the savannah from LandFlux-EVAL, ERA5-Land and MERRA-2. 1989-2005 is the only climatological period shared by all three data sets. For each ecoregion, we compare

the seasonal cycle of evaporation from the two reanalyses against LandFlux-EVAL. Ritter and Munoz-Carpena (2013) state that using a single indicator to assess one data set against another may lead to an incorrect verification. Therefore, we make our judgement on the effectiveness of ERA5-Land and MERRA-2 against LandFlux-EVAL in each ecoregion based upon the collective of the evidence from two indicators: (1) the RMSE statistic against LandFlux-EVAL, and (2) the qualitative fit between the seasonal cycle from the reanalysis and the seasonal cycle from LandFlux-EVAL.

The RMSE statistic is calculated for each reanalysis following the RMSE equation. For each month, we calculate the difference between the reanalysis and LandFlux-EVAL and square the result. We then calculate the mean of the twelve months and take the square root to determine the RMSE. Although there is no globally accepted threshold on the RMSE that should be used for qualitative assessment, a value of less than 0.5 usually indicates that a reanalysis performs well. If both reanalyses are effective, we select the reanalysis with the lowest RMSE to derive the dynamics controlling the seasonal cycle of evaporation. If only one reanalysis is effective, we select this one reanalysis only to derive the evaporation dynamics. If neither reanalysis is effective, then no selection can be made, and we will be unable to make progress.

If a reanalysis is successfully selected for an ecoregion, the following method will be used to derive plausible dynamics controlling the seasonal cycle of evaporation for this ecoregion from the successful reanalysis. Firstly, the seasonal cycle of evaporation and the seasonal cycles of the three evaporation components, transpiration, canopy evaporation and soil evaporation, will be plotted from this reanalysis. Secondly, following

Burnett et al. (2020), the cycle of each component will be compared to hydroclimatic variables to determine possible driver(s) of its shape. Thirdly, plausible dynamics controlling the seasonal cycle of evaporation for the ecoregion will be defined as the collective of the dynamics controlling the individual components. Finally, to provide confidence in the results, following the analysis of Chapter 4, these dynamics will be assessed to examine whether they are consistent with the Budyko evaporation framework. If evaporation and its components are affected by changes in variables other than soil moisture and solar radiation, which would be beyond the scope of the Budyko framework, then to achieve confidence in these derived dynamics, they will be assessed for realism against evidence from the literature.

5.3 Seasonal cycles of evaporation for the rainforest and savannah

Figure 5.2 shows the seasonal cycles of evaporation from LandFlux-EVAL, ERA5-Land and MERRA-2 on the basin-wide average (Figure 5.2a), for the rainforest (Figure 5.2b) and for the savannah (Figure 5.2c), plotted from January to January. Figure 5.2a shows that the MERRA-2 reanalysis overestimates the seasonal cycle of evaporation from LandFlux-EVAL on the basin-wide average, with an RMSE statistic of 0.82, indicating relatively poor agreement. Figures 5.2b and 5.2c show that this poor agreement is reflected in both ecoregions, with RMSE statistics for MERRA-2 of 1.01 in the rainforest and 0.73 in the savannah. The qualitative fit between the MERRA-2 and LandFlux-EVAL cycles is poor, and MERRA-2 substantially overestimates the seasonal cycle of LandFlux-EVAL evaporation in both ecoregions. This combination of factors rules out the further use of MERRA-2 for the rainforest and the savannah in this chapter.

Figure 5.2a also shows that on the basin-wide average, the ERA5-Land reanalysis reproduces the seasonal cycle of evaporation from LandFlux-EVAL with an RMSE of 0.46, indicating improved agreement compared to MERRA-2. However, even though the RMSE is lower in ERA5-Land than MERRA-2 on the basin-wide average, the qualitative fit between the ERA5-Land and LandFlux-EVAL seasonal cycles is sub-par, and ERA5-Land still slightly overestimates the seasonal cycle of LandFlux-EVAL on the basin-wide average, particularly during the wetter months.

In the rainforest (Figure 5.2b), the RMSE of ERA5-Land against LandFlux-EVAL is 0.65, the fit between the two curves is poor, and ERA5-Land substantially overestimates the seasonal cycle of LandFlux-EVAL evaporation. This precludes using ERA5-Land for analysing this ecoregion. However, in the savannah (Figure 5.2c), ERA5-Land effectively reproduces the seasonal cycle of LandFlux-EVAL evaporation. This is because the RMSE is 0.30, and the fit between the ERA5-Land and LandFlux-EVAL seasonal cycles is reasonably good. These factors provide confidence that ERA5-Land produces the seasonal cycle of evaporation in the savannah in a trustworthy manner.

Therefore, to make progress, this chapter uses ERA5-Land to derive plausible dynamics controlling the seasonal cycle of evaporation in the savannah ecoregion only. This ecoregion covers the southern half of the basin domain, which is an area of approximately 900,000 km^2.

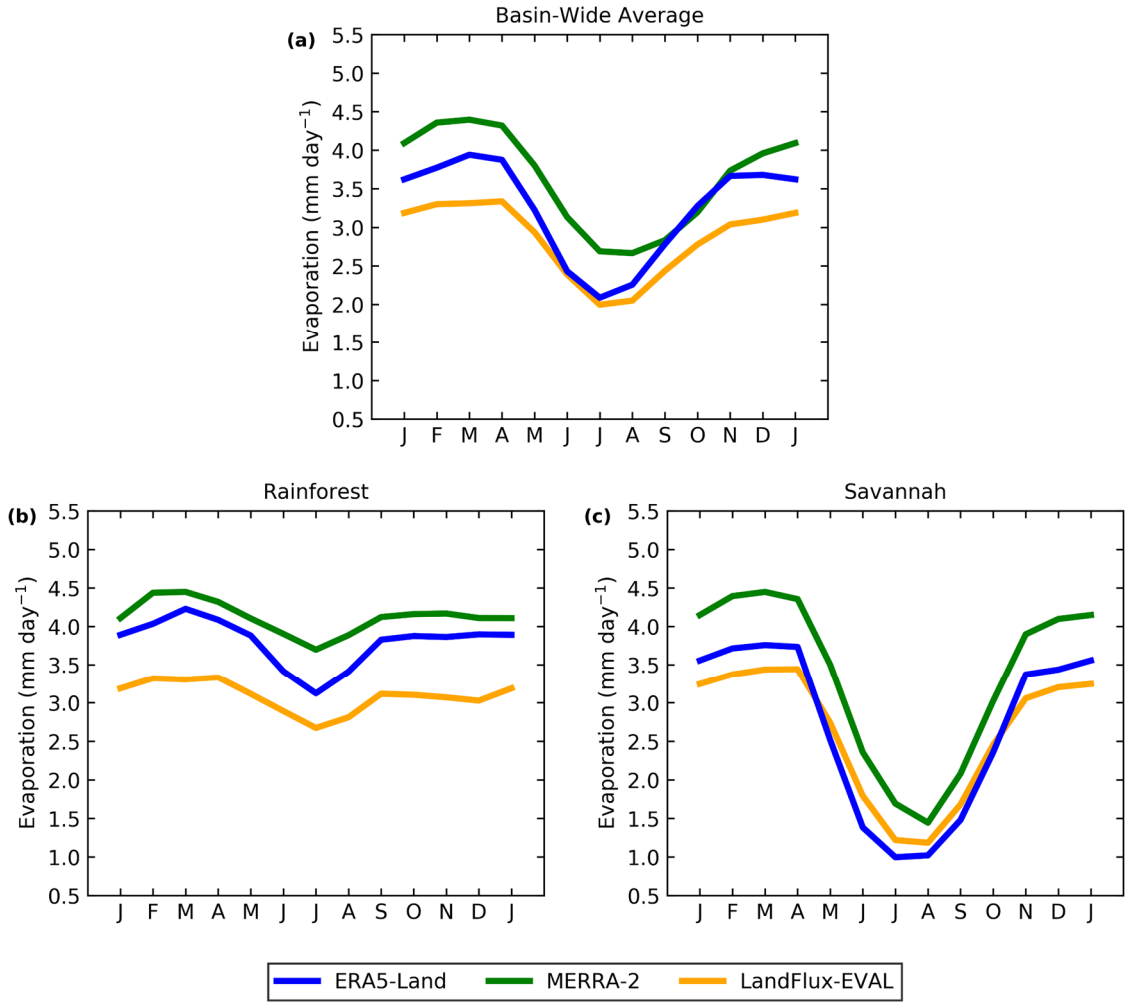


Figure 5.2 Sixteen-year mean (1989-2005) seasonal cycles of evaporation (mm day^{-1}) for **a** the basin-wide average, **b** rainforest, and **c** savannah. Data from ERA5-Land, MERRA-2 and LandFlux-EVAL

5.4 Seasonal cycles of the evaporation components for the savannah

Figure 5.3a shows the seasonal cycles of rainfall and evaporation from ERA5-Land in the savannah, starting in January and ending in January. The seasonal cycle of rainfall shows a wet period from January to March, a dry period from March to November, and a wet period from November to January. However, going forwards, this chapter will make a

graphical adjustment by now analysing the seasonal cycles from November to November, as shown in Figure 5.3b. This adds conciseness by allowing us to explain how evaporation varies during one wet season from November to March when the rain belt is located over the savannah, and during one dry season from March to November when the rain belt migrates northwards away from the savannah between March and July, and then back southwards into the savannah between July and November (Jinga and Palagi 2020).

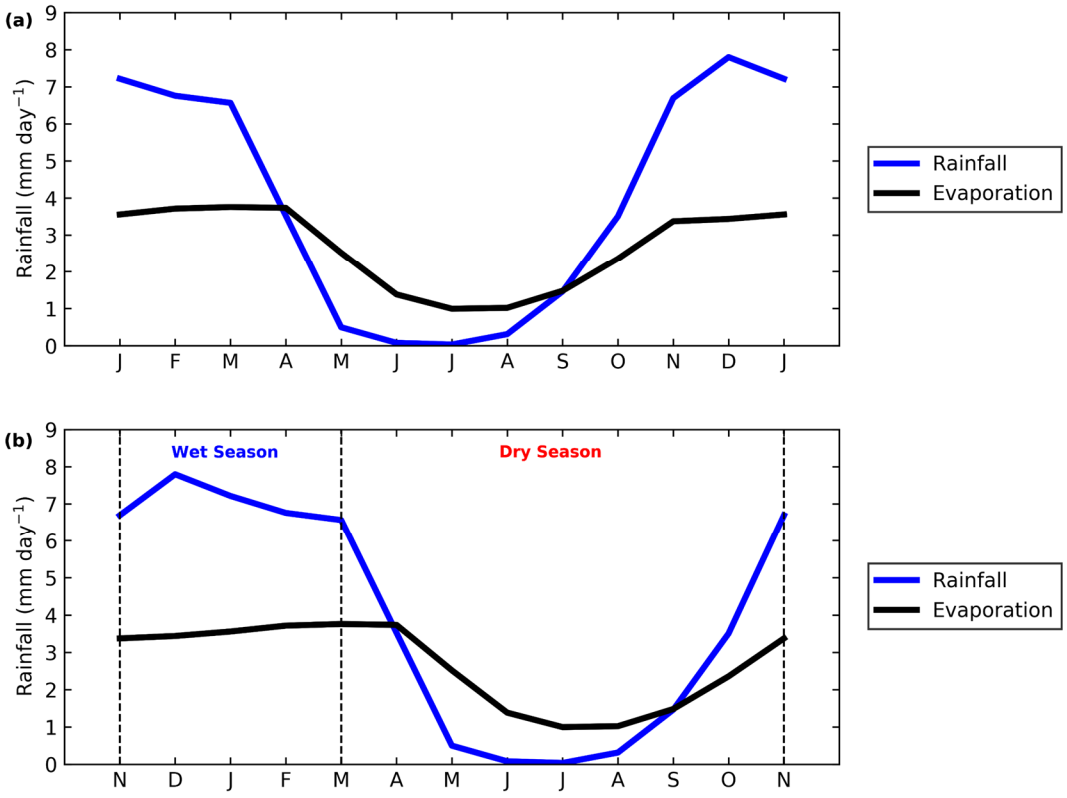


Figure 5.3 Sixteen-year mean (1989-2005) seasonal cycles of rainfall (mm day^{-1}) and evaporation (mm day^{-1}) for the savannah. **a** Seasonal cycles begin in January and end in January. **b** Seasonal cycles begin in November and end in November. All data from ERA5-Land

Figure 5.4 shows the seasonal cycle of evaporation and the seasonal cycles of the three evaporation components for the savannah from ERA5-Land. The figure shows that during the wet season, transpiration accounts for approximately 50%, canopy evaporation 35%,

and soil evaporation 15% of the total evaporation. A high proportion of transpiration and a low proportion of canopy evaporation provides confidence that ERA5-Land is producing evaporation realistically because this is consistent with Wei et al. (2017) for transpiration and Miralles et al. (2010) for canopy evaporation. In the wet season, as canopy evaporation and soil evaporation are broadly stable, the increase in evaporation between November and March is primarily explained by the increase in transpiration.

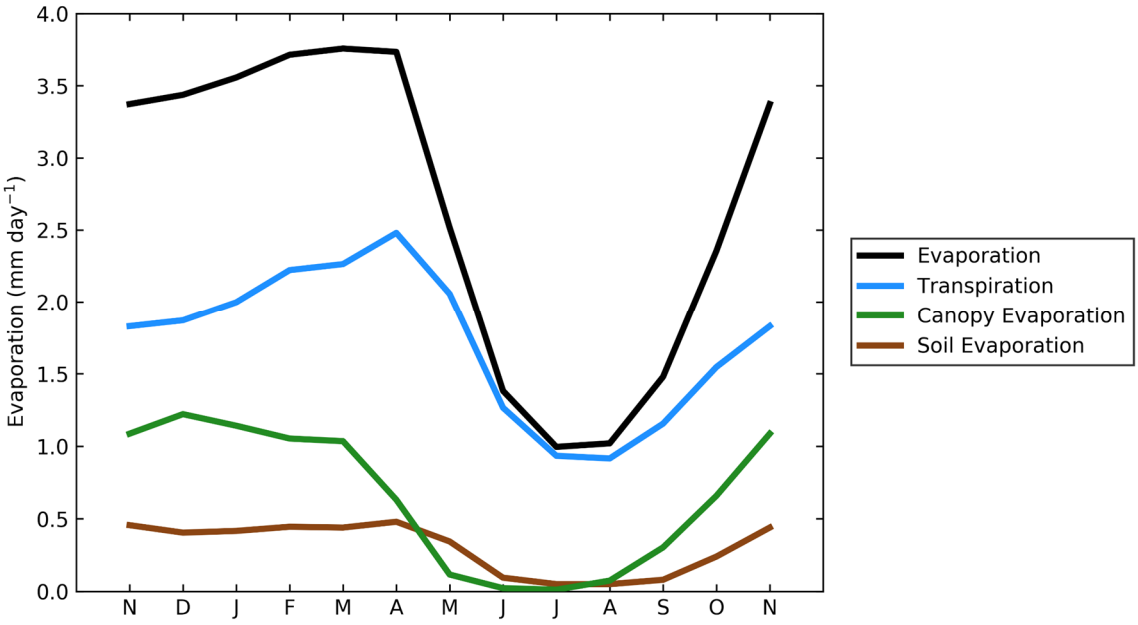


Figure 5.4 Sixteen-year mean (1989-2005) seasonal cycles of evaporation and its three components (mm day^{-1}) for the savannah. All data from ERA5-Land

In March, the first month of the dry season, evaporation remains stable even though rainfall decreases because an increase in transpiration offsets a decrease in canopy evaporation. As rainfall declines further from April, all three evaporation components decline, and the evaporation falls to a trough in July. In the middle of the dry season, the

evaporation flux is almost entirely accounted for by transpiration. Between July and November, evaporation rises because all three of its components increase. Eventually, evaporation returns to its original November level, and the seasonal cycle is complete.

We now progress by deriving plausible dynamics that explain the seasonal cycle of evaporation in the savannah by investigating the dynamics controlling the components that determine the cycle's shape. We consider the dynamics controlling the cycle of transpiration for both the wet and the dry seasons. However, we only consider the dynamics controlling the cycles of canopy and soil evaporation for the dry season. This is because canopy and soil evaporation are broadly stable in the wet season and do not substantially affect the shape of the cycle of evaporation at this time.

5.5 Controls on the seasonal cycle of transpiration in the savannah

5.5.1 Variables for analysis

To investigate controls on the seasonal cycle of transpiration, two hydroclimatic variables will now be compared against this cycle. LAI and vapour pressure deficit (VPD) are selected because they are the main supply and demand variables for transpiration (Lian et al. 2018). LAI is an important control on the supply of water for transpiration because an increase in LAI increases the number of stomata, which in turn increases water loss (Wei et al. 2017). VPD, which is the difference between the saturated vapour pressure (SVP) and the actual vapour pressure (AVP), is believed to be a control on the demand

for transpiration because VPD controls the water potential gradient between the inside of the leaf, with a high water potential, and the surrounding air. When VPD increases, the air becomes drier, and the water potential gradient increases, which increases transpiration (Massmann et al. 2019).

5.5.2 Leaf area index and vapour pressure deficit

Figure 5.5a shows the seasonal cycles of LAI and transpiration from ERA5-Land, while Figure 5.5b shows the seasonal cycles of VPD and transpiration from ERA5-Land. LAI and VPD are derived variables produced following the methods outlined in the Appendix of Chapter 4. As noted in this chapter, monthly LAI values are prescribed in ERA5-Land using the MODIS Collection 5 product (Boussetta et al. 2013).

Figure 5.5a shows that in the wet season, the gradual increase in LAI throughout the wet season between November and March explains why there is a gradual increase in transpiration. Figure 5.5b shows that the VPD and transpiration curves do not vary together, which means that changes in VPD are unlikely to explain the transpiration cycle in this season.

At the beginning of the dry season between March and April, LAI increases, which explains the increase in transpiration. The rate of increase in LAI aligns more closely with the rate of increase in transpiration, suggesting that the increase in LAI, rather than the increase in VPD, is the driver of this increase in transpiration.

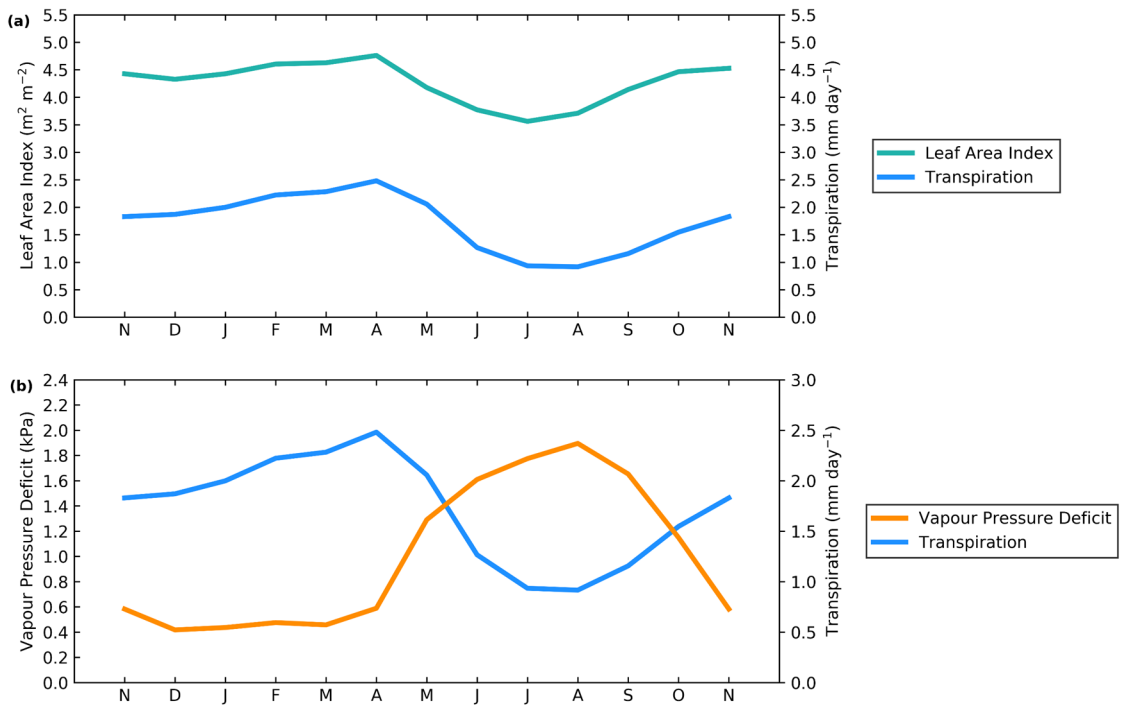


Figure 5.5 Sixteen-year mean (1989-2005) seasonal cycles of **a** LAI (m^2 m^{-2}) and transpiration (mm day^{-1}), and **b** VPD (kPa) and transpiration (mm day^{-1}), for the savannah. All data from ERA5-Land

Between April and July, LAI decreases sharply, which explains the decrease in transpiration. This down-regulation of transpiration suggests that the effect of decreasing LAI outweighs the effect of increasing VPD, and that the decrease in LAI is the driver of the decrease in transpiration.

Between July and November, LAI increases, which explains the increase in transpiration. This up-regulation of transpiration suggests that the effect of increasing LAI outweighs the effect of decreasing VPD, and that the increase in LAI is the driver of the increase in transpiration.

5.5.3 Controls on the seasonal cycle of LAI

We now investigate controls on the savannah's seasonal cycle of LAI in Figure 5.6 to develop a more detailed understanding of the processes which shape the seasonal cycle of LAI, and therefore the seasonal cycle of transpiration. In the natural environment, the main factors which control LAI are soil volumetric water content (VWC) and surface DSR (Cowling and Field 2003; Myneni et al. 2007). We therefore plot seasonal cycles of VWC and surface DSR from ERA5-Land and compare them to the seasonal cycle of LAI. VWC is derived following the method outlined in Chapter 4, while surface DSR is extracted directly from the Copernicus data portal for ERA5-Land. As discussed in Chapter 4, LAI is prescribed from MODIS in ERA5-Land, which means that soil moisture and solar radiation produced by ERA5-Land do not drive LAI in ERA5-Land. Therefore, it is not possible to make causal statements regarding drivers of LAI in ERA5-Land, and this is once more a caveat on our interpretation.

Chapter 4 plotted water budget diagrams to discover the factors responsible for the difference in VWC between the two rainfall peaks. In Figure 5.6, we now plot a water budget diagram for the savannah, and this allows us to investigate what controls the seasonal cycle of VWC in this ecoregion. Chapter 4 also decomposed surface DSR into the sum of three components: (1) top-of-atmosphere (TOA) DSR, (2) the quantity of DSR blocked by cloud ('cloud forcing'), and (3) the quantity of DSR absorbed by the atmosphere ('atmospheric forcing'). (1) is a positive radiation flux directed towards the ground surface, while (2) and (3) are negative fluxes that reduce the radiation reaching the ground surface. This decomposition was performed to understand the factors responsible for the difference in surface DSR between the two rainfall peaks. The present

chapter now decomposes the seasonal cycle of surface DSR into its three components in the savannah in Figure 5.6. This allows us to investigate what controls the seasonal cycle of surface DSR here.

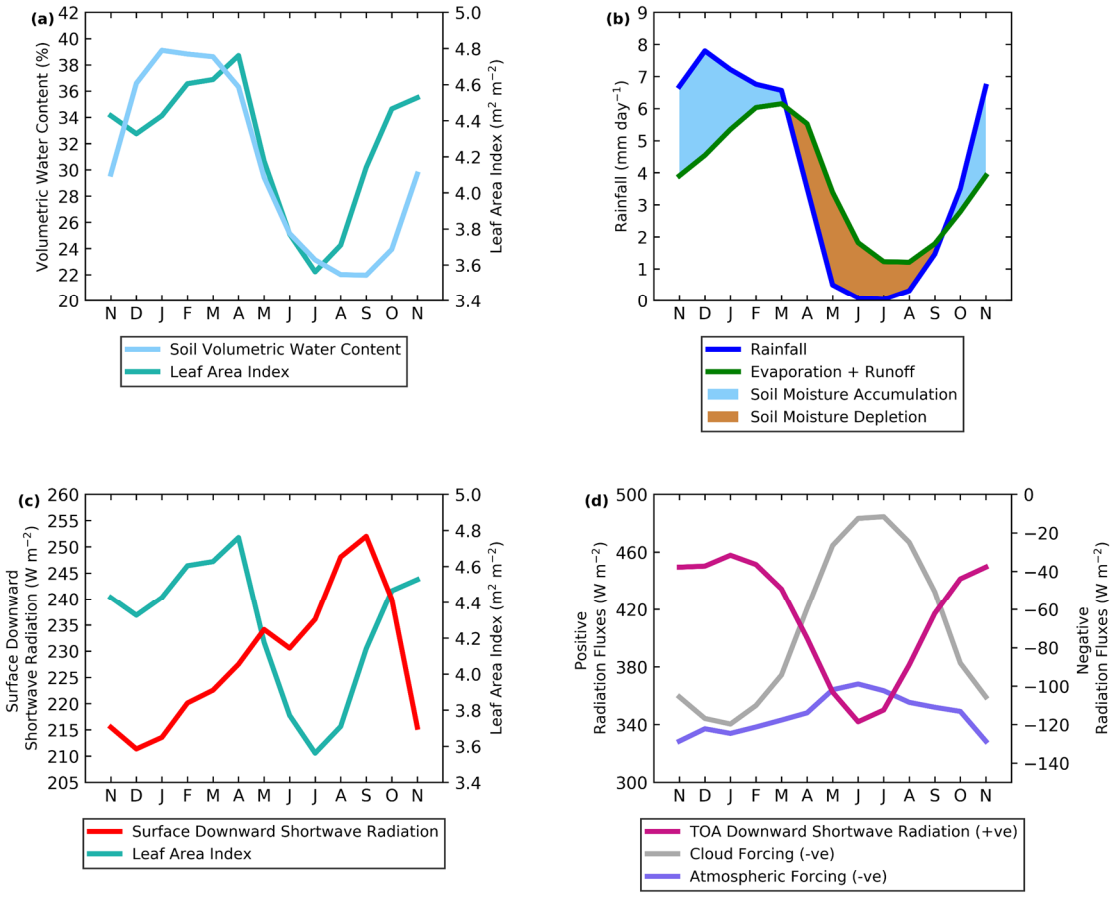


Figure 5.6 Sixteen-year mean (1989-2005) seasonal cycles of **a** soil VWC (%) and LAI (m^2 m^{-2}), **b** rainfall and (evaporation plus runoff) (mm day^{-1}), **c** surface DSR (W m^{-2}) and LAI (m^2 m^{-2}), and **d** TOA DSR, cloud forcing and atmospheric forcing (W m^{-2}), for the savannah. Shadings in panel **b** refer to soil moisture accumulation or soil moisture depletion (mm). All data from ERA5-Land

5.5.3.1 November to April

Figure 5.6a shows that VWC in the savannah accumulates at the beginning of the wet season, as rainfall is higher than the sum of evaporation and runoff (Figure 5.6b). The

savannah is characterised by clay acrisols (Van Engelen et al. 2013) which have a field capacity of 35-40% (Datta et al. 2017). VWC rises to field capacity in November and remains near this level for the duration of the wet season between November and March, and for the first month of the dry season between March and April. Therefore, the overall increase in LAI between November and April is plausibly driven by an increase in surface DSR (Figure 5.6c) because VWC is plentiful and is not a limiting factor for plant productivity. It should be noted that surface DSR decreases slightly between November and December because the cloud forcing increases, but increases between December and April because of decreases in cloud forcing and atmospheric forcing, which outweigh decreases in TOA radiation (Figure 5.6d). These changes in surface DSR possibly drive the dip in LAI between November and December, and a more substantial increase in LAI between December and April. The overall increase in LAI between November and April explains why transpiration and therefore evaporation increase between these two months.

5.5.3.2 April to November

VWC decreases rapidly between April and July (Figure 5.6a) when the rain belt migrates northwards and rainfall declines below the sum of evaporation and runoff (Figure 5.6b). Water availability becomes the limiting factor on ecosystem function as VWC falls well below field capacity. The decrease in VWC is a plausible driver of the decrease in LAI, as plants shed leaves to conserve water loss (Figure 5.6a). This mechanism explains why transpiration decreases and agrees with Vinya et al. (2019), who argued that in the Miombo woodlands, of which the Congo Basin savannah is a part, deciduous tree species mitigate water stress at the beginning of the dry season by shedding leaves.

Although rainfall begins to increase from July, VWC continues to decrease (Figure 5.6a) because rainfall is still below the sum of evaporation and runoff (Figure 5.6b). VWC only begins to recover from September onwards, when rainfall rises above the sum of evaporation and runoff. However, before this recovery in VWC, LAI begins to increase from July onwards (Figure 5.6a). This early green-up has been recognised previously in Southern Tropical Africa (Tobin and Kulmatiski 2018; Vinya et al. 2019) and is able to explain the increase in transpiration that occurs in the savannah between July and November. It is unlikely that the continued decrease in VWC between July and September is the reason for this early green-up because a decrease in water supply should not increase LAI. It is also unlikely that an increase in surface DSR (Figure 5.6c) is the reason for the green-up because surface DSR is sufficient and is not a limiting factor for ecosystem production. A potential explanation could be that early leaf growth allows the vegetation to increase the size of their nutrient stores in preparation for the rain-induced nutrient flush (Ryan et al. 2017).

5.5.4 Controls on the seasonal cycle of VPD

As discussed in Section 5.5.2, the decrease in transpiration during the dry season suggests that the effect of decreasing LAI outweighs the effect of increasing VPD, and that the decrease in LAI is the driver of the decrease in transpiration. Liu et al. (2020) recently confirmed that under conditions of low soil moisture and high VPD, low soil moisture is the dominant driver of dryness stress on vegetation functioning in most semi-arid ecosystems, rather than VPD. The implication is that when soil moisture falls and VPD rises, it is the decrease in soil moisture that causes the decrease in LAI and therefore transpiration, rather than the increase in VPD. Alexander (2011) argued that when soil

moisture decreases, sensible heat flux increases, which increases near-surface air temperature, SVP and therefore VPD. This implies that when soil moisture decreases to low levels, VPD often rises as a residual effect.

This section briefly analyses controls on the seasonal cycle of VPD to assess whether changes in VPD are coupled to land surface properties. The seasonal cycles of several variables which shape VPD are plotted in Figure 5.7. The dry season begins from March as the rain belt migrates northwards away from the savannah, and rainfall declines below evaporation plus runoff, which causes VWC to decrease (Figure 5.7a). This occurs at the same time as an increase in sensible heat flux (Figure 5.7b), which suggests that a coupling between declining VWC and increasing sensible heat flux might occur. However, near-surface temperature only rises gradually (Figure 5.7c), which indicates that other factors are suppressing the expected rise in temperature. At the same time, the northward migration of the rain belt appears to be responsible for a decrease in specific humidity and a decrease in AVP (Figure 5.7d). The main factor causing VPD to rise is the decrease in the AVP (Figure 5.7e). Overall, Figure 5.7 shows that the increase in VPD as the dry season begins is primarily a consequence of decreasing humidity as the rain belt migrates northwards away from the savannah. This increase in VPD is unable to explain the decrease in transpiration, which is instead explained by the decrease in LAI.

The rain belt migrates back southwards into the savannah from July onwards. VWC continues decreasing between July and September (Figure 5.7a), as rainfall is still below the sum of evaporation and runoff. At the same time, there is a rapid increase in sensible heat flux (Figure 5.7b), which suggests that the drying soils are raising the sensible heat flux, near-surface air temperature, SVP and VPD (Figure 5.7c). Simultaneously, the

southward migration of the rain belt appears to be responsible for an increase in specific humidity and an increase in AVP (Figure 5.7d). SVP increases at a faster rate than AVP between July and August, which causes VPD to rise. However, AVP begins to increase at a faster rate than SVP between August and September, which causes VPD to peak and then decline (Figure 5.7e).

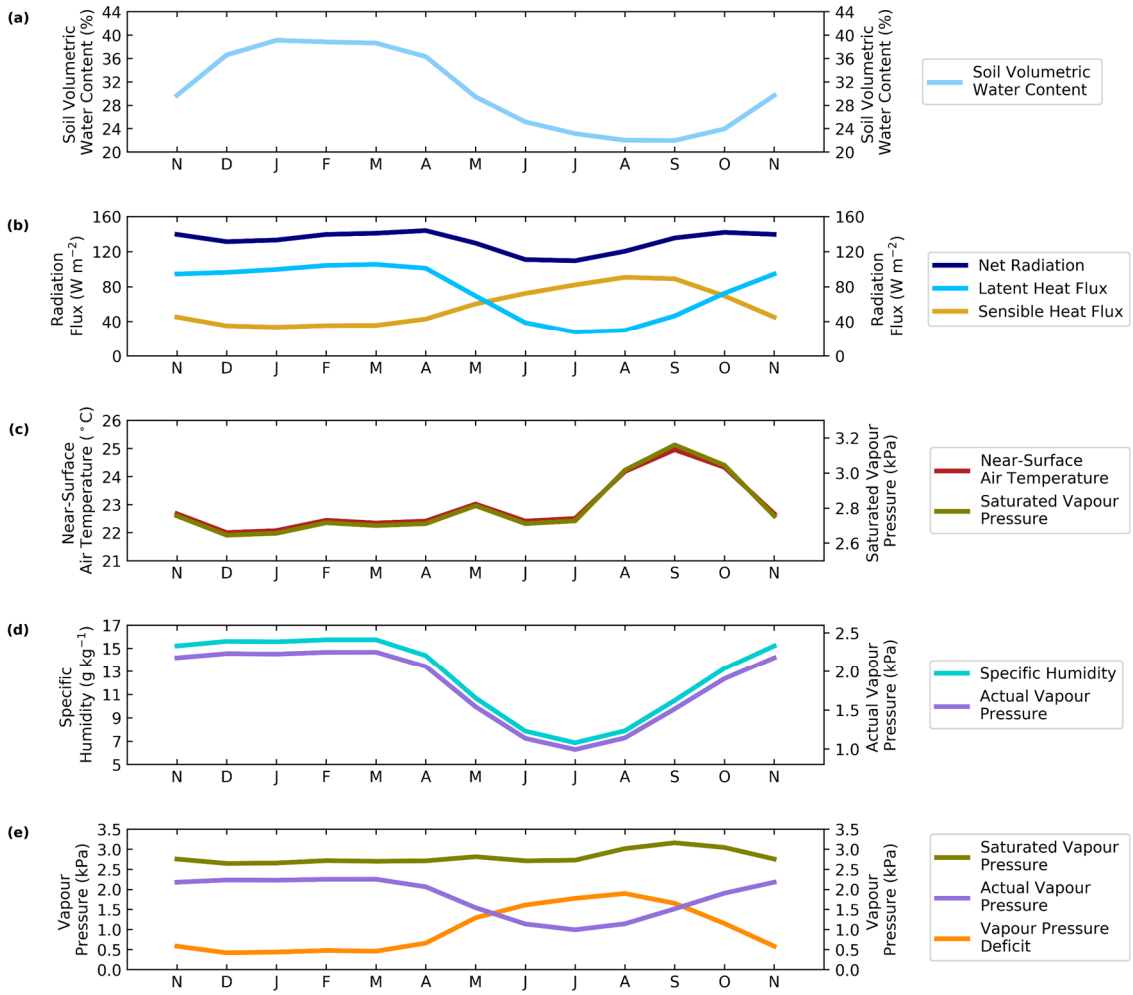


Figure 5.7 Sixteen-year mean (1989-2005) seasonal cycles of **a** soil VWC (%), **b** net radiation, latent heat flux and sensible heat flux (W m^{-2}), **c** near-surface air temperature (°C) and SVP (kPa), **d** specific humidity (g kg^{-1}) and AVP (kPa) and **e** SVP, AVP and VPD (kPa), for the savannah. All data from ERA5-Land

VWC only begins to recover from September onwards (Figure 5.7a) when rainfall increases above the sum of evaporation and runoff. This occurs at the same time as decreases in sensible heat flux (Figure 5.7b), near-surface air temperature and SVP (Figure 5.7c). Therefore, these results suggest that the increase in VWC could decrease the sensible heat flux, near-surface air temperature and SVP, which is a reversal of the coupling described by Alexander (2011). The increase in AVP as the rain belt migrates back southwards into the region continues (Figure 5.7d), and the net result is that VPD decreases between September and November (Figure 5.7e). Overall, Figure 5.7 suggests that the decrease in VPD as the dry season ends is a consequence of an increase in soil moisture and an increase in humidity as the rain belt migrates back southwards. This decrease in VPD is unable to explain the increase in transpiration, which is instead explained by the increase in LAI.

5.6 Controls on canopy and soil evaporation in the savannah's dry season

Equation 3.1 from Chapter 3 shows that canopy evaporation is controlled by the fraction of wet leaf area, which is a function of canopy water storage and canopy water storage capacity. Water storage is determined by rainfall, while LAI determines the water storage capacity. Therefore, rainfall and LAI are important variables that could control the cycle of canopy evaporation. This equation also shows that canopy evaporation is controlled by VPD, and by an aerodynamic resistance, which is a function of wind speed. Therefore, to investigate the controls on canopy evaporation during the savannah's dry season, the cycle of canopy evaporation during this season is compared to the cycles of rainfall, LAI, VPD and wind speed in Figure 5.8.

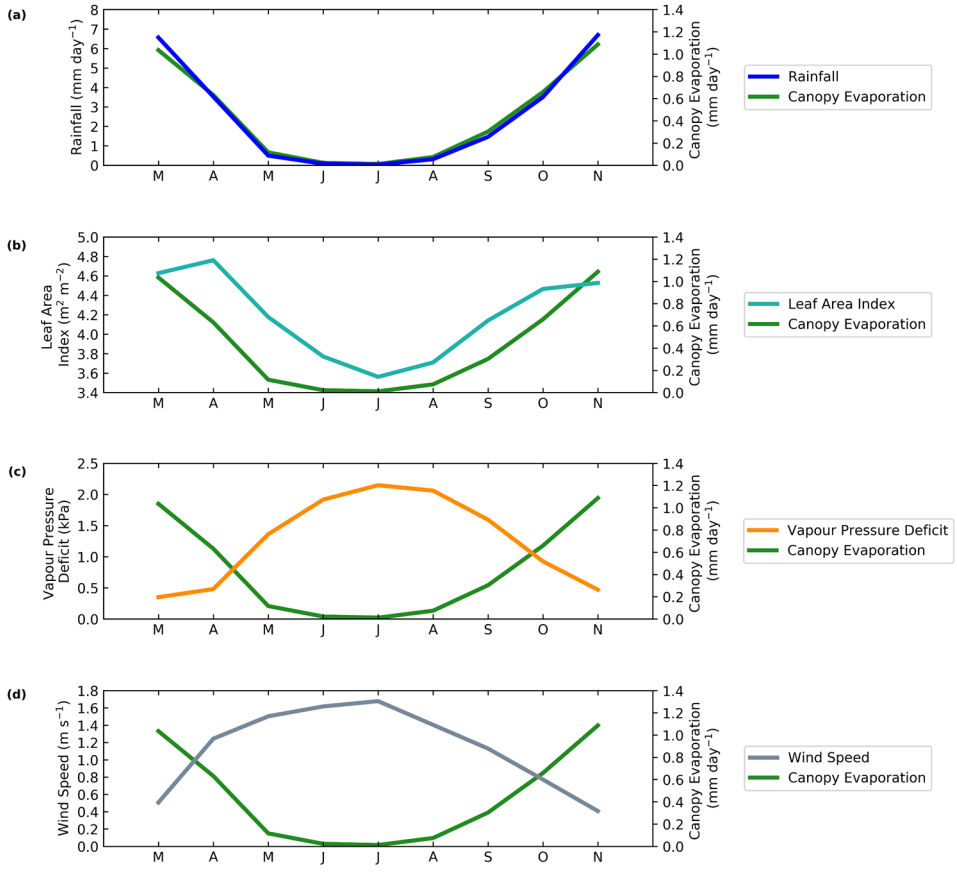


Figure 5.8 Sixteen-year mean (1989-2005) seasonal cycles of **a** rainfall (mm day^{-1}), and canopy evaporation (mm day^{-1}), **b** LAI (m^2 m^{-2}) and canopy evaporation (mm day^{-1}), **c** VPD (kPa) and canopy evaporation (mm day^{-1}), and **d** wind speed (m s^{-1}), and canopy evaporation (mm day^{-1}), for the savannah's dry season. All data from ERA5-Land

Figure 5.8a suggests that rainfall explains the cycle of canopy evaporation in the dry season, as the curves of rainfall and canopy evaporation covary. A plausible explanation for the decrease in canopy evaporation between March and May is that the northward migration of the rain belt and the subsequent decrease in rainfall causes the canopy water store to reduce in size because outputs in the form of evaporation from the canopy store move above inputs from intercepted rainfall. Therefore, as rainfall inputs decrease to near-negligible amounts by May, the canopy water store diminishes. This explains the decrease in canopy evaporation as the water available to meet the atmospheric demand

decreases. The rate of decrease in canopy evaporation could also be affected by the decrease in LAI, which could allow for less rainfall to be intercepted, thereby further decreasing the size of the canopy water store (Figure 5.8b). However, because LAI only decreases to approximately 70% of its initial value, this effect is likely to be small. VPD (Figure 5.8c) and wind speed (Figure 5.8d) increase between March and May, but while their increase should increase canopy evaporation, the opposite happens, suggesting that VPD and wind speed do not drive the decrease in canopy evaporation.

A plausible explanation for the recovery in canopy evaporation between August and November is that the southward migration of the rain belt and subsequent increase in rainfall causes the canopy water store to recover because inputs from intercepted rainfall move above outputs in the form of evaporation (Figure 5.8a). Therefore, water available to meet atmospheric demand increases, and canopy evaporation rises. The rate of increase in canopy evaporation could be affected by the increase in LAI, which could allow for more rainfall to be intercepted, thereby increasing the canopy water store (Figure 5.8b). However, because LAI only increases slightly, this effect is likely to be small. VPD (Figure 5.8c) and wind speed (Figure 5.8d) decrease, but while their decrease should decrease canopy evaporation, the opposite happens, suggesting that VPD and wind speed do not drive the increase in canopy evaporation.

The main controls on soil evaporation investigated by Wang and Liu (2007) were VWC, net radiation and LAI. Therefore, to investigate the controls on soil evaporation during the savannah's dry season, Figure 5.9 compares the cycle of soil evaporation during this season to the cycles of VWC, net radiation and LAI.

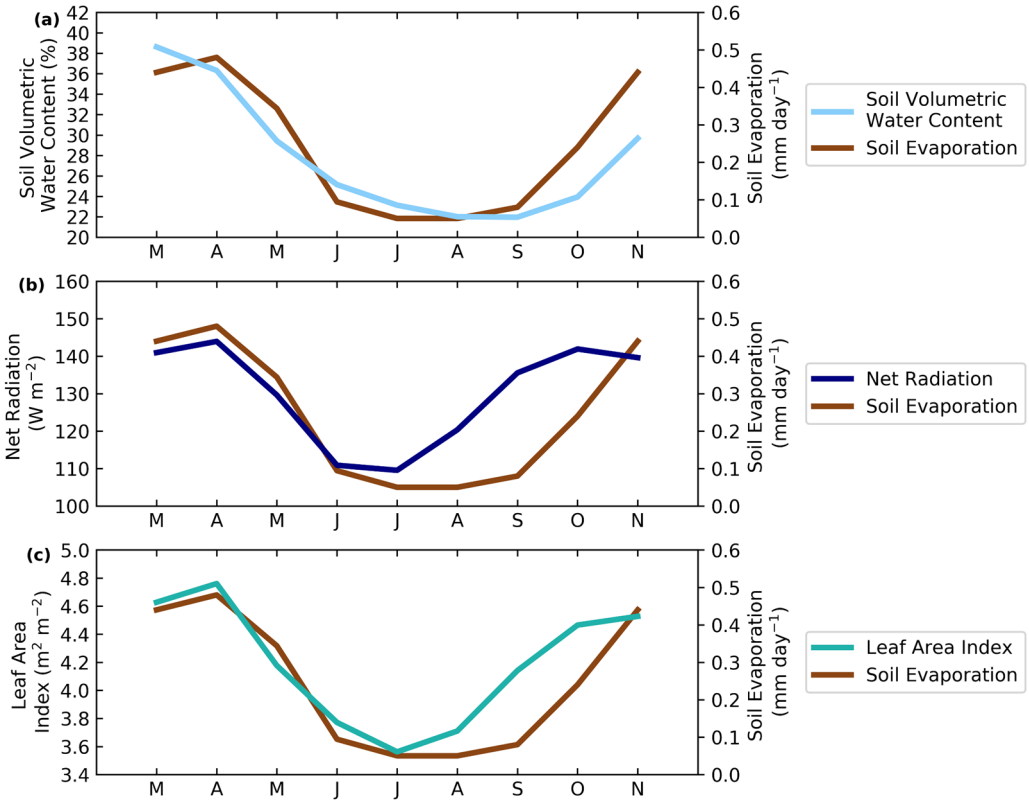


Figure 5.9 Sixteen-year mean (1989-2005) seasonal cycles of **a** soil VWC (%) and soil evaporation (mm day^{-1}), **b** net radiation (W m^{-2}) and soil evaporation (mm day^{-1}), and **c** LAI (m^2 m^{-2}) and soil evaporation (mm day^{-1}), for the savannah's dry season. All data from ERA5-Land

Figure 5.9a suggests that VWC explains the cycle of soil evaporation in the dry season because VWC and soil evaporation covary. Net radiation decreases between March and July (Figure 5.9b), but this does not explain why soil evaporation decreases. This is because VWC falls to low levels and the region moves into a transition evaporation regime, where VWC must be the limiting factor. LAI decreases between April and July (Figure 5.9c), which reduces the shading effect and should increase soil evaporation. However, soil evaporation decreases, which suggests that changes in LAI do not control

the soil evaporation. Therefore, it is plausible to suggest that the decrease in VWC explains the decrease in soil evaporation. When VWC decreases, the location of soil evaporation moves from surface to sub-surface, and a dry surface layer forms which has a greater resistance to evaporation through soil pores (Han and Zhou 2013). Between July and September, soil evaporation remains stable even though net radiation increases (Figure 5.9b). This is further evidence that low VWC is limiting soil evaporation. When VWC rises between September and November, soil evaporation recovers (Figure 5.9a). Net radiation is broadly stable, and is not likely to affect soil evaporation (Figure 5.9b). LAI increases, which increases the shading effect and should decrease soil evaporation (Figure 5.9c). However, soil evaporation increases, which suggests that changes in LAI do not control soil evaporation. Therefore, it is plausible to suggest that the increase in VWC between September and November explains the increase in soil evaporation.

5.7 Overestimation in evaporation in the rainforest in ERA5-Land and MERRA-2

This chapter found that the ERA5-Land and MERRA-2 reanalyses both overestimate evaporation from LandFlux-EVAL in the evergreen rainforest ecoregion of high vegetation density. From Figure 5.2b, we derive the magnitude of the overestimate in evaporation in the rainforest for ERA5-Land and MERRA-2. This is performed by (1) calculating the annual mean evaporation from each reanalysis, (2) calculating the annual mean evaporation from LandFlux-EVAL and (3) subtracting the LandFlux-EVAL value from each reanalysis value. The resulting values are +0.7 mm day^{-1} for ERA5-Land and +1.0 mm day^{-1} for MERRA-2. These overestimates reflect errors in how the reanalyses

produce evaporation, rather than errors in LandFlux-EVAL, which was shown to be a credible benchmark for the Congo Basin (Weerasinghe et al. 2020). The ERA5-Land and MERRA-2 reanalyses therefore need to be improved to bring the evaporation produced by these reanalyses into better agreement with LandFlux-EVAL in the Congo Basin rainforest. This could allow one of these reanalyses to be used to derive the dynamics controlling the seasonal cycle of evaporation here.

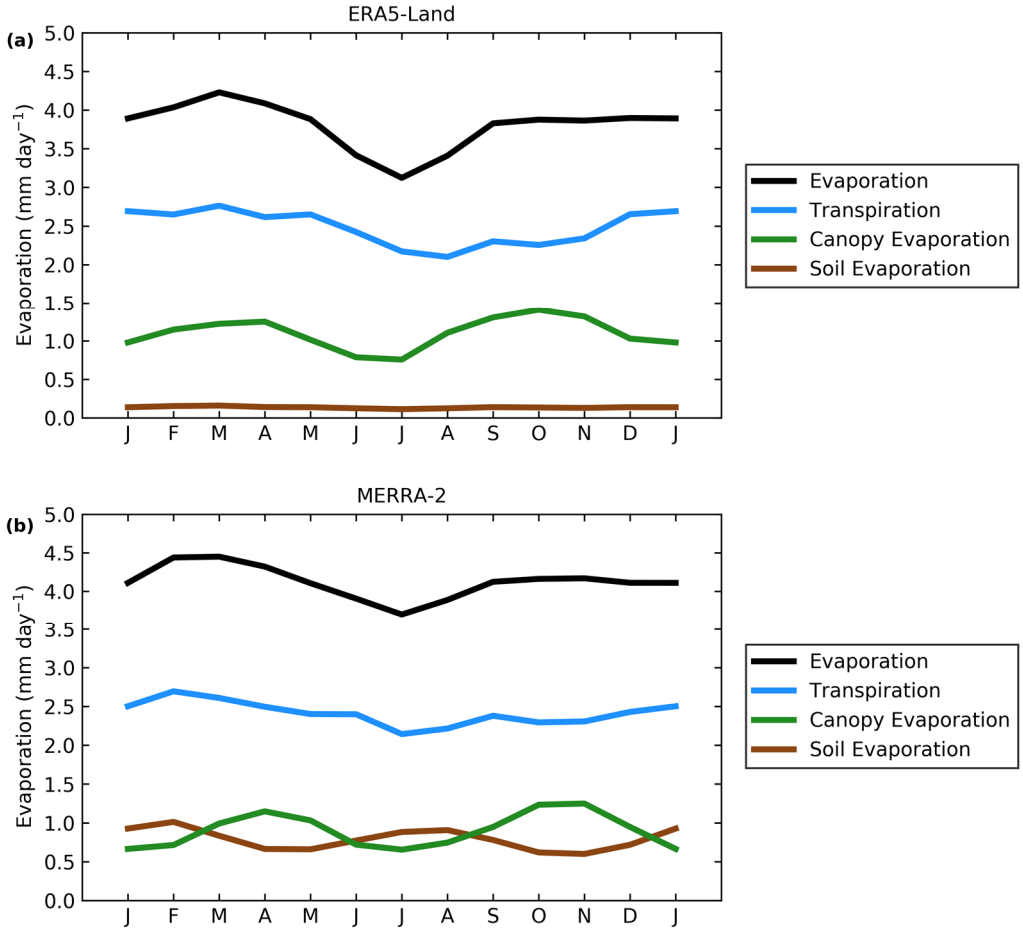


Figure 5.10 Sixteen-year mean (1989-2005) seasonal cycles of evaporation and its three components (mm day^{-1}) for the rainforest. **a** Data from ERA5-Land. **b** Data from MERRA-2

To discover why evaporation is overestimated in the rainforest in these two reanalyses, we first need to determine which components of evaporation are responsible for the overestimation. Figure 5.10 above shows the seasonal cycle of evaporation and the seasonal cycles of the three evaporation components for the rainforest from ERA5-Land and MERRA-2. Each evaporation component will need to be compared to a reference point to quantify its error and the extent to which this error contributes to the overestimation in evaporation. Therefore, where available, we compare the components in each reanalysis to reference points in the literature, if a good level of confidence has been obtained in these reference points through comparisons with in situ observations.

To the knowledge of the authors, no reliable reference points are available in the literature for transpiration against which reanalyses can be compared. However, there is a point of reference for the fraction of transpiration to evaporation from Wei et al. (2017). These authors showed that the annual mean fraction of transpiration to total evaporation in the rainforest is between 0.6-0.65. By calculating this fraction for each month and finding the mean, we find that the annual mean fraction is 0.65 for ERA5-Land (Figure 5.10a), and 0.58 for MERRA-2 (Figure 5.10b). Although these values are consistent with Wei et al. (2017), this comparison does not provide evidence on whether transpiration is overestimated, because absolute values of transpiration from the reanalysis and a reference point are necessary to quantify this. Therefore, at present, it is not possible to determine whether transpiration causes evaporation to be overestimated in the reanalyses.

A reference point for canopy evaporation for which confidence has been achieved through comparison with in situ observations (Figure 2, Miralles et al. 2010) shows that the annual mean canopy evaporation in the basin's rainforest is approximately 0.6 mm day^{-1}. In

ERA5-Land, this value is 1.1 mm day^{-1} (Figure 5.10a). ERA5-Land therefore overestimates the canopy evaporation in the basin's rainforest by approximately 0.5 mm day^{-1}, and this accounts for 71% of the 0.7 mm day^{-1} overestimate in evaporation. Martens et al. (2020) hypothesised that in ERA5, overestimates in canopy evaporation largely explain the overestimation in evaporation in densely vegetated regions, and the result of 71% substantiates this hypothesis for the basin's rainforest in ERA5-Land. MERRA-2 produces an annual mean canopy evaporation of 0.9 mm day^{-1} in the basin's rainforest (Figure 5.10b), which is a 0.3 mm day^{-1} overestimate compared to Miralles et al. (2010), and this accounts for 30% of the 1.0 mm day^{-1} overestimation in evaporation.

To the knowledge of the authors, there is no reliable reference point available in the literature for soil evaporation against which the reanalyses can be compared. Therefore, at present, it is not possible to determine to what extent soil evaporation causes evaporation in ERA5-Land and MERRA-2 to be overestimated in the basin's rainforest. However, it could be argued that the low annual mean soil evaporation in ERA5-Land of 0.1 mm day^{-1} (Figure 5.10a) is plausible because the densely vegetated rainforest canopy should restrict the surface solar radiation, and depress the soil evaporation to low values (Wang and Liu 2007). In MERRA-2, the annual mean soil evaporation is 0.8 mm day^{-1} in the basin's rainforest (Figure 5.10b), which appears to be too high for this vegetation type. The rainforest canopy should restrict surface solar radiation and therefore depress soil evaporation to values below this. High soil evaporation in MERRA-2 is in agreement with previous studies which have argued that soil evaporation in MERRA-2 is likely to be anomalously high along the equator (Schwingshackl et al. 2017; Wartenburger et al. 2018). Therefore, it is plausible to argue that in the basin's rainforest, soil evaporation contributes significantly to the overestimation in evaporation in MERRA-2.

In summary, this section suggests that improving: (1) how the next version of ERA5-Land produces canopy evaporation, and (2) how the next version of MERRA-2 produces canopy evaporation and soil evaporation, could reduce the overestimates in rainforest evaporation in these two reanalyses, and allow their next versions to be used to derive the dynamics controlling the seasonal cycle of evaporation here. It is possible that transpiration does have an effect on the overestimation of evaporation in the basin's rainforest in both reanalyses, but further research will be needed to verify this in future.

5.8 Discussion

Using LandFlux-EVAL, this chapter plotted the seasonal cycles of evaporation for the rainforest and the savannah in the Congo Basin. To investigate the dynamics controlling each of these cycles, it was necessary to find a reanalysis which produced a seasonal cycle of evaporation that compared favourably against LandFlux-EVAL in each ecoregion. However, good agreement was only found between ERA5-Land and LandFlux-EVAL for the savannah, which covers approximately half of the basin domain. The RMSE of ERA5-Land against LandFlux-EVAL was low, the qualitative fit between the seasonal cycles of ERA5-Land and LandFlux-EVAL was good, and ERA5-Land produced a high fraction of transpiration and a low fraction of canopy evaporation during the wet season. This provided confidence that the evaporation from ERA5-Land is produced realistically in the savannah. Therefore, this chapter made progress by deriving plausible dynamics controlling the three components that determine the savannah's seasonal cycle of evaporation. We now define plausible dynamics controlling the savannah's evaporation cycle as the collective of the dynamics controlling its components.

5.8.1 Controls on the seasonal cycle of evaporation in the savannah

During the wet season between November and March, as the canopy evaporation and soil evaporation curves are broadly stable, the radiatively-induced increase in LAI, driven by decreases in cloud forcing and atmospheric forcing, is a plausible driver of the increase in transpiration, and therefore evaporation (Figure 5.11).

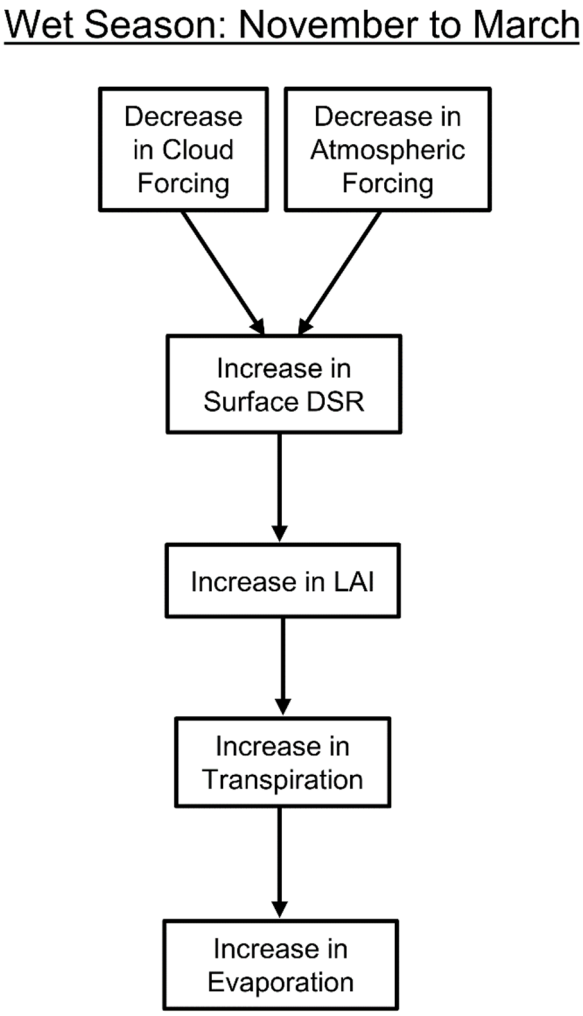


Figure 5.11 Flow chart showing plausible dynamics controlling the seasonal cycle of evaporation between November and March during the savannah's wet season

Between March and April, there is a period of relatively stable evaporation (Figure 5.12). The rain belt migrates northwards away from the savannah, which decreases the amount of rainfall in the savannah. Therefore, canopy interception decreases, which explains a decrease in the size of the canopy water store, and a decrease in canopy evaporation. At the same time, decreases in cloud forcing and atmospheric forcing lead to an increase in surface DSR, which plausibly drives the increase in LAI and therefore the increase in transpiration. The decrease in canopy evaporation and the increase in transpiration offset one another, and the net result is stable evaporation.

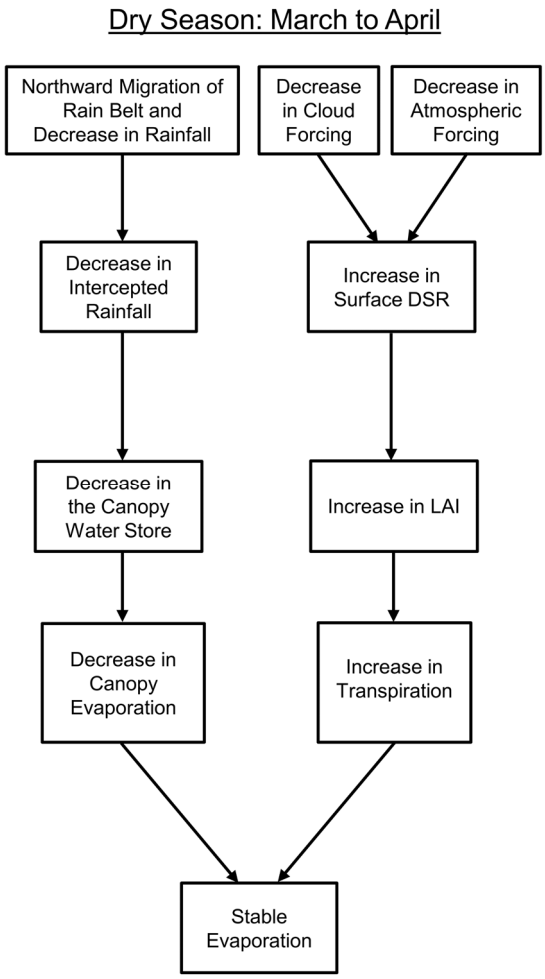


Figure 5.12 Flow chart showing plausible dynamics controlling the seasonal cycle of evaporation between March and April during the savannah's dry season

Between April and July, evaporation drops sharply (Figure 5.13). The rain belt continues to migrate northwards, which means that rainfall in the savannah decreases to negligible amounts and intercepted rainfall decreases. As the atmospheric demand is high, the canopy water store gradually diminishes, explaining why canopy evaporation also decreases to negligible values. The decline in rainfall explains why VWC declines, which is a plausible explanation for why LAI, and therefore transpiration, decrease. The decline in VWC also explains why soil evaporation decreases. The net effect of a decrease in all three evaporation components is a decrease in evaporation.

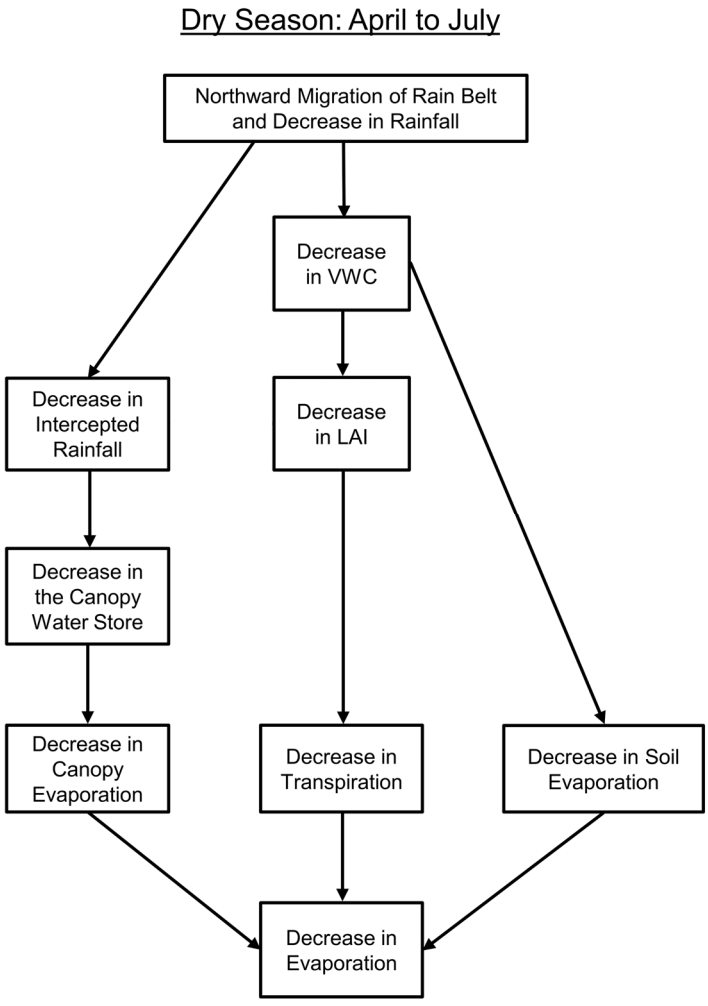


Figure 5.13 Flow chart showing plausible dynamics controlling the seasonal cycle of evaporation between April and July during the savannah's dry season

Between July and November, evaporation increases (Figure 5.14). The rain belt migrates southwards back into the savannah between July and November, which increases the amount of rainfall and the interception of rainwater by the canopy. The canopy water store recovers, and this explains the increase in canopy evaporation. Early green-up, or an early increase in LAI, also occurs from July onwards, which explains why transpiration increases. Finally, the increase in rainfall causes VWC to increase from September onwards, explaining the increase in soil evaporation. The net effect of an increase in all three evaporation components is an increase in evaporation.

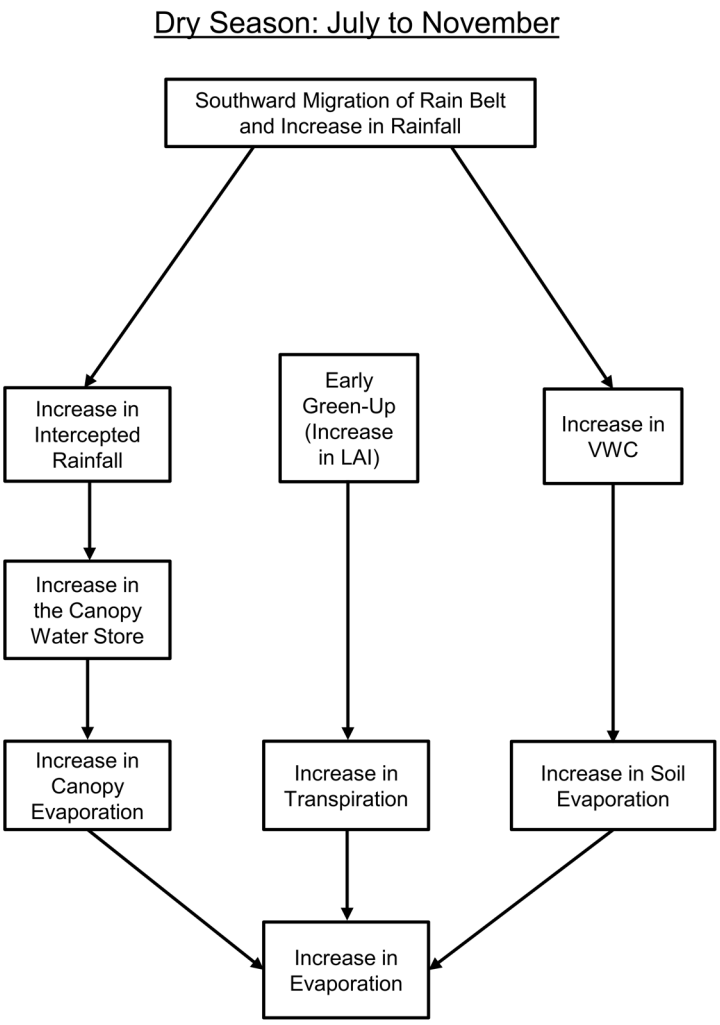


Figure 5.14 Flow chart showing plausible dynamics controlling the seasonal cycle of evaporation between July and November during the savannah's dry season

5.8.2 Consistency with the Budyko framework

We have confidence in the dynamics which control the seasonal cycle of evaporation in the savannah's wet season between November and March because they are consistent with the framework set out by Budyko (1961), which defines how evaporation behaves under different soil moisture conditions. When soil moisture availability is plentiful in wet regimes, evaporation is controlled by surface DSR (Figure 5, Seneviratne et al. 2010). The results show that the savannah fits into this regime between November and March. Soil moisture is close to field capacity throughout this period. An increase in surface DSR is a plausible driver of the increase in LAI, transpiration, and therefore evaporation, in agreement with the Budyko framework.

Between March and April, VWC continues to remain close to field capacity. An increase in surface DSR is a plausible driver of the increase in LAI and therefore transpiration, in agreement with the Budyko framework. Simultaneously, the results suggest that the northward migration of the rain belt away from the savannah and the resultant decrease in rainfall reduces the size of the canopy water store, thereby decreasing canopy evaporation. While not represented in the Budyko framework, the decrease in the canopy evaporation component is effectively explained by the northward migration of the rain belt and the decrease in rainfall (Washington et al. 2013; Creese and Washington 2016). The increase in transpiration and the decrease in canopy evaporation offset one another, and the net result is stable evaporation.

Between April and July, a decrease in VWC plausibly drives a decrease in LAI and therefore decrease in transpiration. The decrease in VWC also explains why soil evaporation decreases. This is consistent with the Budyko framework, which states that when a region moves from a wet regime with high soil moisture to a transition regime with lower soil moisture, a decrease in soil moisture causes evaporation to decrease (Figure 5, Seneviratne et al. 2010). The northward migration of the rain belt and the resultant decrease in rainfall also explains a decrease in canopy evaporation. We have confidence in this phenomenon as the decrease in canopy evaporation is again effectively explained by the northward migration of the rain belt and decrease in rainfall. The net effect of a reduction in all three evaporation components is a decrease in evaporation.

Between July and November, an increase in VWC explains why soil evaporation increases. This is consistent with the Budyko framework, which states that when a region moves from a transition regime to a wet regime, an increase in soil moisture causes evaporation to increase (Figure 5, Seneviratne et al. 2010). The results also suggest that early green-up, or an early increase in LAI, explains the increase in transpiration. Even though early green-up is not represented in the Budyko framework, this mechanism is ubiquitous in southern Tropical Africa (Ryan et al. 2017). Given that LAI and transpiration vary closely together (Wei et al. 2017), it is plausible that the early green-up is driving the increase in transpiration. Furthermore, the southward migration of the rain belt and the resultant increase in rainfall explains the increase in canopy evaporation. Although canopy evaporation is not part of the Budyko framework, we again have confidence in this phenomenon as the increase in canopy evaporation is explained by the southward migration of the rain belt and the subsequent increase in rainfall. The net effect of an increase in all three evaporation components is an increase in evaporation.

5.8.3 Improving rainforest evaporation in ERA5-Land and MERRA-2

Section 5.7 showed that ERA5-Land produces too much canopy evaporation in the basin's rainforest (Figure 5.10a) and that this is largely responsible for its overestimation in evaporation in this ecoregion. The failure to account for convective rainfall occurring beneath the scale of a typical grid box in ERA5-Land may be a contributing factor to the overestimation of the canopy evaporation.

The LSM in ERA5-Land, CH-TESSEL, is driven by total precipitation from the ERA5 reanalysis, which is produced from cycle 41r2 of the Integrated Forecasting System from ECMWF (Muñoz-Sabater et al. 2021). This cycle produces rainfall as a grid-box average value, and the fine spatial scales associated with convective rainfall are not adequately resolved (Lavers et al. 2021). Generating rainfall uniformly over the grid box in a lighter than expected form means that in the rainforest ecoregion, which often has heavy convective rainfall, the rainfall intensity is too light. The reanalysis LSM produces a large canopy water store because the high LAI can easily intercept and hold light rain. Therefore, there is excessive evaporation of water from the canopy into the atmosphere to instantaneously satisfy the atmospheric demand for evaporation.

Chapter 3 investigated the parameterisations that LSMs of 11 GCMs from the fifth phase of the Atmospheric Model Intercomparison Project (AMIP) use to produce evaporation and found that GCMs which performed well in the basin for evaporation contain sub-grid rainfall schemes in their LSMs. The authors argued that using sub-grid rainfall schemes in the LSMs of all GCMs could improve how the GCMs produce Congo Basin

evaporation by reducing canopy evaporation. When sub-grid rainfall is added to the LSM, convective rainfall occurs in a smaller fraction of the grid box, and incoming rainfall is distributed according to a probability density function (Pitman 1991; Wang et al. 2006). On the grid-box average, rainfall intensity increases, canopy throughfall increases, the high LAI intercepts less rainwater, the canopy water store reduces in size, and canopy evaporation decreases. This means that evaporation is lowered to more realistic values.

Muñoz-Sabater et al. (2021) confirmed that the CH-TESSEL LSM included in ERA5-Land does not include a correction to the ERA5 rainfall forcing to account for rainfall on sub-grid scales. Therefore, we suggest that including a sub-grid rainfall scheme in the LSM of the next version of ERA5-Land, as already included in some CMIP5 GCMs, could increase the rainfall intensity, decrease the canopy evaporation, and reduce evaporation to more realistic values in areas of high LAI. This could bring the evaporation into good agreement with LandFlux-EVAL in the basin's rainforest and allow the next version of the ERA5-Land reanalysis to be used to derive the dynamics controlling the seasonal cycle of evaporation in this ecoregion.

MERRA-2 was shown to produce too much canopy evaporation in the basin's rainforest (Figure 5.10b) which partially explains its overestimation in evaporation. MERRA-2 has a lower overestimation of canopy evaporation than ERA5-Land. One reason for this could be that model-generated rainfall over Africa in MERRA-2 is corrected with rainfall from the CPC Merged Analysis of Precipitation product before producing the final rainfall output. This corrected rainfall explains why MERRA-2 has the best performance of seven reanalyses in its rainfall estimates when compared against the NIC131-Gridded reference

data set (Hua et al. 2019), and the improved input rainfall could lead to improved canopy evaporation in the reanalysis. A further reason could be that in the Catchment LSM included in MERRA-2, convective rainfall is assumed to occur over only 2% of the canopy leaf area (Reichle et al. 2011; Reichle et al. 2017), which means that MERRA-2 corrects the input rainfall to account for convective rainfall on fine spatial scales. By increasing the rainfall intensity on the grid-box average and reducing the size of the canopy water store, this adjustment could also lead to improved canopy evaporation.

However, despite these two favourable features, MERRA-2 still overestimates canopy evaporation in the basin's rainforest. Reichle et al. (2017) argued that even though daily rainfall totals are prescribed, the intensity of rainfall in MERRA-2 is too low at sub-daily timescales, due to the use of diurnal rainfall as the background field in the rainfall correction algorithm. This could produce an excessively large canopy water store that contributes to the overestimation of canopy evaporation. Therefore, future work is necessary to investigate this issue, as resolving it could further lower the overestimation.

MERRA-2 also appears to produce too much soil evaporation in the basin's rainforest (Figure 5.10b) The Catchment LSM included in MERRA-2 calculates the resistance to soil evaporation as a function of surface soil moisture alone (Koster and Suarez 1996; Koster et al. 2000). The LSM might not take into account the fact that soil evaporation depends on surface solar radiation at the first stage of the process (Wang and Liu 2007). This is important in a rainforest, because surface solar radiation is considerably restricted by the canopy, and soil evaporation should be depressed (Or and Lehmann 2019). However, further work is needed to confirm the causes of the overestimation in soil evaporation in MERRA-2, and to design a solution to address this.

5.9 Conclusions

This chapter has moved towards a complete understanding of the dynamics controlling the seasonal cycle of Congo Basin evaporation on the basin-wide average. This was achieved by deriving plausible dynamics which explain the seasonal cycle of evaporation in the savannah, which covers approximately half of the basin. These dynamics were derived using the ERA5-Land reanalysis, which effectively reproduces the seasonal cycle of evaporation in the savannah from LandFlux-EVAL. We have confidence in these dynamics because they are consistent with the Budyko framework or evidence from the literature. The seasonal cycle of evaporation was analysed from November to November to account for evaporation during one wet season between November and March, and one dry season between March and November.

In the savannah ecoregion, between November and March an increase in surface DSR is a plausible driver of an increase in LAI, transpiration and therefore evaporation. Between March and April, a decrease in rainfall explains why canopy evaporation decreases, while an increase in surface DSR is a plausible driver of an increase in LAI and therefore transpiration, and the net effect is stable evaporation. Between April and July, a decrease in rainfall as the rain belt migrates northwards away from the savannah is a plausible explanation for why the three components of evaporation decrease, and the net effect is that evaporation falls to a trough. Between July and November, an increase in rainfall as the rain belt migrates back southwards explains why canopy evaporation increases, early green-up occurs, which explains why transpiration increases, and the increase in rainfall causes soil VWC to increase from September onwards, which explains why soil evaporation increases. The net effect is a recovery in evaporation.

Using sub-grid rainfall in the LSM of the next version of ERA5-Land could bring its seasonal cycle of evaporation into good agreement with LandFlux-EVAL in the rainforest and allow the next version of this reanalysis to be used to derive the dynamics controlling the seasonal cycle of evaporation here. Collectively, the previously researched dynamics on why evaporation is suppressed at the November rainfall peak relative to the March rainfall peak, the dynamics researched in this chapter controlling the seasonal cycle of evaporation in the savannah, and the dynamics controlling the seasonal cycle of evaporation in the rainforest still to be investigated, will achieve a full understanding on the basin-wide average of the seasonal cycle of Congo Basin evaporation.

Acknowledgements

The land cover map used in this chapter is from the European Space Agency Climate Change Initiative Land Cover Project (2017) and contains modified Copernicus data. This chapter uses the LandFlux-EVAL merged benchmark synthesis products of ETH Zurich produced under the aegis of the Global Energy and Water Exchanges (GEWEX) and Integrated Land-Ecosystem Atmosphere Process Study (ILEAPS) projects (http://www.iac.ethz.ch/url/research/LandFlux-EVAL/). The authors acknowledge the data providers for the ERA5-Land and MERRA-2 reanalysis data sets used in this chapter. David Crowhurst is funded by the U.K. Natural Environment Research Council (NERC) through the Doctoral Training Partnership in Environmental Research (Grant NE/L002612/1). Richard Washington is partly supported by the NERC-Department for International Development (DfID) Uncertainty reduction in Models For Understanding deveLopment Applications (UMFULA) project (Grant NE/M020207/1).

6 Conclusions

6.1 Introduction

Although the atmospheric leg of the land-atmosphere coupling in the Congo Basin has been studied, the terrestrial leg has received less research attention, and the dynamics that control the climatological seasonal cycle of the Congo Basin evaporation were previously unclear. This thesis aimed to address this lack of clarity by making progress towards an understanding of these evaporation dynamics.

Long term in situ observations of evaporation and its controls were unavailable for the basin. Therefore, this thesis sought to contribute to knowledge on evaporation dynamics by using GCMs and reanalyses. The thesis also sought to identify ways to improve reanalyses where no agreement was found between evaporation from reanalyses and evaporation from LandFlux-EVAL. Achieving agreement could allow data from these reanalyses to be used to advance understanding of the dynamics controlling the seasonal cycle of Congo Basin evaporation in future work.

For each of the research questions, this conclusion summarises the findings of the thesis which answer the question, discusses the limitations of the research approach which influence the findings, and outlines the implications of the findings for the field. The conclusion continues by addressing the extent to which the thesis aim was fulfilled, and details the contribution to knowledge that the thesis has made. Finally, the conclusion suggests directions for future work.

6.2 Research question 1

6.2.1 Findings

The purpose of the first research question was to reveal information from GCM and reanalysis data about the dynamics controlling the climatological seasonal cycle of Congo Basin evaporation.

Chapter 3 provided initial insights from LandFlux-EVAL, CHIRPS2 and CMIP5 GCMs on the characteristics of the seasonal cycle of Congo Basin evaporation. These insights set the foundations for the research to follow. The seasonal cycle of evaporation was plotted from LandFlux-EVAL on the basin-wide average and showed that evaporation increases from January to its one peak in March, remains at its peak between March and April, decreases from April to a trough in July, and recovers between July and January. Evaporation was shown to be lower in July than at the two rainfall peaks in March and November in the basin, and it was argued that the factors responsible for this were unclear. The results also showed that evaporation is lower at the November rainfall peak than the March rainfall peak, despite similar rainfall in CHIRPS2.

GCMs which performed well against LandFlux-EVAL evaporation were shown to have a similar canopy and soil evaporation in March and November, but lower transpiration in November than March. Therefore, it was concluded that lower transpiration is likely to explain why evaporation is lower in November than March. Chapter 3 argued that the dynamics controlling lower transpiration, and therefore evaporation, were not understood.

As a result of these findings, Chapter 4 aimed to discover the dynamics responsible for the lower evaporation at the November rainfall peak than the March rainfall peak on the basin-wide average. A decision was taken to use reanalyses in preference to GCMs to investigate these dynamics for the reason set out in Section 1.1.

Data from the ERA5-Land reanalysis, which effectively reproduced the magnitude and pattern of the evaporation difference between the two rainfall peaks in LandFlux-EVAL, were used to derive plausible dynamics controlling this feature of the evaporation seasonal cycle as follows: lower surface DSR in November is a plausible driver of lower LAI, transpiration and therefore evaporation in the northern rainforest, southern rainforest, and north-eastern savannah, while lower VWC is a plausible driver of lower LAI, transpiration and therefore evaporation in the south-eastern savannah. Collectively, these contrasting controls were shown to provide a plausible explanation for the lower evaporation in November than March on the basin-wide average. As discussed in Section 4.4.2, a caveat on this interpretation is that it is not possible to make causal statements regarding drivers of LAI in ERA5-Land, because LAI is prescribed to this reanalysis.

The regional approach used in Chapter 4 provided a plausible answer to the problem posed in Chapter 3 on the evaporation difference between March and November on the basin-wide average because this difference was understood as the collective of contrasting controls on evaporation in different basin regions. In each region, lower evaporation was plausibly driven by either lower solar radiation or lower soil moisture, and the results for each region were therefore consistent with the Budyko framework. Chapter 4 concluded by arguing that to understand the full seasonal cycle of evaporation on the basin-wide average, a regional approach was also necessary.

To expand beyond the peaks and move towards a more complete understanding of the dynamics controlling the seasonal cycle of evaporation, a regional approach was therefore used in Chapter 5, which sought to derive plausible dynamics that control the seasonal cycles of evaporation in the rainforest and savannah. Good agreement was not found between reanalyses and LandFlux-EVAL in the rainforest, meaning that reanalyses could not provide information about the dynamics controlling the seasonal cycle of evaporation in this ecoregion. However, good agreement was found between ERA5-Land and LandFlux-EVAL in the savannah.

ERA5-Land was therefore used to derive plausible dynamics controlling the seasonal cycle of evaporation in the savannah as follows: between November and March an increase in surface DSR is a plausible driver of an increase in LAI, transpiration and therefore evaporation. Between March and April, a decrease in rainfall explains why canopy evaporation decreases, while an increase in surface DSR is a plausible driver of an increase LAI and therefore transpiration, and the net effect is stable evaporation. Between April and July, a decrease in rainfall as the rain belt migrates northwards away from the savannah explains why the three components of evaporation decrease, and the net effect is that evaporation falls to a trough. Between July and November, an increase in rainfall as the rain belt migrates back southwards into the savannah explains why canopy evaporation increases, early green-up occurs, which explains why transpiration increases, and the increase in rainfall causes soil VWC to increase from September onwards, which explains why soil evaporation increases. The net effect is a recovery in evaporation. As discussed in Section 5.5.3, a caveat on this interpretation is that it is not possible to make causal statements regarding drivers of LAI in ERA5-Land, because LAI is prescribed to this reanalysis. By deriving these plausible dynamics, Chapter 5 also

showed that a decrease in rainfall in the savannah contributes to answering the remaining problem posed in Chapter 3 on why evaporation falls to a trough between April and July on the basin-wide average.

6.2.2 Limitations of the research approach

A limitation of the approach used to answer Research Question 1 was that model experiments were not conducted. Therefore, a caveat of the findings is that cause and effect was not ascertained. However, there is confidence in the findings despite this caveat because the findings were shown to be consistent with the Budyko framework or with evidence from the literature.

Another limitation of the research approach is that only supply (LAI) and demand (VPD) drivers of transpiration were investigated. Lian et al. (2018) showed that a range of other environmental drivers could have small contributions to make. However, these drivers are unlikely to have much of an effect on the seasonal cycle of evaporation.

Finally, as discussed in Chapter 2, a further caveat on the results is that LandFlux-EVAL has not been validated against in situ observations from within the Congo Basin. However, we have confidence in the use of LandFlux-EVAL as a reliable reference point for the reasons set out in Section 2.2.1.

6.2.3 Implications of the findings for the field

The improved scientific understanding of the dynamics controlling the climatological seasonal cycle of Congo Basin evaporation developed in this thesis has implications for the field of Congo Basin climate science.

Firstly, by adding to the literature on the Congo Basin climate, this thesis has contributed to developing a theoretical framework on hydrological science and land-atmosphere coupling in the basin (Ndehedehe et al. 2018). As terrestrial land-atmosphere coupling is an essential part of the climate system of the basin, this contribution could motivate future studies on the basin's climate and its links with other regions (James et al. 2020). Insights on the seasonal cycle of basin evaporation and the dynamics that control this cycle could also be important for scientific applications within basin climate research and other fields such as environmental management (Fisher et al. 2017).

Secondly, as this thesis has provided plausible dynamics responsible for the lower evaporation at the November rainfall peak relative to the March rainfall peak, and the seasonal cycle of evaporation in the basin's savannah, GCMs can now be evaluated against a baseline to assess how well they reproduce these dynamics. GCMs must effectively reproduce present-day evaporation to have confidence in their simulations and projections of evaporation, and therefore rainfall.

Thirdly, this thesis has made progress by understanding evaporation on the domain-wide average as the collective of processes operating in different basin regions. The implication

is that future studies on evaporation in the Congo Basin and further afield should recognise that evaporation can vary substantially within the domain studied. Scientific research which averages across large domains might not produce satisfactory outcomes.

6.3 Research question 2

6.3.1 Findings

The purpose of the second research question was to identify possible ways to improve reanalyses where no agreement could be found between evaporation from reanalyses and evaporation from LandFlux-EVAL. This could bring reanalyses into good agreement with LandFlux-EVAL for part(s) of the basin where this is needed and allow further evaporation dynamics for the basin to be derived from reanalyses in future work. As many contemporary reanalyses include improved convective parameterisations, the focus was to identify how to improve the LSMs in the reanalyses.

The results from Chapter 3 showed that two CMIP5 GCMs which perform well for evaporation against LandFlux-EVAL include sub-grid rainfall parameterisations in their LSMs. These schemes could explain why the GCMs have a lower proportion of canopy evaporation and a higher proportion of transpiration at the two rainfall peaks, compared to GCMs which do not include them. Including sub-grid rainfall in an LSM increases grid box average rainfall intensity, increases canopy throughfall, reduces canopy water storage, reduces canopy evaporation, and increases transpiration to satisfy the

atmospheric demand for evaporation. The increase in transpiration is less than the decrease in canopy evaporation, because transpiration has an additional resistance associated with stomatal closure and is slower than canopy evaporation. This change in the evaporation partitioning means that evaporation is lowered to more realistic values.

Chapter 3 therefore suggested that using sub-grid rainfall schemes in the LSMs of all GCMs could improve how GCMs produce basin evaporation. This improvement could propagate through the hydrological cycle, leading to improvements in how individual GCMs generate Congo Basin rainfall. If implemented across all GCMs, this could narrow the wide spread in Congo Basin rainfall.

As both GCMs and reanalyses include LSMs, it was possible to use the finding from Chapter 3 on the importance of sub-grid rainfall schemes in LSMs to suggest ways to improve evaporation from reanalyses in the Congo Basin. In Chapter 5, good agreement could not be found between ERA5-Land and LandFlux-EVAL, and MERRA-2 and LandFlux-EVAL, for the basin's rainforest. This precluded the use of these two reanalyses to understand the dynamics controlling the seasonal cycle of evaporation in this ecoregion. Therefore, ERA5-Land and MERRA-2 need improving before they can be used to discover these dynamics.

Chapter 5 showed that the main reason for the overestimation in rainforest evaporation in ERA5-Land is that it overestimates canopy evaporation. The chapter therefore used the findings from Chapter 3 to suggest that adding a sub-grid rainfall scheme to the LSM of the next version of ERA5-Land could increase grid-box average rainfall intensity,

decrease the canopy evaporation, and reduce evaporation to more realistic values. This could bring its evaporation into good agreement with LandFlux-EVAL in the rainforest, allowing the next version of ERA5-Land to be used to understand the seasonal cycle of evaporation in this ecoregion. Chapter 5 also showed that the main reasons for the overestimation in evaporation in MERRA-2 are that it overestimates both canopy evaporation and soil evaporation. Following Reichle et al. (2017), the chapter argued that a reason for the overestimate in canopy evaporation could be that the intensity of rainfall in MERRA-2 on sub-daily timescales is too low. Future work is necessary to investigate this issue, as resolving it could further lower the overestimate in canopy evaporation. In addition, the chapter suggested that it is possible that the LSM in MERRA-2 does not take into account the low surface solar radiation in tropical rainforests when calculating soil evaporation, and argued that this could explain the overestimation in soil evaporation. However, further research is needed to confirm the causes of the overestimation in soil evaporation in MERRA-2, and to design a solution to address this. If both canopy evaporation and soil evaporation were improved in MERRA-2, this could bring evaporation from this reanalysis into good agreement with LandFlux-EVAL, allowing it to be used to understand the seasonal cycle of evaporation in the basin's rainforest.

6.3.2 Limitations of the research approach

Chapter 3 suggested that including sub-grid rainfall schemes in more LSMs could improve how GCMs and reanalyses produce Congo Basin evaporation. This finding was derived using composite analysis to identify the parameterisations present in models that perform well, but absent in models that perform less well. A limitation of this approach is that it does not allow for model experiments to be conducted to prove that there is a

causal link between adding sub-grid rainfall schemes to LSMs and improvements in GCM evaporation. However, Wang et al. (2006) found that including sub-grid rainfall in the Community Land Model decreased canopy evaporation and increased transpiration in Central Africa, reducing evaporation to more realistic values.

It is therefore plausible that adding sub-grid rainfall schemes to the LSMs of GCMs and reanalyses which do not currently use them could ensure that these data products produce evaporation more realistically in the basin. Nonetheless, before decisions are taken to implement sub-grid rainfall schemes, developers need to perform experiments to determine whether adding these schemes does improve evaporation in their data products without negatively impacting other aspects of the local hydrological cycle.

Another limitation of the approach is that only eleven models from CMIP5 were analysed in Chapter 3 due to data availability constraints. Analysing more models could have provided additional information on the parameterisations included in the models which perform well, and this would have been helpful information for model developers.

6.3.3 Implications of the findings for the field

The finding on the potential importance of sub-grid rainfall schemes for evaporation in the Congo Basin has implications for model evaluation and model development.

Firstly, as Chapter 3 successfully identified the potential importance of sub-grid rainfall schemes using an approach that analysed evaporation parameterisations, there is potential to apply this approach more widely in climate science to assess how models behave. For

example, this approach could be used to investigate why some GCMs and reanalyses produce better convective rainfall in the basin than others by outlining how their convective parameterisations differ. The information on why some GCMs and reanalyses perform well could then be used by developers whose GCMs and reanalyses perform less well, to improve how their atmospheric models produce basin rainfall. Pathak et al. (2019) used an approach of this kind to analyse convective parameterisations in CMIP5 models in South Asia, and a similar study would be of benefit for the Congo Basin.

Secondly, the knowledge on the potential importance of sub-grid rainfall in LSMs could guide developers in a direction that leads to improvements in how GCMs and reanalyses produce basin evaporation. For example, using a sub-grid rainfall scheme in the LSM of ERA5-Land could reduce its evaporation to achieve agreement with LandFlux-EVAL in the basin's rainforest, and allow the dynamics controlling the seasonal cycle of evaporation to be discovered in this ecoregion.

However, it is important to note that implementing sub-grid rainfall will impact evaporation beyond the basin. Therefore, model experiments conducted by developers should confirm that sub-grid rainfall has benefits for evaporation both within the basin and further afield, without negatively impacting the global hydrological cycle. At least two modelling centres have already included sub-grid rainfall parameterisations in their LSMs, indicating that sub-grid rainfall could be included in more models without difficulty. It is possible that using sub-grid rainfall could reduce overestimates in evaporation in regions of higher LAI specifically, both within the basin and further afield.

6.4 Fulfilment of thesis aim and thesis contribution to knowledge

This thesis aimed to make progress towards an understanding of the dynamics controlling the climatological seasonal cycle of Congo Basin evaporation. This aim was fulfilled because the thesis has made substantial progress towards understanding these dynamics. The thesis has provided two significant contributions to knowledge on the dynamics controlling this cycle, and has begun developing a theoretical framework useful for advancing hydrological science in the basin. The first contribution to knowledge was to highlight and explain a key feature of the evaporation seasonal cycle on the basin-wide average. This feature is that evaporation is lower at the November rainfall peak than the March rainfall peak, despite similar rainfall. Plausible dynamics responsible for this feature were derived, consistent with the Budyko framework. The second contribution was to explain the seasonal cycle of evaporation for the basin's savannah, which covers the southern half of the studied domain. Plausible dynamics controlling this cycle were derived, consistent with the Budyko framework or with evidence from the literature.

Although the aim was fulfilled, it is important to recognise that future research still needs to be carried out to derive the dynamics controlling the seasonal cycle of evaporation in the basin's rainforest, which covers the northern half of the studied domain. This is because collectively, the dynamics which explain why evaporation is suppressed at the November rainfall peak relative to the March rainfall peak, and the dynamics controlling the seasonal cycles of evaporation in the basin's rainforest and savannah, will explain what controls the seasonal cycle of evaporation on the basin-wide average. This thesis was unable to derive the dynamics in the rainforest using a reanalysis because good agreement was not found between a reanalysis and LandFlux-EVAL.

However, the thesis has suggested that using a sub-grid rainfall parameterisation in the LSM of the next version of ERA5-Land could improve how this reanalysis produces evaporation in the basin's rainforest. This could bring the seasonal cycle of evaporation from ERA5-Land into good agreement with LandFlux-EVAL in the rainforest, and allow the next version of this reanalysis to be used to derive the dynamics controlling the seasonal cycle of evaporation in this ecoregion.

6.5 Suggestions for future work

This section provides suggestions for future work that build upon the findings of this thesis. These suggestions are divided into two categories: (1) scientific understanding of Congo Basin climate dynamics, and (2) use of sub-grid rainfall schemes in future GCMs and reanalyses to improve how they represent evaporation.

6.5.1 Congo Basin climate dynamics

The main finding of Chapter 4 was that higher cloud cover is largely responsible for lower surface DSR, which in turn is largely responsible for lower LAI, lower transpiration, and therefore lower evaporation at the November rainfall peak than the March rainfall peak on the basin-wide average. However, this thesis did not explore why there is higher cloud cover in November than March, and future research could investigate reasons for this. Factors that could play a role include faster LLW in SON than MAM, which deliver more moisture to the basin per unit time in SON (Pokam et al. 2014), and the development of a hotspot of MCS activity at the coordinates 2°S, 28°E in SON but not in MAM (Jackson

et al. 2009; Hart et al. 2019). Hartman (2021) argued that there is a need for further research on why this convective hotspot develops in the SON season and why it is not present in the MAM season.

Although this thesis has discovered a plausible reason for the difference in evaporation between the two rainfall peaks, the reason for the rainfall difference between these peaks is not yet understood. CHIRPS2 was shown in Chapter 4 to have similar rainfall amounts at the two peaks, but Figure 6.1 shows that the rainfall difference varies regionally within the basin. Future research is therefore required to explain the key characteristics of this figure. The hotspot of convection at 2°S, 28°E has much higher rainfall in November than March, which further highlights the need to understand this feature of the basin's climate.

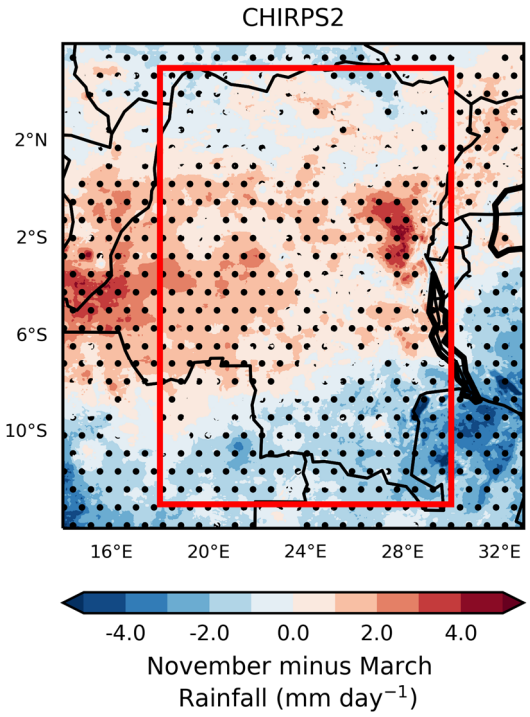


Figure 6.1 Sixteen-year mean (1989-2005) November minus March rainfall (mm day^{-1}) difference map from CHIRPS2. The domain used in this thesis is shown with a red box (14°S to 4°N, 18°E to 30°E). Dots are grid points where the difference between March and November is statistically significant ($p<0.05$)

ERA5-Land and MERRA-2 overestimated the seasonal cycle of evaporation in the Congo Basin rainforest. Therefore, further development of these reanalyses is required to achieve good agreement with LandFlux-EVAL and allow the next versions of these reanalyses to be used to derive the evaporation dynamics in this ecoregion. In particular, using sub-grid rainfall in the LSM of the next version of ERA5-Land could be a successful way to reduce overestimates in rainforest evaporation and achieve good agreement between ERA5-Land and LandFlux-EVAL.

The seasonal cycle of evaporation for the rainforest is presented from LandFlux-EVAL in Figure 5.2b. The curve shows that evaporation is flat, except for boreal summer, when evaporation falls slightly between April and July, and recovers between July and September. Philippon et al. (2016) argued that in a region to the north-west of the basin, outside of the domain studied in this thesis, a pronounced drop in solar radiation in the boreal summer is likely to be responsible for reduced EVI. Therefore, it is possible that a drop in solar radiation in the boreal summer is also responsible for reduced evaporation in the Congo Basin rainforest, but further research is required to confirm this.

As plausible dynamics responsible for the difference in evaporation at the two rainfall peaks and the seasonal cycle of evaporation in the savannah have now been discovered, future research could evaluate how well current generation GCMs reproduce these dynamics. When confidence is achieved that individual GCMs can adequately reproduce these two aspects of the cycle, evaporation projections could then be analysed for these two aspects of the cycle from the GCMs that perform well. Understanding how evaporation will change in the savannah is of particular importance, as a large percentage of the population rely on subsistence agriculture in this ecoregion. Changes in evaporation

can affect water availability for agriculture, both directly as evaporation extracts water from the soil, and indirectly as evaporation affects rainfall, which then feeds back to the soil. Additionally, once an understanding of the dynamics controlling the seasonal cycle of evaporation is achieved for the rainforest, then GCMs could also be evaluated to discover which GCMs effectively simulate the seasonal cycle of evaporation in this region. Projections from these GCMs could then be analysed to understand how and why the seasonal cycle of evaporation in the rainforest will change.

6.5.2 Use of sub-grid rainfall in GCMs and reanalyses to improve evaporation

This thesis has highlighted the potential importance of using sub-grid rainfall schemes in the LSMs of GCMs and reanalyses to improve how these products produce the seasonal cycle of evaporation in the Congo Basin. This could enable the dynamics controlling this cycle to be discovered for the rainforest ecoregion. CMIP5 GCMs which performed well for evaporation in the Congo Basin were shown to contain sub-grid rainfall schemes in their LSMs. Therefore, the results demonstrate the need to bring a consideration of using sub-grid rainfall schemes to the forefront of GCM and reanalysis development.

As discussed in Section 6.3.2, this thesis did not perform model experiments to determine whether including a sub-grid rainfall scheme in a LSM would have benefits for evaporation in the basin and further afield without negatively impacting other aspects of the hydrological cycle. To justify implementing sub-grid rainfall schemes into their LSMs, GCM and reanalysis developers should produce experimental simulations of global evaporation and rainfall with and without a sub-grid rainfall scheme, to confirm

that the benefits of including these schemes in their LSMs outweigh any potential drawbacks on global scales. Berg and Sheffield (2019) argued that a tension exists between implementing modifications to increase transpiration and reduce canopy evaporation, and possible unintended consequences on other aspects of simulated climate. Wang and Eltahir (2000) found that when a sub-grid rainfall scheme was added to a coupled climate model, evaporation in West Africa was improved, and rainfall was increased to more realistic values. Wang et al. (2006) found a similar evaporation improvement for the Congo Basin in a LSM, but the authors did not assess the effect on rainfall. If model rainfall were to increase in the basin, then this would negatively impact how the model represents the basin's climate. If replicated across the globe, this could mean that sub-grid rainfall schemes should not be included in the LSM in question.

Pitman (1991) argued that including a sub-grid rainfall scheme in most LSMs could be a computationally cheap way to improve how they produce evaporation. However, an alternative way to improve evaporation in the basin and further afield could be to improve the representation of rainfall intensity in the atmospheric models of climate data products.

The development of atmospheric models is the subject of current work, and there have been recent improvements. For example, the atmospheric model included in ERA5-Land includes an enhanced convective parameterisation, which has led to better rainfall intensity against Tropical Rainfall Measuring Mission data (Hersbach et al. 2020) and therefore better evaporation relative to ERA-Interim (Martens et al. 2020). If convective parameterisations were improved in other GCMs and reanalyses, this could lead to improved rainfall intensity and therefore evaporation in the basin and further afield.

As discussed in Section 6.3.3, a future study could investigate how to improve convective parameterisations by following the approach used in Chapter 3. This study could determine why some GCMs and reanalyses produce better convective rainfall than others in the basin by outlining how their convective parameterisations differ (Hart et al. 2018). The information on why some GCMs and reanalyses produce convective rainfall more effectively could then be used by developers whose GCMs and reanalyses produce convective rainfall less effectively. This could help to improve how their atmospheric models produce rainfall, with positive impacts on LSM evaporation.

Another way to improve rainfall intensity and therefore evaporation could be to improve the resolution of atmospheric models. Some research has investigated the benefits of moving to a higher resolution on the simulation of rainfall intensity over Africa. Tamoffo et al. (2020) used a process-based analysis to investigate the added value of using 25 km x 25 km regional climate model (RCM) simulations of rainfall in Central Africa instead of coarser resolution GCMs. They found that using RCMs can improve rainfall intensity in Central Africa, but not always for the right reasons, which indicates that moving to an RCM may not always be the best approach. A better way forward could be to move to even finer spatial resolutions, which allow atmospheric models to resolve convection without the need for convective parameterisations. This could enable atmospheric models to produce rainfall intensity adequately and for the right reasons.

Senior et al. (2021) examined the impact of moving from a 25 km x 25 km resolution RCM (R25-Africa) to an even finer 4.5 km x 4.5 km RCM (CP4-Africa) on the land surface hydrology of Africa. Results showed that with improved rainfall intensity, the

fraction of canopy interception loss falls from 22% in R25-Africa to less than 6% in CP4-Africa in the Congo Basin. This brings canopy interception loss into better agreement with observations of approximately 10% from Miralles et al. (2010). Improving the resolution of the atmospheric model to very fine spatial scales could therefore explicitly resolve the convective rainfall and correct errors in rainfall intensity for the right reasons, resulting in a positive effect on model evaporation both within the basin and further afield without the need for a sub-grid rainfall parameterisation in the LSM. Senior et al. (2021) anticipated that more of these high resolution simulations will be developed in future work and argued that they should become routine.

An additional way to improve rainfall intensity and therefore evaporation could be to make use of machine learning. Rasp et al. (2018) trained a neural network to represent atmospheric sub-grid processes by learning from a model with explicit convection. The trained neural network replaced the traditional sub-grid parameterisations in a GCM. Results showed that the GCM performed reasonably well for key aspects of climate variability. The authors suggested that machine learning can improve how sub-grid processes are represented, and further work is needed to explore the use of these methods.

Aside from rainfall intensity, model developers could also investigate how to rectify errors in the simulation of lateral water flow within the soil (Fatichi and Papas 2017) and errors in how reanalyses produce soil evaporation (Or and Lehmann 2019). Resolving these errors where appropriate could lead to further improvements in how GCMs and reanalyses represent evaporation both within the basin and beyond.

GCM and reanalysis developers therefore have a range of options that could be used to improve evaporation in their data products both for the Congo Basin and further afield, and developers should decide which is the best combination to use for their particular product(s). It is important to note that there has been model development between CMIP5 and CMIP6, and future work should investigate CMIP6 parameterisations to gain further insights on how to improve GCMs and reanalyses. Wild (2020) found that CMIP6 models still have a wide spread in evaporation on global scales, which suggests that across the spectrum of CMIP6 models, many of the issues present in CMIP5 related to evaporation have not been addressed.

6.6 Concluding comments

Alsdorf et al. (2016) argued that overcoming the challenge of data constraints is not straightforward and will require concerted efforts by the community of scientists working on the climate of the Congo Basin. However, despite the scarcity of long-term climate records, this thesis has made a significant contribution towards understanding the dynamics controlling the seasonal cycle of Congo Basin evaporation.

The thesis justified the LandFlux-EVAL evaporation product as a credible reference data set for evaporation in the basin, and made progress using data from the ERA5-Land reanalysis where good agreement between ERA5-Land and LandFlux-EVAL was found. This approach allowed the thesis to advance knowledge on the terrestrial leg of the basin's land-atmosphere coupling, thereby adding to the body of literature on the basin's climate.

7 References

Adebiyi AA, Zuidema P (2016) The role of the southern African easterly jet in modifying the southeast Atlantic aerosol and cloud environments. Q J R Meteorol Soc 142:1574–1589. https://doi.org/10.1002/qj.2765

Adole T, Dash J, Rodriguez-Galiano V, Atkinson PM (2019) Photoperiod controls vegetation phenology across Africa. Commun Biol 2:1-13. https://doi.org/10.1038/s42003-019-0636-7

Alber K, Raghavendra A, Zhou L et al (2021) Analyzing intensifying thunderstorms over the Congo Basin using the Gálvez-Davison index from 1983-2018. Clim Dyn 56:949-967. https://doi.org/10.1007/s00382-020-05513-x

Alexander L (2011) Climate science: Extreme heat rooted in dry soils. Nat Geosci 4:12-13. https://doi.org/10.1038/ngeo1045

Aloysius NR, Sheffield J, Saiers JE et al (2016) Evaluation of historical and future simulations of precipitation and temperature in central Africa from CMIP5 climate models. J Geophys Res Atmos 121:130-152. https://doi.org/10.1002/2015JD023656

Alsdorf D, Beighley E, Laraque A et al (2016) Opportunities for hydrologic research in the Congo Basin. Rev Geophys 54:378-409. https://doi.org/10.1002/2016RG000517

Anav A, Murray-Tortarolo G, Friedlingstein P et al (2013) Remote Sensing Evaluation of Land Surface Models in Reproducing Satellite-Derived Leaf Area Index over the High-Latitude Northern Hemisphere. Part II: Earth System Models. Remote

Sens 5:3637-3661. https://doi.org/10.3390/rs5083637

Baker J, Garcia-Carreras L, Gloor M et al (2021) Evapotranspiration in the Amazon: spatial patterns, seasonality and recent trends in observations, reanalysis and CMIP models. Hydrol Earth Syst Sci 25:2279-2300. https://doi.org/10.5194/hess-25-2279-2021

Balas N, Nicholson SE, Klotter D (2007) The relationship of rainfall variability in West Central Africa to sea-surface temperature fluctuations. Int J Climatol 27:1335-1349. https://doi.org/10.1002/joc.1456

Balsamo G, Beljaars A, Scipal K et al (2009) A Revised Hydrology for the ECMWF Model: Verification from Field Site to Terrestrial Water Storage and Impact in the Integrated Forecast System. J Hydrometeorol 10:623-643. https://doi.org/10.1175/2008JHM1068.1

Barkhordarian A, Saatchi SS, Behrangi A et al (2019) A Recent Systematic Increase in Vapor Pressure Deficit over Tropical South America. Sci Rep 9:1-12. https://doi.org/10.1038/s41598-019-51857-8

Bele MY, Sonwa DJ, Tiani AM (2015) Adapting the Congo Basin forests management to climate change: Linkages among biodiversity, forest loss, and human well-being. For Policy Econ 50:1-10. https://doi.org/10.1016/J.FORPOL.2014.05.010

Bentsen M, Bethke I, Debernard JB et al (2013) The Norwegian Earth System Model, NorESM1-M - Part 1: Description and basic evaluation of the physical climate. Geosci Model Dev 6:687-720. https://doi.org/10.5194/gmd-6-687-2013

Berg A, Sheffield J (2019) Evapotranspiration Partitioning in CMIP5 Models: Uncertainties and Future Projections. J Clim 32:2653-2671.

https://doi.org/10.1175/JCLI-D-18-0583.1

Bonal D, Burban B, Stahl C et al (2016) The response of tropical rainforests to drought-lessons from recent research and future prospects. Ann For Sci 73:27-44. https://doi.org/10.1007/s13595-015-0522-5

Boussetta S, Balsamo G, Beljaars A et al (2013) Impact of a satellite-derived leaf area index monthly climatology in a global numerical weather prediction model. Int J Remote Sens 34:3520-3542. https://doi.org/10.1080/01431161.2012.716543

Budyko MI (1961) The Heat Balance of the Earth's Surface. Sov Geogr 2:3-13. https://doi.org/10.1080/00385417.1961.10770761

Bultot F, Griffiths J (1972) The equatorial wet zone. In: Climates of Africa: World Survey of Climatology. Elsevier, Amsterdam, pp 259-311

Burnett MW, Quetin GR, Konings AG (2020) Data-driven estimates of evapotranspiration and its controls in the Congo Basin. Hydrol Earth Syst Sci 24:4189-4211. https://doi.org/10.5194/hess-24-4189-2020

Chang LL, Dwivedi R, Knowles JF et al (2018) Why Do Large-Scale Land Surface Models Produce a Low Ratio of Transpiration to Evapotranspiration? J Geophys Res Atmos 123:9109-9130. https://doi.org/10.1029/2018JD029159

Congoflux (2020) Measuring greenhouse gas exchange to better understand the contribution of the Congo Basin's forests to fight climate change. https://www.cifor.org/publications/pdf_files/flyer/7786-CongoFlux-Flyer.pdf. Accessed 21 July 2021

Cook KH, Vizy EK (2016) The Congo Basin Walker circulation: dynamics and connections to precipitation. Clim Dyn 47:697-717.

https://doi.org/10.1007/s00382-015-2864-y

Cook KH, Liu Y, Vizy EK (2020) Congo Basin drying associated with poleward shifts of the African thermal lows. Clim Dyn 54:863-883. https://doi.org/10.1007/s00382-019-05033-3

Cooper H, Bennett E, Blake J et al (2021) COSMOS-UK: National soil moisture and hydrometeorology data for empowering UK environmental science. Earth Syst Sci Data 13:1737-1757. https://doi.org/10.5194/essd-13-1737-2021

Cowling SA, Field CB (2003) Environmental control of leaf area production: Implications for vegetation and land-surface modeling. Global Biogeochem Cycles 17:1-14. https://doi.org/10.1029/2002GB001915

Creese A (2018) Climate change in the Congo basin: Evaluating coupled models. DPhil Thesis, University of Oxford

Creese A, Washington R (2016) Using qflux to constrain modeled Congo Basin rainfall in the CMIP5 ensemble. J Geophys Res Atmos 121:13415-13442. https://doi.org/10.1002/2015JD024524

Creese A, Washington R (2018) A process-based assessment of CMIP5 rainfall in the Congo basin: The September-November rainy season. J Clim 31:7417-7439. https://doi.org/10.1175/JCLI-D-17-0818.1

Creese A, Washington R, Jones R (2019a) Climate change in the Congo Basin: processes related to wetting in the December-February dry season. Clim Dyn 53:3583-3602. https://doi.org/10.1007/s00382-019-04728-x

Creese A, Washington R, Munday C (2019b) The Plausibility of September-November Congo Basin Rainfall Change in Coupled Climate Models. J Geophys Res Atmos

124:5822-5846. https://doi.org/10.1029/2018JD029847

Crowhurst D, Morrison R, Evans J et al (2019) Actual evaporation data system for COSMOS-UK. In: Hydro-JULES: Next Generation Land Surface and Hydrological Predictions, The Royal Society, London, 11 Sept 2019. http://nora.nerc.ac.uk/id/eprint/525105. Accessed 21 July 2021

Dai Y, Zeng X, Dickinson RE et al (2003) The common land model. Bull Am Meteorol Soc 84:1013-1023. https://doi.org/10.1175/BAMS-84-8-1013

Damour G, Simonneau T, Cochard H, Urban L (2010) An overview of models of stomatal conductance at the leaf level. Plant Cell Environ 33:1419-1438. https://doi.org/10.1111/j.1365-3040.2010.02181.x

Dargie GC, Lewis SL, Lawson IT et al (2017) Age, extent and carbon storage of the central Congo Basin peatland complex. Nature 542:86-90. https://doi.org/10.1038/nature21048

Dargie GC, Lawson IT, Rayden TJ et al (2018) Congo Basin peatlands: threats and conservation priorities. Mitig Adapt Strateg Glob Chang 24:669-686. https://doi.org/10.1007/s11027-017-9774-8

Datta S, Tagvaeian S, Stivers J (2017) Understanding Soil Water Content and Thresholds for Irrigation Management. Oklahoma Coop Ext Serv. https://doi.org/10.13140/RG.2.2.35535.89765

Decharme B, Douville AH (2007) Global validation of the ISBA sub-grid hydrology. Clim Dyn 29:21-37. https://doi.org/10.1007/s00382-006-0216-7

Dezfuli A (2017) Climate of Western and Central Equatorial Africa. In: Oxford Research Encyclopaedia of Climate Science, Oxford, pp 1-46.

https://doi.org/10.1093/acrefore/9780190228620.013.511

Dezfuli AK, Zaitchik BF, Gnanadesikan A (2015) Regional atmospheric circulation and rainfall variability in south equatorial Africa. J Clim 28:809-818. https://doi.org/10.1175/JCLI-D-14-00333.1

Dirmeyer PA (2011) The terrestrial segment of soil moisture-climate coupling. Geophys Res Lett 38:L16702. https://doi.org/10.1029/2011GL048268

Dirmeyer PA, Wang Z, Mbuh MJ, Norton HE (2014) Intensified land surface control on boundary layer growth in a changing climate. Geophys Res Lett 41:1290-1294. https://doi.org/10.1002/2013GL058826

Dufresne J-L, Foujols M-A, Denvil S et al (2013) Climate change projections using the IPSL-CM5 Earth System Model: from CMIP3 to CMIP5. Clim Dyn 40:2123-2165. https://doi.org/10.1007/s00382-012-1636-1

Dunning C (2018) Characterising and understanding trends and variability in African rainfall seasonality. PhD Thesis, University of Reading

Dyer ELE, Jones DBA, Nusbaumer J et al (2017) Congo Basin precipitation: Assessing seasonality, regional interactions, and sources of moisture. J Geophys Res Atmos 122:6882-6898. https://doi.org/10.1002/2016JD026240

Eltahir EAB, Bras RL (1993) A Description of Rainfall Interception over Large Areas. J Clim 6:1002-1008. https://doi.org/10.1175/1520-0442(1993)006<1002:ADORIO>2.0.CO;2

European Space Agency (2017) Climate Change Initiative Land Cover - Prototype 20m Land Cover Map of Africa 2016. http://2016africalandcover20m.esrin.esa.int. Accessed 21 July 2021

Evans JG, Ward HC, Blake JR et al (2016) Soil water content in southern England derived from a cosmic-ray soil moisture observing system - COSMOS-UK. Hydrol Process 30:4987-4999. https://doi.org/10.1002/hyp.10929

Eyring V, Bony S, Meehl GA et al (2016) Overview of the Coupled Model Intercomparison Project Phase 6 (CMIP6) experimental design and organization. Geosci Model Dev 9:1937-1958. https://doi.org/10.5194/gmd-9-1937-2016

Farnsworth A, White E, Williams CJR et al (2011) Understanding the Large Scale Driving Mechanisms of Rainfall Variability over Central Africa. In: African Climate and Climate Change. Springer, Dordrecht, pp 101-122

Fatichi S, Pappas C (2017) Constrained variability of modeled T:ET ratio across biomes. Geophys Res Lett 44:6795-6803. https://doi.org/10.1002/2017GL074041

Fisher JB, Melton F, Middleton E et al (2017) The future of evapotranspiration: Global requirements for ecosystem functioning, carbon and climate feedbacks, agricultural management, and water resources. Water Resour Res 53:2618-2626. https://doi.org/10.1002/2016WR020175

Fisher RA, Koven CD (2020) Perspectives on the Future of Land Surface Models and the Challenges of Representing Complex Terrestrial Systems. J Adv Model Earth Syst 12:e2018MS001453

Funk C, Peterson P, Landsfeld M et al (2015) The climate hazards infrared precipitation with stations - A new environmental record for monitoring extremes. Sci Data 2:150066. https://doi.org/10.1038/sdata.2015.66

Gelaro R, McCarty W, Suarez MJ et al (2017) The Modern-Era Retrospective Analysis for Research and Applications, Version 2 (MERRA-2). J Clim 30:5419-5454.

https://doi.org/10.1175/JCLI-D-16-0758.1

Gond V, Fayolle A, Pennec A et al (2013) Vegetation structure and greenness in Central Africa from Modis multi-temporal data. Philos Trans R Soc B Biol Sci 368:20120309. https://doi.org/10.1098/rstb.2012.0309

Guan K, Pan M, Li H et al (2015) Photosynthetic seasonality of global tropical forests constrained by hydroclimate. Nat Geosci 8:284-289. https://doi.org/10.1038/ngeo2382

Haensler A, Saeed F, Jacob D (2013) Assessing the robustness of projected precipitation changes over central Africa on the basis of a multitude of global and regional climate projections. Clim Change 121:349-363. https://doi.org/10.1007/s10584-013-0863-8

Han J, Zhou Z (2013) Dynamics of soil water evaporation during soil drying: Laboratory experiment and numerical analysis. Sci World J 2013:240280. https://doi.org/10.1155/2013/240280

Hart NCG, Washington R, Stratton RA (2018) Stronger Local Overturning in Convective-Permitting Regional Climate Model Improves Simulation of the Subtropical Annual Cycle. Geophys Res Lett 45:11334-11342. https://doi.org/10.1029/2018GL079563

Hart NCG, Washington R, Maidment RI (2019) Deep Convection over Africa: annual cycle, ENSO, and trends in the hotspots. J Clim 32:8791-8811. https://doi.org/10.1175/jcli-d-19-0274.1

Hartman AT (2021) Tracking mesoscale convective systems in central equatorial Africa. Int J Climatol 41:469-482. https://doi.org/10.1002/joc.6632

Hasler N, Avissar R (2007) What controls evapotranspiration in the Amazon basin? J Hydrometeorol 8:380-395. https://doi.org/10.1175/JHM587.1

Hersbach H, Bell B, Berrisford P et al (2020) The ERA5 global reanalysis. Q J R Meteorol Soc 146:1999-2049. https://doi.org/10.1002/qj.3803

Hohenegger C (2020) Land-Atmosphere Interaction in Tropical Africa. In: Oxford Research Encyclopaedia of Climate. https://doi.org/10.1093/acrefore/9780190228620.013.779

Hosaka M (2011). A new MRI land surface model HAL. AGU Fall Meeting Abstracts

Howard E, Washington R (2019) Drylines in Southern Africa: Rediscovering the Congo Air Boundary. J Clim 32:8223-8242. https://doi.org/10.1175/JCLI-D-19-0437.1

Hua W, Zhou L, Nicholson SE et al (2019) Assessing reanalysis data for understanding rainfall climatology and variability over Central Equatorial Africa. Clim Dyn 53:651-669. https://doi.org/10.1007/s00382-018-04604-0

Hurrell JW, Hack JJ, Shea D et al (2008) A new sea surface temperature and sea ice boundary dataset for the community atmosphere model. J Clim 21:5145-5153. https://doi.org/10.1175/2008JCLI2292.1

Hutyra LR, Munger JW, Saleska SR et al (2007) Seasonal controls on the exchange of carbon and water in an Amazonian rain forest. J Geophys Res Biogeosci 112:G03008. https://doi.org/10.1029/2006JG000365

Integrated Carbon Observing System (ICOS) (2020) Congoflux eddy covariance tower. https://www.icos-belgium.be/ESCongoFlux.php. Accessed 21 July 2021

Jackson B, Nicholson SE, Klotter D (2009) Mesoscale Convective Systems over Western Equatorial Africa and Their Relationship to Large-Scale Circulation. Mon

Weather Rev 137:1272-1294. https://doi.org/10.1175/2008MWR2525.1

Jacquemin B, Noilhan J (1990) Sensitivity study and validation of a land surface parameterization using the HAPEX-MOBILHY data set. Boundary Layer Meteorol 52:93-134. https://doi.org/10.1007/BF00123180

James R, Washington R, Abiodun B et al (2018) Evaluating climate models with an African lens. Bull Am Meteorol Soc 99:313-336. https://doi.org/10.1175/BAMS-D-16-0090.1

James R, Hart NCG, Munday C et al (2020) Coupled climate model simulation of tropical-extratropical cloud bands over Southern Africa. J Clim 33:8579-8602. https://doi.org/10.1175/JCLI-D-19-0731.1

Jarvis PG, McNaughton KG (1986) Stomatal Control of Transpiration: Scaling Up from Leaf to Region. Adv Ecol Res 15:1-49. https://doi.org/10.1016/S0065-2504(08)60119-1

Ji D, Wang L, Feng J et al (2014) Description and basic evaluation of Beijing Normal University Earth System Model (BNU-ESM) version 1. Geosci Model Dev 7:2039-2064. https://doi.org/10.5194/gmd-7-2039-2014

Ji JJ, Huang M, Li KR (2008) Prediction of carbon exchanges between China terrestrial ecosystem and atmosphere in 21st century. Sci China Ser D Earth Sci 51:885-898. https://doi.org/10.1007/s11430-008-0039-y

Jinga P, Palagi J (2020) Dry and wet miombo woodlands of south-central Africa respond differently to climate change. Environ Monit Assess 192:1-16. https://doi.org/10.1007/s10661-020-08342-x

Jung M, Reichstein M, Ciais P et al (2010) Recent decline in the global land

evapotranspiration trend due to limited moisture supply. Nature 467:951-954. https://doi.org/10.1038/nature09396

Jury MR, Mpeta EJ (2009) African climate variability in the satellite era. Theor Appl Climatol 98:279-291. https://doi.org/10.1007/s00704-009-0106-0

Kanamitsu M, Ebisuzaki W, Woollen J et al (2002) NCEP-DOE AMIP-II Reanalysis. Bull Am Meteorol Soc 83:1631-1644. https://doi.org/10.1175/BAMS-83-11-1631

Keller M, Alencar A, Asner GP et al (2004) Ecological research in the Large-scale Biosphere-Atmosphere Experiment in Amazonia: Early results. Ecol Appl 14:3-16. https://doi.org/10.1890/03-6003

Kim Y, Moorcroft PR, Aleinov I et al (2015) Variability of phenology and fluxes of water and carbon with observed and simulated soil moisture in the Ent Terrestrial Biosphere Model (Ent TBM version 1.0.1.0.0). Geosci Model Dev 8:3837-3865. https://doi.org/10.5194/gmd-8-3837-2015

Koster RD, Suarez MJ (1996) Energy and water balance calculations in the Mosaic LSM. NASA Tech Memo 9:104606. https://purl.fdlp.gov/GPO/gpo60361

Koster RD, Suarez MJ, Ducharne A et al (2000) A catchment-based approach to modeling land surface processes in a general circulation model: 1. Model structure. J Geophys Res Atmos 105:24809–24822. https://doi.org/10.1029/2000JD900327

Krinner G, Viovy N, de Noblet-Ducoudré N et al (2005) A dynamic global vegetation model for studies of the coupled atmosphere-biosphere system. Global Biogeochem Cycles 19(1):1-33. https://doi.org/10.1029/2003GB002199

Kuete G, Pokam Mba W, Washington R (2020) African Easterly Jet South: control, maintenance mechanisms and link with Southern subtropical waves. Clim Dyn

54:1539-1552. https://doi.org/10.1007/s00382-019-05072-w

Lavers DA, Harrigan S, Prudhomme C (2021) Precipitation Biases in the ECMWF Integrated Forecasting System. J Hydrometeorol 22:1187–1198. https://doi.org/10.1175/JHM-D-20-0308.1

Lawrence DM, Thornton PE, Oleson KW, Bonan GB (2007) The Partitioning of Evapotranspiration into Transpiration, Soil Evaporation, and Canopy Evaporation in a GCM: Impacts on Land-Atmosphere Interaction. J Hydrometeorol 8:862-880. https://doi.org/10.1175/JHM596.1

Lian X, Piao S, Huntingford C et al (2018) Partitioning global land evapotranspiration using CMIP5 models constrained by observations. Nat Clim Chang 8:640-646. https://doi.org/10.1038/s41558-018-0207-9

Liu L, Gudmundsson L, Hauser M et al (2020) Soil moisture dominates dryness stress on ecosystem production globally. Nat Commun 11:1-9. https://doi.org/10.1038/s41467-020-18631-1

Longandjo GNT, Rouault M (2020) On the Structure of the Regional-Scale Circulation over Central Africa: Seasonal Evolution, Variability, and Mechanisms. J Clim 33:145-162. https://doi.org/10.1175/jcli-d-19-0176.1

Maeda EE, Ma X, Wagner FH et al (2017) Evapotranspiration seasonality across the Amazon Basin. Earth Syst Dynam 8:439-454. https://doi.org/10.5194/esd-8-439-2017

Mahfouf JF, Manzi AO, Noilhan J et al (1995) The land surface scheme ISBA within the Meteo-France climate model ARPEGE. Part I: implementation and results. J Clim 8:2039-2057. https://doi.org/10.1175/1520-

0442(1995)008<2039:TLSSIW>2.0.CO;2

Mahowald N, Lo F, Zheng Y et al (2016) Projections of leaf area index in earth system models. Earth Syst Dynam 7:211-229. https://doi.org/10.5194/esd-7-211-2016

Maidment RI, Allan RP, Black E (2015) Recent observed and simulated changes in precipitation over Africa. Geophys Res Lett 42:8155-8164. https://doi.org/10.1002/2015GL065765

Martens B, Miralles DG, Lievens H et al (2017) GLEAM v3: Satellite-based land evaporation and root-zone soil moisture. Geosci Model Dev 10:1903-1925. https://doi.org/10.5194/gmd-10-1903-2017

Martens B, Schumacher DL, Wouters H et al (2020) Evaluating the land-surface energy partitioning in ERA5. Geosci Model Dev 13:4159-4181. https://doi.org/10.5194/gmd-13-4159-2020

Massmann A, Gentine P, Lin C (2019) When Does Vapor Pressure Deficit Drive or Reduce Evapotranspiration? J Adv Model Earth Syst 11:3305-3320. https://doi.org/10.1029/2019MS001790

Matsuyama H, Oki T, Shinoda M, Masuda K (1994) The seasonal change of the water budget in the Congo River Basin. J Meteorol Soc Japan 72:281-299. https://doi.org/10.2151/jmsj1965.72.2_281

Maxwell RM, Condon LE (2016) Connections between groundwater flow and transpiration partitioning. Science 353:377-380. https://doi.org/10.1126/science.aaf7891

Mercado LM, Bellouin N, Sitch S et al (2009) Impact of changes in diffuse radiation on the global land carbon sink. Nature 458:1014-1017.

Milly PCD, Malyshev SL, Shevliakova E et al (2014) An Enhanced Model of Land Water and Energy for Global Hydrologic and Earth-System Studies. J Hydrometeorol 15:1739-1761. https://doi.org/10.1175/JHM-D-13-0162.1

Miralles DG, Brutsaert W, Dolman AJ, Gash JH (2020) On the Use of the Term "Evapotranspiration." Water Resour Res 56:e2020WR028055. https://doi.org/10.1029/2020WR028055

Miralles DG, Gash JH, Holmes TRH et al (2010) Global canopy interception from satellite observations. J Geophys Res Atmos 115:D16122. https://doi.org/10.1029/2009JD013530

Miralles D, Jimenez C, Jung M et al (2016) The WACMOS-ET project - Part 2: Evaluation of global terrestrial evaporation data sets. Hydrol Earth Syst Sci 20:823-842. https://doi.org/10.5194/hess-20-823-2016

Mizuta R, Yoshimura H, Murakami H et al (2012) Climate Simulations Using MRI-AGCM3.2 with 20-km Grid. J Meteorol Soc Japan 90A:233-258. https://doi.org/10.2151/jmsj.2012-A12

Mueller B, Seneviratne SI (2014) Systematic land climate and evapotranspiration biases in CMIP5 simulations. Geophys Res Lett 41:128-134. https://doi.org/10.1002/2013GL058055

Mueller B, Hirschi M, Jimenez C et al (2013) Benchmark products for land evapotranspiration: LandFlux-EVAL multi-data set synthesis. Hydrol Earth Syst Sci 17:3707-3720. https://doi.org/10.5194/hess-17-3707-2013

Munday C, Washington R (2017) Circulation controls on southern African precipitation in coupled models: The role of the Angola Low. J Geophys Res Atmos 122:861–

877. https://doi.org/10.1002/2016JD025736

Munday C, Washington R, Hart N (2021) African Low-Level Jets and Their Importance for Water Vapor Transport and Rainfall. Geophys Res Lett 48:e2020GL090999. https://doi.org/10.1029/2020GL090999

Muñoz-Sabater J, Dutra E, Agusti-Panareda A et al (2021) ERA5-Land: A state-of-the-art global reanalysis dataset for land applications. Earth Syst Sci Data Discuss. https://doi.org/10.5194/ESSD-2021-82

Myneni RB, Yang W, Nemani RR et al (2007) Large seasonal swings in leaf area of Amazon rainforests. Proc Natl Acad Sci U S A 104:4820-4823. https://doi.org/10.1073/pnas.0611338104

Ndehedehe CE, Okwuashi O, Ferreira VG, Agutu NO (2018) Exploring evapotranspiration dynamics over Sub-Sahara Africa (2000-2014). Environ Monit Assess 190:400. https://doi.org/10.1007/s10661-018-6780-6

Neupane N (2016) The Congo basin zonal overturning circulation. Adv Atmos Sci 33:767-782. https://doi.org/10.1007/s00376-015-5190-8

Nicholson SE (2018a) The ITCZ and the seasonal cycle over equatorial Africa. Bull Am Meteorol Soc 99:337-348. https://doi.org/10.1175/BAMS-D-16-0287.1

Nicholson SE, Grist JP (2003) The seasonal evolution of the atmospheric circulation over West Africa and equatorial Africa. J Clim 16:1013-1030. https://doi.org/10.1175/1520-0442(2003)016<1013:TSEOTA>2.0.CO;2

Nicholson SE, Dezfuli AK (2013) The relationship of rainfall variability in western equatorial Africa to the tropical oceans and atmospheric circulation. Part I: The boreal spring. J Clim 26:45-65. https://doi.org/10.1175/JCLI-D-11-00653.1

Nicholson SE, Klotter D (2021) The Tropical Easterly Jet over Africa, its representation in six reanalysis products, and its association with Sahel rainfall. Int J Climatol 41:328-347. https://doi.org/10.1002/joc.6623

Nicholson SE, Kim J, Ba MB, Lare AR (1997) The mean surface water balance over Africa and its interannual variability. J Clim 10:2981-3002. https://doi.org/10.1175/1520-0442(1997)010<2981:TMSWBO>2.0.CO;2

Nicholson SE, Klotter D, Dezfuli AK, Zhou L (2018b) New rainfall datasets for the Congo basin and surrounding regions. J Hydrometeorol 19:1379-1396. https://doi.org/10.1175/JHM-D-18-0015.1

Nicholson SE, Klotter D, Zhou L, Hua W (2019) Validation of satellite precipitation estimates over the Congo Basin. J Hydrometeorol 20:631-656. https://doi.org/10.1175/JHM-D-18-0118.1

Nikulin G, Hewitson B (2019) A simple set of indices describing the Tropical Rain Belt over central and southern Africa. Atmos Sci Lett 20:e946. https://doi.org/10.1002/asl.946

Oleson K, Dai Y, Bonan B et al (2004) Technical Description of the Community Land Model (CLM). National Center for Atmospheric Research. https://doi.org/10.5065/D6N877R0

Oleson W, Lawrence M, Bonan B et al (2010) Technical Description of version 4.0 of the Community Land Model (CLM). National Center for Atmospheric Research. https://doi.org/10.5065/D6FB50WZ

Or D, Lehmann P (2019) Surface Evaporative Capacitance: How Soil Type and Rainfall Characteristics Affect Global-Scale Surface Evaporation. Water Resour Res

55:519–539. https://doi.org/10.1029/2018WR024050

Parker WS (2016) Reanalyses and Observations: What's the Difference? Bull Am Meteorol Soc 97:1565-1572. https://doi.org/10.1175/BAMS-D-14-00226.1

Pathak R, Sahany S, Mishra SK, Dash SK (2019) Precipitation Biases in CMIP5 Models over the South Asian Region. Sci Rep 9:1-13. https://doi.org/10.1038/s41598-019-45907-4

Peng J, Loew A, Chen X et al (2016) Comparison of satellite-based evapotranspiration estimates over the Tibetan Plateau. Hydrol Earth Syst Sci 20:3167-3182. https://doi.org/10.5194/hess-20-3167-2016

Philip JR (1957) Evaporation, and Moisture and Heat Fields in the Soil. J Meteorol 14. https://doi.org/10.1175/1520-0469(1957)014<0354:EAMAHF>2.0.CO;2

Philippon N, de Lapparent B, Gond V et al (2016) Analysis of the diurnal cycles for a better understanding of the mean annual cycle of forests greenness in Central Africa. Agric For Meteorol 223:81-94. https://doi.org/10.1016/j.agrformet.2016.04.005

Pitman AJ (1991) Sensitivity of the land surface to sub-grid scale processes: implications for climate simulations. Plant Ecol 91:121-134. https://doi.org/10.1007/BF00036052

Pitman AJ (2003) The evolution of, and revolution in, land surface schemes designed for climate models. Int J Climatol 23:479-510. https://doi.org/10.1002/joc.893

Pokam WM, Djiotang LAT, Mkankam FK (2012) Atmospheric water vapor transport and recycling in Equatorial Central Africa through NCEP/NCAR reanalysis data. Clim Dyn 38:1715-1729. https://doi.org/10.1007/s00382-011-1242-7

Pokam WM, Bain CL, Chadwick RS et al (2014) Identification of processes driving low-level westerlies in West Equatorial Africa. J Clim 27:4245-4262. https://doi.org/10.1175/JCLI-D-13-00490.1

Raghavendra A, Zhou L, Jiang Y, Hua W (2018) Increasing extent and intensity of thunderstorms observed over the Congo Basin from 1982 to 2016. Atmos Res 213:17-26. https://doi.org/10.1016/j.atmosres.2018.05.028

Raghavendra A, Zhou L, Roundy PE et al (2020) The MJO's impact on rainfall trends over the Congo rainforest. Clim Dyn 54:2683-2695. https://doi.org/10.1007/s00382-020-05133-5

Rasp S, Pritchard MS, Gentine P (2018) Deep learning to represent subgrid processes in climate models. Proc Natl Acad Sci U S A 115:9684-9689. https://doi.org/10.1073/pnas.1810286115

Reichle RH, Koster RD, De Lannoy GJM et al (2011) Assessment and enhancement of MERRA land surface hydrology estimates. J Clim 24:6322–6338. https://doi.org/10.1175/JCLI-D-10-05033.1

Reichle RH, Draper CS, Liu Q et al (2017) Assessment of MERRA-2 Land Surface Hydrology Estimates. J Clim 30:2937–2960. https://doi.org/10.1175/JCLI-D-16-0720.1

Restrepo-Coupe N, da Rocha HR, Hutyra LR et al (2013) What drives the seasonality of photosynthesis across the Amazon basin? A cross-site analysis of eddy flux tower measurements from the Brazil flux network. Agric For Meteorol 182:128-144. https://doi.org/10.1016/j.agrformet.2013.04.031

Richter I, Chang P, Doi T et al (2016) An Overview of coupled GCM Biases in the

Tropics. Indo-Pacific Clim Var Predict 8:213-263. https://doi.org/10.1142/9789814696623_0008

Ritter A, Munoz-Carpena R (2013) Performance evaluation of hydrological models: Statistical significance for reducing subjectivity in goodness-of-fit assessments. J Hydrol 480:33-45. https://doi.org/10.1016/j.jhydrol.2012.12.004

Running S, Zhao M (2015) User's Guide: Daily GPP and Annual NPP (MOD17A2/A3) Products: NASA Earth Observing System MODIS Land Algorithm. NASA: Washington DC, USA

Running S, Mu Q, Zhao M, Moreno A (2017) User's Guide: MODIS Global Terrestrial Evapotranspiration (ET) Product (NASA MOD16A2/A3): NASA Earth Observing System MODIS Land Algorithm. NASA: Washington DC, USA.

Ryan CM, Williams M, Grace J et al (2017) Pre-rain green-up is ubiquitous across southern tropical Africa: implications for temporal niche separation and model representation. New Phytol 213:625-633. https://doi.org/10.1111/nph.14262

Saha S, Moorthi S, Pan HL et al (2010) The NCEP climate forecast system reanalysis. Bull Am Meteorol Soc 91:1015-1057. https://doi.org/10.1175/2010BAMS3001.1

Samba G, Nganga D (2012) Rainfall variability in Congo-Brazzaville: 1932-2007. Int J Climatol 32:854-873. https://doi.org/10.1002/joc.2311

Sandjon AT, Nzeukou A, Tchawoua C (2012) Intraseasonal atmospheric variability and its interannual modulation in Central Africa. Meteorol Atmos Phys 117:167-179. https://doi.org/10.1007/s00703-012-0196-6

Schmidt GA, Ruedy R, Hansen JE et al (2006) Present-day atmospheric simulations using GISS ModelE: Comparison to in situ, satellite, and reanalysis data. J Clim

19:153-192

Schmidt GA, Kelley M, Nazarenko L et al (2014) Configuration and assessment of the GISS ModelE2 contributions to the CMIP5 archive. J Adv Model Earth Syst 6:141-184. https://doi.org/10.1002/2013MS000265

Schwingshackl C, Hirschi M, Seneviratne SI (2017) Spatiotemporal Variations of Soil Moisture Control on Surface Energy Balance and Near-Surface Air Temperature. J Clim 30:7105-7124. https://doi.org/10.1175/JCLI-D-16-0727.1

Seneviratne SI, Corti T, Davin EL et al (2010) Investigating soil moisture-climate interactions in a changing climate: A review. Earth Science Rev 99:125-161. https://doi.org/10.1016/j.earscirev.2010.02.004

Senior CA, Marsham JH, Berthou S et al (2021) Convection permitting regional climate change simulations for understanding future climate and informing decision making in Africa. Bull Am Meteorol Soc. https://doi.org/10.1175/BAMS-D-20-0020.1

Shem WO (2006) Biosphere-atmosphere interaction over the Congo Basin and its influence on the regional hydrological cycle. PhD Thesis, Georgia Institute.

Shevliakova E, Pacala SW, Malyshev S et al (2009) Carbon cycling under 300 years of land use change: Importance of the secondary vegetation sink. Global Biogeochem Cycles. https://doi.org/10.1029/2007GB003176

Siam MS, Demory ME, Eltahir EAB et al (2013) Hydrological Cycles over the Congo and Upper Blue Nile Basins: Evaluation of GCM Simulations and Reanalysis Products. J Clim 26:8881-8894. https://doi.org/10.1175/JCLI-D-12-00404.1

Sitch S, Smith B, Prentice IC et al (2003) Evaluation of ecosystem dynamics, plant

geography and terrestrial carbon cycling in the LPJ dynamic vegetation model. Glob Chang Biol 9:161-185. https://doi.org/10.1046/j.1365-2486.2003.00569.x

Sjöström M, Zhao M, Archibald S et al (2013) Evaluation of MODIS gross primary productivity for Africa using eddy covariance data. Remote Sens Environ 131:275-286. https://doi.org/10.1016/J.RSE.2012.12.023

Sonwa DJ, Oumarou Farikou M, Martial G, Felix FL (2020) Living under a Fluctuating Climate and a Drying Congo Basin. Sustainability 12:2936. https://doi.org/10.3390/su12072936

Sonwa DJ, Dieye A, El Mzouri E-H et al (2017) Drivers of climate risk in African agriculture. Clim Dev 9:383-398. https://doi.org/10.1080/17565529.2016.1167659

Sori R, Nieto R, Vicente-Serrano SM et al (2017) A Lagrangian perspective of the hydrological cycle in the Congo River basin. Earth Syst Dyn 8:653-675. https://doi.org/10.5194/esd-8-653-2017

Taguela TN, Vondou DA, Moufouma-Okia W et al (2020) CORDEX Multi-RCM Hindcast Over Central Africa: Evaluation Within Observational Uncertainty. J Geophys Res Atmos 125:e2019JD031607. https://doi.org/10.1029/2019JD031607

Takata K, Emori S, Watanabe T (2003) Development of the minimal advanced treatments of surface interaction and runoff. Glob Planet Change 38:209-222. https://doi.org/10.1016/S0921-8181(03)00030-4

Tamoffo AT, Dosio A, Vondou DA, Sonkoue D (2020) Process-Based Analysis of the Added Value of Dynamical Downscaling Over Central Africa. Geophys Res Lett 47:e2020GL089702. https://doi.org/10.1029/2020GL089702

Taylor CM, Fink AH, Klein C et al (2018) Earlier Seasonal Onset of Intense Mesoscale

Convective Systems in the Congo Basin Since 1999. Geophys Res Lett 45:13458-13467. https://doi.org/10.1029/2018GL080516

Taylor KE, Stouffer RJ, Meehl GA et al (2012) An Overview of CMIP5 and the Experiment Design. Bull Am Meteorol Soc 93:485-498. https://doi.org/10.1175/BAMS-D-11-00094.1

Tobin RL, Kulmatiski A (2018) Plant identity and shallow soil moisture are primary drivers of stomatal conductance in the savannas of Kruger National Park. PLoS One 13:e0191396. https://doi.org/10.1371/journal.pone.0191396

Trambauer P, Dutra E, Maskey S et al (2014) Comparison of different evaporation estimates over the African continent. Hydrol Earth Syst Sci 18:193-212. https://doi.org/10.5194/hess-18- 193-2014

Trenberth KE (1999) Atmospheric moisture recycling: Role of advection and local evaporation. J Clim 12:1368-1381. https://doi.org/10.1175/1520-0442(1999)012<1368:amrroa>2.0.co;2

Van Der Ent RJ, Savenije HHG, Schaefli B, Steele-Dunne SC (2010) Origin and fate of atmospheric moisture over continents. Water Resour Res 46:1-12. https://doi.org/10.1029/2010WR009127

Van Engelen VW, Verdoot A, Dijkshoorn JA, Batjes NH (2013) Soil and Terrain Database of Central Africa (ver. 1.0). SOTERCAF. World Soil Information

Verseghy DL (2000) The Canadian land scheme (CLASS): Its history and future. Atmosphere - Ocean 38:1-13. https://doi.org/10.1080/07055900.2000.9649637

Vinya R, Malhi Y, Brown ND et al (2019) Seasonal changes in plant–water relations influence patterns of leaf display in Miombo woodlands: evidence of water

conservation. Tree Physiol 39:104–112. https://doi.org/10.1093/treephys/tpy062

Voldoire A, Sanchez-Gomez E, Salas y Mélia D et al (2013) The CNRM-CM5.1 global climate model: description and basic evaluation. Clim Dyn 40:2091-2121. https://doi.org/10.1007/s00382-011-1259-y

Volodin EM, Lykosov VN (1998) Parameterization of Heat and Moisture Transfer in the Soil-Vegetation System for Use in Atmospheric General Circulation Models: 1. Formulation and Simulations. Atmos Ocean Phy 34:405-416.

Volodin EM, Dianskii NA, Gusev AV (2010) Simulating present-day climate with the INMCM4.0 coupled model of the atmospheric and oceanic general circulations. Izv Atmos Ocean Phys 46:414-431. https://doi.org/10.1134/S000143381004002X

Von Salzen K, Scinocca JF, Mcfarlane NA et al (2013) The Canadian Fourth Generation Atmospheric GCM (CanAM4). Representation of Physical Processes. Atmosphere-Ocean 51:104-125. https://doi.org/10.1080/07055900.2012.755610

Wang D, Anagnostou EN, Wang G (2006) The effect of sub-grid rainfall variability on the water balance and flux exchange processes resolved at climate scale: The European region contrasted to Central Africa and Amazon rainforests. Adv Geosci 7:269-274. https://doi.org/10.5194/adgeo-7-269-2006

Wang G, Eltahir EAB (2000) Modeling the Biosphere-Atmosphere System: The Impact of the Subgrid Variability in Rainfall Interception. J Clim 13:2887-2899. https://doi.org/10.1175/1520-0442(2000)013<2887:MTBAST>2.0.CO;2

Wang HX, Liu CM (2007) Soil Evaporation and its Affecting Factors under Crop Canopy. Commun Soil Sci Plant Anal 38:259-271. https://doi.org/10.1080/00103620601094213

Wang K, Dickinson RE (2012) A review of global terrestrial evapotranspiration: Observation, modeling, climatology, and climatic variability. Rev Geophys 50. https://doi.org/10.1029/2011RG000373

Wartenburger R, Seneviratne SI, Hirschi M et al (2018) Evapotranspiration simulations in ISIMIP2a-Evaluation of spatio-temporal characteristics with a comprehensive ensemble of independent datasets. Environ Res Lett 13:075001. https://doi.org/10.1088/1748-9326/aac4bb

Washington R, Harrison M, Conway D et al (2006) African climate change: Taking the shorter route. Bull Am Meteorol Soc 87:1355-1366. https://doi.org/10.1175/BAMS-87-10-1355

Washington R, James R, Pearce H et al (2013) Congo basin rainfall climatology: Can we believe the climate models? Philos Trans R Soc B Biol Sci 368:20120296. https://doi.org/10.1098/rstb.2012.0296

Watanabe M, Suzuki T, O'ishi R et al (2010) Improved Climate Simulation by MIROC5: Mean States, Variability, and Climate Sensitivity. J Clim 23:6312-6335. https://doi.org/10.1175/2010JCLI3679.1

Webster P (1983) The large-scale structure of the tropical atmosphere. In: General Circulation of the Atmosphere, London, Academic Press, pp 235-275

Weerasinghe I, Bastiaanssen W, Mul M et al (2020) Can we trust remote sensing evapotranspiration products over Africa? Hydrol Earth Syst Sci 24:1565-1586. https://doi.org/10.5194/hess-24-1565-2020

Wei Z, Yoshimura K, Wang L et al (2017) Revisiting the contribution of transpiration to global terrestrial evapotranspiration. Geophys Res Lett 44:2792-2801.

https://doi.org/10.1002/2016GL072235

Werth D, Avissar R (2004) The regional evapotranspiration of the Amazon. J Hydrometeorol 5:100-109. https://doi.org/10.1175/1525-7541(2004)005<0100:TREOTA>2.0.CO;2

Whalley WR, Ober ES, Jenkins M (2013) Measurement of the matric potential of soil water in the rhizosphere. J Exp Bot 64:3951-3963. https://doi.org/10.1093/jxb/ert044

Wild M (2020) The global energy balance as represented in CMIP6 climate models. Clim Dyn 55:553-577. https://doi.org/10.1007/s00382-020-05282-7

Williams CJR, Allan RP, Kniveton DR (2012) Diagnosing atmosphere-land feedbacks in CMIP5 climate models. Environ Res Lett 7:044003. https://doi.org/10.1088/1748-9326/7/4/044003

Wu MLC, Reale O, Schubert SD et al (2009) African easterly jet: Structure and maintenance. J Clim 22:4459–4480. https://doi.org/10.1175/2009JCLI2584.1

Wu T, Song L, Li W et al (2014) An overview of BCC climate system model development and application for climate change studies. J Meteorol Res 28:34-56. https://doi.org/10.1007/s13351-014-3041-7

Xu L, Saatchi SS, Shapiro A et al (2017) Spatial Distribution of Carbon Stored in Forests of the Democratic Republic of Congo. Sci Rep 7:15030. https://doi.org/10.1038/s41598-017-15050-z

Yan D, Zhang X, Yu Y, Guo W (2017) Characterizing Land Cover Impacts on the Responses of Land Surface Phenology to the Rainy Season in the Congo Basin. Remote Sens 9:461. https://doi.org/10.3390/rs9050461

Yang W, Seager R, Cane MA, Lyon B (2015) The annual cycle of East African precipitation. J Clim 28:2385-2404. https://doi.org/10.1175/JCLI-D-14-00484.1

Yu M, Wang G, Chen H (2016) Quantifying the impacts of land surface schemes and dynamic vegetation on the model dependency of projected changes in surface energy and water budgets. J Adv Model Earth Syst 8:370-386. https://doi.org/10.1002/2015MS000492

Zhao M, Held IM, Lin SJ, Vecchi GA (2009) Simulations of global hurricane climatology, interannual variability, and response to global warming using a 50-km resolution GCM. J Clim 22:6653-6678. https://doi.org/10.1175/2009JCLI3049.1

Zhou L, Tian Y, Myneni RB et al (2014) Widespread decline of Congo rainforest greenness in the past decade. Nature 508:86-90. https://doi.org/10.1038/nature13265

Zhou ZQ, Xie SP, Zhang GJ, Zhou W (2018) Evaluating AMIP skill in simulating interannual variability over the Indo-western Pacific. J Clim 31:2253-2265. https://doi.org/10.1175/JCLI-D-17-0123.1